2014-01-29

Unraveling mechanisms behind cross presentation during phagocytic signaling

Hari, Aswin

UNIVERSITY OF CALGARY

Unraveling mechanisms behind cross presentation during phagocytic signaling

by

Aswin Hari

A THESIS

SUBMITTED TO THE FACULTY OF GRADUATE STUDIES

IN PARTIAL FULFILMENT OF THE REQUIREMENTS FOR THE

DEGREE OF DOCTOR OF PHILOSOPHY

DEPARTMENT OF MICROBIOLOGY AND INFECTIOUS DISEASES

CALGARY, ALBERTA

JANUARY 2014.

Abstract

MHC class I antigens come from endogenous syntheses, while class II antigens are obtained extracellularly via endocytosis. Cross presentation is the link between the two by which external antigens are targeted to the MHC class I pathway. It is generally accepted that particulate antigens are more efficient in this pathway switch. However the reason behind this phenomenon is unknown. We report that dendritic cell engagement of a phagocytic target limits endocytic maturation and inhibits the associated proteolytic activities. In this scenario, early endosomes show reduced progression towards late endosomes/lysosomes and remain spatially close to the cell membrane. In phagocytosis, the microtubular (MT) system, including tubulin filaments and microtubule organization centers (MTOCs), are heavily skewed toward the engulfed particulate matter; the remaining cytoplasmic volumes are relatively devoid of MT presence. This is accompanied by a reduced centripetal movement inward and the maturation of endosomes. The antigen processing in these arrested endosomes is under the control of Nicotinamide adenine dinucleotide phosphate-oxidase (NAPDH)-associated ROS. We also show that cathepsin S is responsible for the generation of the class I epitope for cross presentation. The rerouted antigen presentation is at least 40 fold more efficient than the same amount of antigen delivered through the phagocytic pathway, and is operational *in vivo*. Our results suggest that in DCs in addition to solid structure uptake, phagocytosis directs a coordinated set of enzymatic and cytoskeletal events that regulate endosomal trafficking and maturation. As a consequence, external soluble antigens are driven away from their conventional MHC class II processing, into the class I cross presentation pathway.

Acknowledgements

I would like to thank Melanie Stenner for all her hard labour and patience that helped me to finish this thesis. I would like to thank Anutosh Ganguly, Shevaun Davis, Aileen Yang, Pankaj Tailor, Dale Balce, Joanna Rybicka, Raymond Lam, Fay Munro, Inana Namet, Enaam Alghamdi, Randy, Michael Schoel, Tobias, Wei Dong and Libing for their extensive technical advice and help. I would like to thank Sue, Xavier, Barry, Dr. Fernando Cabral and Dr. Li Yu for methodological help. I would like to acknowledge Marcy Brett for administrative help and Jennifer Tran for thesis review. I would like to acknowledge Martha and Jaime in the mouse facilities for putting up with my complex requests for mice however untimely they were. *In vivo* work wouldn't have been possible without the expertise of Yie Ping and Laurie Kennedy at the FACS facility. I would like to thank Dr. Jim McGee for access to the super resolution microscope. I would also like to acknowledge core facilities at university of Calgary: LCI (Dr. Pina Colarusso and Jen Amon), MIF and at Tshingua University. I would like to thank Dr. Matthias Amrein for access to the AFM and expert guidance to complete the work especially in imaging experiments. I would like to thank Dr. Robin Yates for his valuable input in different experiments and access to equipment in his laboratory. I would like to thank Dr. Kenneth Rock and Dr. LJ Shen for mice, materials and constructive criticism on the study. I am indebted to my supervisory committee members Dr. Amrein, Dr. Patel and Dr. Yates for their constant guidance and support that has helped me to come this far. I would like to thank my supervisor Dr. Yan Shi for his faith in me, his mentorship and support all through my graduate study. I would like to thank the funding agencies that have made it all possible: Canada Foundation for Innovation (MIF and LCI), grants from US NIH, NSERC and CIHR, QE II and William Davies scholarships. Last but not the least I am grateful to all my friends and family for supporting me all along in this endeavor.

Dedication

I would like to dedicate this thesis to my family, Hari and Lakshmi, Karthik and Krithika, and all the Higher Beings for their nurturing care and lifelong support. They have provided me love and comfort through the ups and downs of this journey.

Table of Contents

List of Figures and Illustrations

Video Legends

Movie 1- Control Super-resolution shows image projection of the 3D model of MT staining in an untreated dendritic cell. The projection was made from the Z stack images taken 0.2 micro-meter apart. A total of around 60 images from stacks were embedded to make a projection using ImageJ.

Movie 2- Control Super-resolution shows 360 degree rotation of the 3D model shown above. A total of around 60 images from stacks were embedded to make a 3D model using ImageJ 3D projection.

Movie 3- Crystal Super-resolution shows image projection of the 3D model of MT staining in a dendritic cell that had phagocytosed an MSU. The MSU crystal from DIC acquisition was manually embedded in the SIM data. The position of the crystal is shown in blue color.

Movie 4- crystal super resolution shows 360 degree rotation of the 3D model above. Note the 3D rotation shows that the microtubules form tunnel like structure in the position of the crystal.

Movie 5-7: Total Internal Reflection Fluorescence Microscopy (TIRFM) shows the time series of an untreated DC 2.4 cell that had been fed with Alexa 488 labeled OVA. A total of 61 images for each cell were embedded to make the movies.

Movie 8-10: TIRFM shows the time series of a DC2.4 cell that had internalized a MSU crystal. A total of 61 images for each cell were embedded to make the movies.

Movie 11: Structured Illumination Microscopy (SIM) shows 360 degree rotation of the 3D model of a DC2.4 cell stained with clathrin antibody. A total of 450 images were embedded to make the model.

Movie 12: SIM shows 360 degree rotation of the 3D model of a DC2.5 that had phagocytosed a MSU crystal. A total of 450 images were embedded to make the model.

List of Symbols, Abbreviations and Nomenclature

Symbol	Definition
ADCC	Antibody-dependent cell-mediated cytotoxicity
APC	Antigen presenting cell
ARF6	ADP-ribosylation factor 6
CARD	Caspase activation and recruitment domains
CD-	Cluster of differentiation
CDC42	Cell division control protein 42
CLEC9a	C-type lectin 9a
CTL	Cytotoxic T lymphocyte
CTLA4	Cytotoxic T-lymphocyte antigen 4
DAI	DNA-dependent activator of IFN-regulatory factors
DAMP	Danger associated molecular pattern
DC	Dendritic cell
DNA	Deoxyribonucleic acid
ER	Endoplasmic reticulum
FLT3L	Fms-like tyrosine kinase 3
GATA-3	Trans-acting T-cell-specific transcription factor 3
GM-CSF	Granulocyte-macrophage colony-stimulating factor
GTPase	GTP binding hydrolases

HLA	Human leukocyte antigen
IFN-ɣ	Interferon-ɣ
IgG	Immunoglobulin
IL-	Interleukins
ITAM	Immunoreceptor tyrosine-based activation motif
LRR	Leucine-rich repeat
MAPK	Mitogen-activated protein kinase
MHC	Major histocompatibility complex
MTOC	Microtubule-organizing center
MyD88	Myeloid differentiation primary response gene (88)
NF κ B	Nuclear factor kappa-light-chain-enhancer of activated B cells
NLR	NOD like receptor
NOD	Nucleotide-binding oligomerization domain
NOX2	NADPH oxidase
PAMP	Pathogen associated molecular pattern
PD1	Programmed cell death protein 1
PI3kinase	Phosphatidylinositide 3-kinase
PRR	Pattern recognition receptor
Ras	Rat sarcoma protein
RIG	Retinoic acid-inducible gene 1
RNA	Ribonucleic acid

ROS	Reactive oxygen species
SNARE	Soluble NSF attachment Protein receptor
TAP	Transporter associated with antigen processing
T-bet	T-box transcription factor-1
TCR	T cell receptor
TGF-β	Transforming growth factor-β
TLR	Toll like receptor
Treg	Regulatory T cell
TRIF	TIR-domain-containing adapter-inducing interferon-β
ZAP70	Zeta-chain-associated protein kinase 70

Chapter One: **Introduction**

1.1 Antigen presentation

1.1.1 Background

An antigen is any substance that can generate an immune response. The term was coined in 1899 by Ladislas Deutsch as a new compound word from *anti*body *gen*erator. Immunology, the study of the body's immune system is a relatively new science. Although relatively unknown to most people, the WHO noted in a 1988 report that the Indians and Chinese experimented with cutaneous and respiratory variolation respectively in the early 10th century A.D. [1]. The procedures, however crude with some painful side effects, did endow some level of protection. The origin of modern immunology is generally attributed to Edward Jenner, who experimented with vaccination in 1796. Edward Jenner was the first to demonstrate the efficacy of inoculating people with cowpox virus to offer protection against small pox and called the procedure *vaccination* [2]. His work led to the complete eradication of small pox by 1979. Louis Pasteur developed a successful vaccine against rabies in humans in the 1880s and tried to develop a cholera vaccine against chicken cholera. In the following decade, Behring and Kitasato discovered that the serum of animals immune to diphtheria or tetanus had a specific "antitoxic" activity. The modern concept of antigen identification by T cells, when they are presented on self MHC molecules, was the result of the seminal work by Zinkernagel and Doherty [3]. There are two arms of the immune system, the innate and the adaptive system. The innate immune system is generic and non-specific with its activation mainly dependent on pattern recognition receptors (PRRs) that recognize different microbial and cellular products. The innate immune system does not need priming for its functions. The innate immune machinery is not only the first in line for defence against any pathogen, but also provides crucial activation signals and partly drives the

adaptive response. The adaptive response of the immune system is specific and needs to be primed effectively to be activated. The Russian pioneer and Nobel Laureate, Elie Metchnikoff discovered that there were certain cells in the body capable of engulfing many microorganisms. He named them macrophages and they are one of the frontline defenses of the body in fighting pathogens. Macrophages, belonging to a special group of cells known as antigen presenting cells (APCs) which includes dendritic cells (DCs) and B cells, are capable of capturing antigens and priming T cells. The adaptive arm consists of B and T lymphocytes that, upon activation, mount specific responses against antigens. In the course of evolution to discriminate infectious foreign entities from the non-infectious host, the body requires three signals before the priming of the adaptive system can occur [4]. These signals include MHC/peptide complex, activation of PRRs and cytokines [5]. Antigen presentation on MHC molecules to cognate T cells is the first and critical signal needed in this process. Antigen presentation can be classified into three types: presentation of endogenous antigens on MHC I molecules, presentation of exogenous antigens on MHC II molecules and presentation of exogenous antigens on MHC I molecules (cross presentation) [6].

1.1.2 Endogenous antigen presentation

All cells survey their cytoplasm for any abnormalities and target malfunctioning proteins to the proteasome for cleavage [7]. These include defective self-proteins, alternative translation products, proteins that have been retrotranslocated from the endoplasmic reticulum (ER) for sampling purposes and viral antigens which are produced internally. Cytosolic chaperones protect proteolytic intermediates of the antigen from exhaustive degradation and preserve epitopes for MHC I loading [8]. The resulting peptides enter the ER through TAP (Transporter associated with antigen processing) and further trimming of antigen is performed by amino

peptidases in the ER. The ER aminopeptidases can either trim peptides bound to the MHC I molecules or trim peptides to generate an epitope that can tightly bind to MHC class I molecule [9]. All nucleated cells are capable of processing endogenous antigens. The epitope bound MHC I molecules are directed to the plasma membrane (PM) (through the Golgi) to be presented to CD8 T cells [10] (Illustration 1). An infected host cell presenting viral antigens can be identified and killed by a CD8 T cell.

1.1.3 Presentation of exogenous antigens on MHC II molecules on APCs

The immune system generally presents external antigens by MHC II system. The source of antigen can be bacterial, fungal or viral and includes pathogenic products like toxins or self-proteins, and allergens in the extracellular local environment. Exogenous antigens can be taken in by macropinocytosis, clathrin mediated endocytosis, endocytosis or phagocytosis [9, 11, 12]. Other than these processes, peptides for loading on MHC II molecules can be derived from sampling apoptotic bodies and through autophagy [13, 14]. Once the antigen is internalized, the vesicles containing the antigen merge with compartments that carry degradative proteases including amino peptidases, aspartic peptidases and cysteine proteases [15] . The pH of these compartments are modulated to optimise degradation, prevent excessive damage and assist in peptide loading to MHC II molecules [16]. This mechanism and the site of peptide loading however are current topics of research. The main candidates for the site of antigen degradation are endosomes, late endosomes and lysosomes [9-11]. Before MHC class II molecules leave the ER, they are bound by an invariant chain (li) that fills the peptide binding pocket and prevents premature or non-specific binding, provides stability to the MHC II molecule and targets it to the requisite compartments [17-19]. The MHC II molecules travel through the Golgi before they reach the site of peptide degradation. The li chain is cleaved by resident proteases in the loading

compartment, resulting in a small peptide called CLIP (Class II-associated invariant chain peptide) remaining in the MHC II binding groove. Subsequently, CLIP is exchanged for an antigenic peptide in the presence of the chaperone protein HLA DM (Human leukocyte antigen chaperone DM) along with another chaperone HLA DO (Human leukocyte antigen chaperone DO) that acts as a regulator of HLA DM [20]. Once the peptide is loaded onto an MHC II molecule, it is sent to the PM to be presented to CD4 T cells [10](Illustration 1).

1.1.4 Cross presentation

The final antigen processing pathway is cross presentation and it is observed mainly in DCs and macrophages. Cross presentation is the engulfment and processing of exogenous cell bodies or particles by APCs for presentation on MHC I molecules to CD8 T cells through a relatively unknown pathway or pathways [21](Illustration 1). Generally, exogenous antigens are presented on MHC II molecules to T cells to initiate an immune response, but this would make it impossible for the immune system to react to viruses that do not infect APCs, and against cancer cells [22]. This difficulty is overcome because DCs can sample cellular debris and particles from their surroundings. When virally infected and malignant cells die and become fragmented they are cleared by macrophages and DCs. In the process they get sampled and processed by DCs to induce a CD8 T cell response. DCs can cross-present a wide range of exogenous antigens such as cell-associated, bacterial, immunocomplex and soluble proteins [11, 23]. There are many mechanisms of antigen uptake for cross presentation; they include phagocytosis [24], uptake of apoptotic bodies [25] and endocytosis [26]. Upon uptake, antigens are subjected to proteolytic digestion.

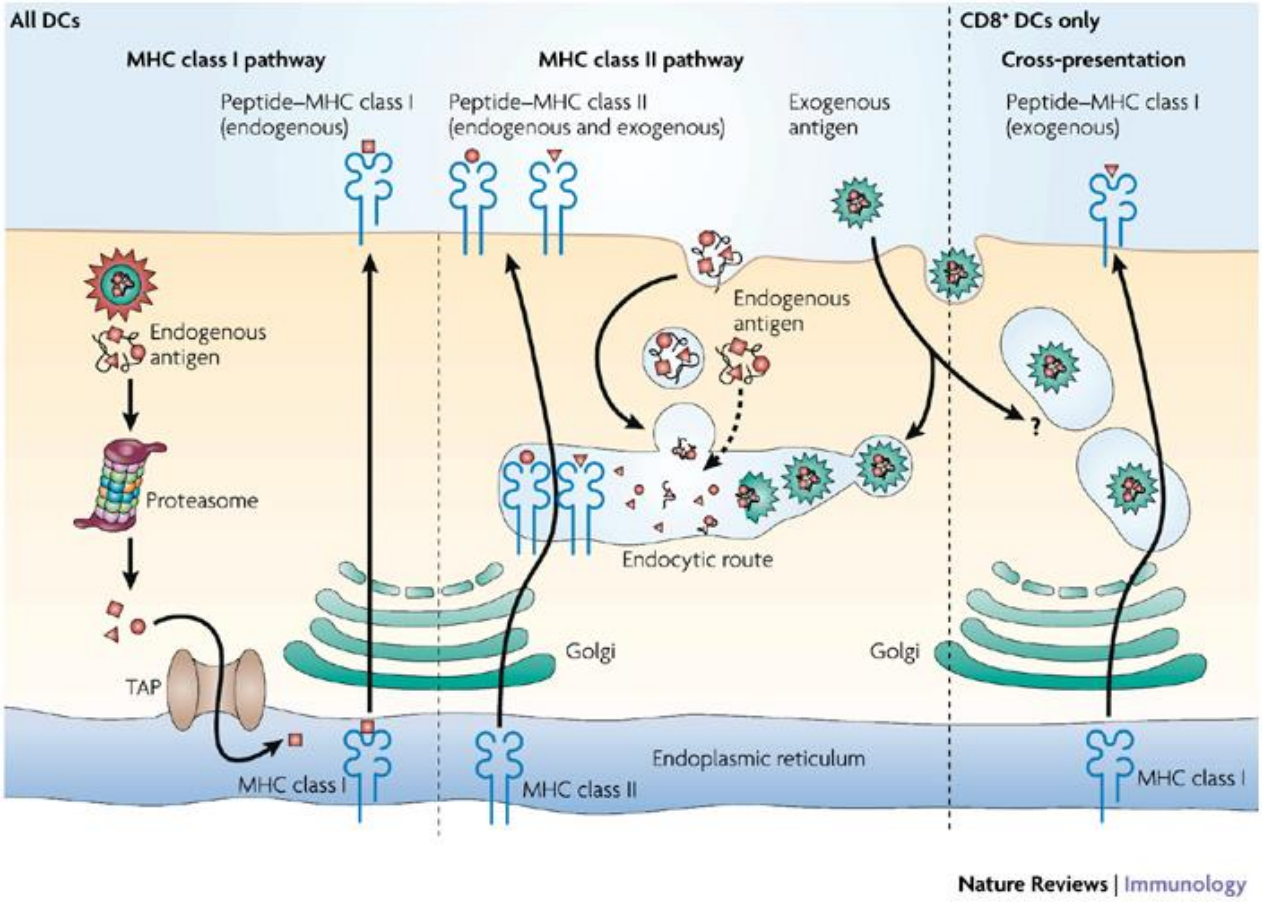

Illustration 1: Types of antigen presentation.

Antigen presentation can be divided broadly into three types [27]. The endogenous MHC I pathway allows endogenous antigens sampled via the proteosome to be loaded on MHC I molecules in the ER. The MHC II pathway, which is restricted to professional APCs, processes exogenous antigens in the lysosomal system and loads them on MHC II molecules. The last type is the cross presentation pathway, which allows external antigens to be presented on MHC I molecules instead of MHC II. Although different DC subtypes can cross present, CD8+ DCs are generally considered the most efficient at cross presentation.

This mechanism is crucial in promoting cytotoxic T cell responses against tumour and viral antigens. In both cases, antigens are ingested, processed and presented on MHC I molecules to CD8 T cells [23, 28].

There are two variants of cross presentation that are currently proposed：the vesicular pathway and the cytosolic pathway.

1.1.4.1 Vesicular pathway

In the vesicular pathway, upon uptake of antigen, the phagosome that is formed after internalization was shown not to mature into a phagolysosome. In this proteasome independent pathway, the trimming of foreign antigen is accomplished by cathepsin S. In the study where OVA bound to biodegradable polymer polylactide polyglycolide (PLGA) microspheres were used, proteasome independence was confirmed using TAP knock-out mice for antigen presentation [29]. However, the mechanism by which MHC I and related apparatus such as calnexin reach the site of processing remains unclear. There are many proposals to explain the presence of these proteins that are from the ER in the early endo/phagosomal vesicles. One possibility in the case of vesicular cross presentation is the fusion of the early endo/phagosomal compartment with an ER derived vesicle. The early phagosomal compartment contained the MHC I molecule, calnexin and ERp57 which are important for loading of the peptide on the MHC I molecule [24, 30]. Calnexin and ERp57 act as chaperones for proper folding of MHC I molecules and along with calreticulin they ensure proper loading of peptide. The ER vesicles were reported to travel through the Golgi to the early phagosome using a soluble N-ethylmaleimide-sensitive factor attachment protein receptor (SNARE) known as sec22b [31]. SNAREs are vesicular addressins that help in fusion/fission of appropriate vesicles through attaching to specific partner SNAREs. Another proposed mechanism by which the MHC I

molecule and related proteins reach early endosomes is the contribution of the ER membrane towards formation of new phagosomes. This proposal, although interesting, was challenged by another study that failed to obtain similar results [31]. However neither of these proposals reported by different groups has been validated.

1.1.4.2 Cytosolic pathway

In the cytosolic pathway, the antigen is in the endo/phagosomal compartment upon uptake. The antigens are sent out to be degraded by cytosolic proteasomes. The cleaved peptides are transported into the ER or the endo/phagosome for loading [32]. The mechanism by which antigen from the compartment reaches the site of degradation and into the ER is controversial. It has been hypothesised that the Sec61 complex helps the protein exit the compartment [33]. Sec61 is part of the endoplasmic reticulum associated protein degradation (ERAD) complex that shuttles misfolded proteins from the ER to the proteasome. However this has been disputed based on the pore size of sec61 being too small [34]. Another study where a co-localization study was used concluded that TAP is involved in shuttling back the peptide for loading [35]. Viral and tumor antigens produced internally in affected host cells can also be cross presented through autophagy [36, 37]. Saveanu et al. identified insulin regulated aminopeptidase (IRAP) as a marker for the endosomal compartment involved in cross presentation [38]. The IRAP protease is related to an ER resident aminopeptidase that is known to trim peptides to assist in loading of MHC-I molecules. Ultimately the peptide is loaded on MHC I and sent to the plasma membrane.

Many aspects of cross presentation are under debate. Since MHC I molecules are unstable in the ER and TAP deficient animals express very low levels of MHC I, it is very difficult to dissect the precise role of either type of cross presentation [32]. The site of origin of MHC I is also under considerable debate due to these experimental constraints. While one report

points at a conserved cytoplasmic domain as imperative for cross presentation, thereby pointing to recycling MHC I as the source, others have identified lipid droplets carrying cargo or CD74, Rab3b/c being used as a SNARE needed for their trafficking of MHC I molecules from the ER[6, 32, 39]. Finally, the relative contribution of cytosolic and vesicular cross presentation to the adaptive response is not easy to determine *in vivo* or *in vitro* as no such effort has been attempted to address the difference. .

1.1.4.3 Receptor based enhancement of cross presentation

Receptor mediated endocytosis has been shown to enhance the efficiency of cross presentation by many groups. For instance, it has been reported that some antigens endocytosed through mannose receptor trigger better class I cross presentation [26]. In other cases, engagement of cell surface receptors, such as DNGR-1 and Dectin-1 promotes cross presentation [40-42]. Fc receptor based phagocytosis induces cross presentation as well [40]. It was recently demonstrated that soluble antigen internalized by the DEC 205 receptor, also a member of C-type lectin family, initiated a strong CD8 response [43]. However, the precise reason behind this phenomenon is poorly understood. In most cases, the receptors signal through some variants of an ITAM motif leading to a signal through Syk kinase [44]. An exception to this is the mannose receptor which is able to achieve the effect without an ITAM motif. Interestingly, mannose receptor mediated endocytosis involves F-actin, myosin and talin, factors related to the cytoskeleton [45].

1.1.4.4 Soluble antigen and non-receptor based cross presentation

In a previous report, soluble antigen coated on different sized beads was used to prove that size can be a critical factor when it comes to the format of antigen used in antigen presentation studies. 1µm beads coated with ovalbumin were shown to cross present efficiently [46].

Particulate bacterial antigens taken up by phagocytic means in another study showed better cross presentation as well. They also reported that cytosolic processing may not be essential in cross presentation which hinted at the involvement of the vesicular pathway instead [47]. Germain's group reported that in a subset of macrophages, adding solid structures enhanced soluble antigen presentation through the class I pathway [48]. They observed that solid particles of different sizes could help induce cross presentation with varied efficiencies. The bigger particles were said to be more efficient than smaller ones, which was supported by a more recent paper [49]. The mechanism behind these observations was not probed, but they hypothesised that the uptake of soluble antigen into phagosomes helped them to escape into the cytoplasm for processing through the proteasome leading to MHC I loading. Another study reported that soluble antigen could be cross presented, but required higher concentrations and that activators such as phorbol esters be given at the same time [50]. It is well-established that particulate antigen is consistently better cross presented than its soluble counterpart. In a study published in 2001, it was reported that cell associated antigen was cross presented with much higher efficiency than soluble antigen in an *in vivo* setting [28]. Thus the biggest deciding factor when it comes to antigen getting cross presented is the physical state of antigens involved [6].

1.1.4.5 Solid structures and antigen presentation

It was Polly Matzinger who proposed the danger hypothesis in the 1990s. In this proposal the APCs such as DCs could sense endogenous signals released under sterile conditions [51]. This gave rise the idea of danger associated molecular patterns (DAMPs). The first DAMPs identified were heat shock proteins followed by monosodium urate crystals [52]. Since then there have been many other DAMPs such as host double stranded DNA added to the list. Monosodium urate crystals have been shown to have an adjuvant effect for CD8+T cell responses [52]. These

crystals were shown to act in a receptor independent manner, with the plasma membrane lipids able to transduce a signal upon engagement [53]. The signal was mediated by Syk kinase and PI3 kinase in the cytosol leading to activation that included release of pro-inflammatory cytokines and expression of activation markers. The same group reported in another article that alum, the most commonly used human adjuvant, utilized a similar pathway to achieve its signaling [54]. Dunne's group reported in a recent article that basic calcium phosphate crystals that are associated with osteoarthritis induced the production of pro-inflammatory cytokines through the activation of Syk kinase and PI3 kinase [55]. In another article published in 2010, the authors reported that macrophages can sense physical properties of their target such as geometry and topography [56]. They used latex beads and other targets in their study. Therefore, it is likely that cross presentation involves the recognition of solid structures through Syk kinase, PI3kinase and a host of other machinery [57, 58].

Nonetheless, the literature available to date presents a dilemma of a unique kind. While phagocytosis seems essential for cross presentation in many cases, cytosolic processing appears dispensable. On one hand, receptors were shown to be crucial, but receptors by themselves cannot be used to explain the whole phenomenon needed during cross presentation [44]. What seems to be missing is a connecting piece between all the different fragments and a logical way to reconcile the observations made.

1.1.5 Dendritic cells

Among the three different APCs, DCs discovered by Nobel Laureate Ralph Steinman are generally accepted as being the most efficient in antigen presentation [4, 59, 60]. They can capture a variety of antigens and are able to process them in exogenous and cross presentation pathways efficiently. Compared to B cells and macrophages, the primary purpose of DCs appears to be antigen presentation. The presence of 'dendrites' or extensions may help them to better sample the environment. DCs in the gut have been shown to directly sample the lumen of the small intestine by forming transepithelial dendrites which extend across the capillary wall [61]. DCs have adapted their antigen presentation machinery to present even minute amounts of antigen for extended periods [43, 62]. DCs are known to have decreased proteolytic activity in the endocytic pathway, which can be attributed to presence of a lower level of proteases and a lesser activity of the enzymes [63]. Another way to regulate protease activity is through the NOX2 (NADPH oxidase) enzyme derived ROS (reactive oxygen species) in the endocytic system. Phagosomal protease action was altered by direct oxidation of protease active sites by the ROS generated [64, 65]. In contrast to another report ruling out pH involvement [65], alkalization of this vesicle was proposed to aid in cross presentation by preventing activation of lysosomal proteases, thereby making the antigen available to be sent to the cytoplasm [66].
In addition, DCs are known to constantly sample the environment and migrate to the draining lymph nodes upon encountering stimuli along with antigens to present them to naive T cells [9, 11, 26, 62, 67].

DCs can be divided broadly into three types: conventional or classical DCs (cDCs), plasmacytoid DCs (pDCs) and inflammatory DCs[68]. They are mainly originated from common DC precursors (CDP). cDCs and pDCs are derived from the CDPs, and in the case of cDCs, with

a blood borne intermediary pre-cDCs[69]. pDCs are a set of DCs found in circulation that are capable of detecting viral nucleic acids and release large quantities of type I interferon. Inflammatory DCs mainly arise from monocytic precursors and, as the name suggests, are only seen under inflammatory settings as monocytes migrate to the inflamed tissues and convert into DCs (also into macrophages). Thus different DCs arise from one of three different sources and the division appears to be based on final destination and function. *In vitro,* bone marrow derived DCs are generated from precursors using a combination of GM-CSF and IL4 for inflammatory DCs and FLT3 ligand for resident DCs [69]. A specific subset of DCs known as the $CD8^+$ DCs are generally accepted as the most efficient at cross presentation while the $CD8^-$ subset is more efficient at MHC II presentation [70, 71].

Most DCs under non-inflammatory steady state conditions are located in the non-lymphoid tissues with a small number in the spleen. Some tissues have a specific set of DCs localised only in that region and are not seen in any other part of the body. The skin for instance has Langerhans cells and dermal DCs located in different sectors of the skin layers [72]. The mucosa, including the lung, intestines and liver, have DCs that can be classified based on the expression of CD103 and CD11b levels [73]. Furthermore, there are other subsets of DCs such as CD4 DCs in the spleen whose functions are not completely understood[70]. In summary, with so much division of labor and specialisation it is clear that mapping out DC subsets and lineages is a laborious endeavor.

1.1.6 T cells

T cells are the central players of cellular immunity. They were first discovered in the 1960s when the modern concept of "immune system" was still new. Waldman and colleagues in the 1970s, revealed that they came from a group of precursor cells: thymocytes, based on their origin in the thymus [74]. Precursor lymphocytes enter the blood stream from the bone marrow and travel to the thymus for a process called "thymic selection". It is in this selection process that the body programs the difference between self and non-self into T cells through presentation of various self-antigens in the thymic dendritic and epithelial cells. Thymus is also the site where the TCRs are selected for their modest affinity for MHC, ensuring that upon arrival in the periphery, they operate in MHC restricted manner. This is achieved through positive selection where in T cells that can bind to peptide bound self MHC molecules with low affinity alone are given survival signals and the rest die via apoptosis. During selection, majority of these cells are deleted to prevent accidental auto immunity, a process known as negative selection. The TCR (T cell receptor) was discovered by teams led by Marrack, Mak and Davis [75-77]. The TCR has two transmembrane subunits, α and β that interact with the peptide bearing MHC molecule. These two highly variable subunits form a complex with the non-polymorphic CD3 units that help in signal transduction via various kinases. The interaction between a T cell and an APC occurs through a cluster of proteins. This interface between the two cells is called the immune synapse. It contains a central supramolecular part that includes the TCR, Zeta-chain-associated protein kinase 70 (ZAP70) and Phosphatidylinositide 3-kinase (PI 3-kinase) that are needed for signaling and a peripheral supramolecular complex with proteins such as integrins that help in adhesion. The immune synapse formation is accompanied by cytoskeletal modifications to assist in signal transduction. Upon strong binding between MHC and TCR, the ITAMs in the CD3 subunits

transduce a signal through ZAP70 [78]. The signal sent from ZAP70 branches into different cascades leading to the activation of nuclear factor kappa-light-chain-enhancer of activated B cells (NFkB) and nuclear factor of activated T-cells (NFAT). The signals from the co-stimulatory molecules, CD80/CD86, go through CD28 to enhance the TCR signals and complete activation along with cytokines to tune the response accordingly [79]. The inhibitory receptors CTLA4 and PD1 on the other hand, function to shut down TCR and associated signals by binding to the ligands of CD28 and PD1 ligand respectively with much higher affinity.

There are many T cell types based on phenotype and function. CD4 T cells are one of the major subsets and the most abundant in number. CD4 T cells in their naïve form traverse the lymphoid regions of the body, scanning for antigenic epitope loaded MHC II molecules on activated APCs. Once they encounter such a cell, they become activated and differentiate into CD4 helper T effector cells. Effector CD4 T cells are crucial for providing activation signals to B cells via cytokines and CD40/CD40L signaling to help determine which antibody subtypes will be generated. CD8 T cells on the other hand patrol the lymphoid areas, scanning for cognate MHC I molecules bearing antigenic peptides on APCs. Once activated the CD8 T cell differentiate into CTLs to perform their duties in cell-mediated immunity with a small subset becoming memory CD8 T cells.

1.2 Modulation of adaptive response

The adaptive response relies on multiple signals to kick start a robust immune response. These include antigen presentation, co-stimulatory signals and cytokines secreted by the APCs [80].

1.2.1 DC maturation

DCs constantly survey the local environment. An immature DC is highly endocytic and is capable of reacting to a variety of PAMPs and DAMPs. The combination of PAMPs, DAMPs and local inflammatory cytokines provides the maturation signals for the DCs. The maturing DCs move to lymph nodes where they prime their cognate T cells. In other cases even after they reach the lymph node, they anergize the T cells under tolerogenic conditions [81]. Tolerogenic conditions are created when a DC takes up antigen but does not receive accompanying maturation signals that drive complete maturation. Another feature for DC maturation is transient upregulation of co-stimulatory markers including CD86, CD80 and CD40 for T cell priming followed by their down regulation. At that time, DCs were presumed to have stopped endocytosis and sampling of the local environment [80]. However this notion has been questioned recently. For instance, there was an assumption that a mature DC stops endocytosis to ensure the T cell response generated is against the original antigen encountered [82]. A recent study showed that *in vivo* mature DCs retained their ability to endocytose a soluble antigen and even load MHC II and MHC I molecules with peptides efficiently. That report concluded that under inflammatory conditions, mature DCs may contribute to T cell priming against newly captured antigens instead of waiting for their immature counterparts to reach the site [82]. Another study revealed similar conclusions to show that mature DCs were still competent of endocytic uptake [83]. The authors of the second study questioned use of antigen presentation

models and the exaggerated concentration of tracers and antigens used in various manuscripts from drawing generalized conclusions. Moreover all the studies that gave rise to the current model of DC maturation were performed using specific DC subtypes in an *in vitro* setting. As we know now, there are many different DC types and models in an *in vivo* setting. Another possibility in antigen presentation *in vivo* is that mature DCs that migrate to lymph nodes can deliver the antigens to lymph node resident DCs for T cell priming [84].

1.2.2 PRRs

The second set of signals to upregulate co-stimulatory molecules comes from PRRs. Based on their cellular distribution, PRRs can be on the plasma membrane or intracellular. Membrane bound PRRs include the Toll like receptor (TLR) and C-type lectin receptor (CLR) families of receptors. The TLR family consists of 12 receptors found in mice and 10 receptors in humans. In mice, three TLR members TLR3, TLR7 and TLR9 are present inside endosomes for recognition of nucleic acids. The remaining TLRs present on the plasma membrane recognise a variety of PAMPs, including zymosan, LPS, lipoproteins, flagelin among others [85]. Almost all TLRs signal though Myeloid Differentiation primary response gene (88) (MyD88) or TIR-domain-containing adapter-inducing interferon-β (TRIF) adaptors to induce activation and production of cytokines. The CLR family consists of receptors that sense fungal PAMPs. Dectin-1, Dectin-2 and Mincle belong to this family [86]. Signalling pathways for these differ from TLRs in that these do not use MyD88 or TRIF for their signal modulation. Instead they connect an ITAM or a hemi-ITAM motif signal to a Syk kinase leading up to NFkB activation. The CLR family is a relatively new group of PRRs and their signaling networks are not completely worked out.

The diverse group of membrane bound PRRs are complemented by cytosolic PRRs which detect cytosolic bacteria and viruses. There are three groups of cytosolic PRRs known so

far, retinoic acid-inducible gene 1 (RIG-I) like receptors, DNA sensors and NLRs (NOD like receptors). RIG like receptors are cytosolic RNA helicases that get activated by RNA from double stranded or single stranded viruses. Upon detection, these receptors activate the NF-κB pathway and can also connect to the inflammasome cascade. DNA sensors like DAI (DNA-dependent activator of IFN-regulatory factors) can sense other forms of DNA and RNA from viruses to activate IFN-β [87].

The last group of cytosolic PRRs are the NLR group of receptors. They are a common set of sensors found in the cytosol and are characterised by a leucine-rich repeat (LRR) domain predicted to be responsible for the ligand binding and a variable N terminal domain for signal transduction. Even though no physical ligand binding has been discovered so far, the role of these sensors is assumed to be very critical [87]. NLRC1 (Nucleotide-binding oligomerization domain-containing protein 1 like receptor, NOD1) and NLRC2 (Nucleotide-binding oligomerization domain-containing protein 1 like receptor, NOD2), the Caspase activation and recruitment domains (CARD) domain containing receptors detect bacterial cell wall component called peptidoglycans. The signaling pathway for these receptors is not as clear as TLRs but they generally end in NF-κB activation and interferon gene transcription. The most famous member of the NLR family is the NACHT, LRR and PYD domains-containing protein 3 (NALP3) inflammasome which is part of NLRP group of PRRs. These receptors form a multimeric complex leading to caspase-1 activation, resulting in the processing and secretion of IL-1β and IL-18 [88]. The inflammasome field is currently an area under intense research. There are opposing schools of thought as to whether the inflammasome directly senses various stimuli like ATP or is the effect of sensing disturbance or pathogen in the locality [87].

1.2.3 The cytokine milieu

T cell activation occurs in the lymph nodes and spleen. One of the functions of these structures is to increase the probability for an encounter between an antigen bearing APC and a rare cognate T cell. Since T cell activation does not occur at the site of infection, a microenvironment is created in the secondary lymphoid areas to facilitate the T cell response [89]. When a pathogen is detected in the periphery, local innate cells and DCs are activated through the PRRs. If the activation signals are sufficiently strong, DCs undergo maturation and move through the afferent lymph vessels to the local lymph node for antigen presentation to T cells. The cytokine milieu of the microenvironment in the secondary lymphoid regions can have a profound influence on the differentiation of naïve CD4 T cells. For instance NK cells and eosinophils can secrete IL4 and create a bias towards a Th2 profile or NK T cells can secrete IFN-ɣ and direct a Th1 response. It is proposed that each species or group of microbes is identified by DCs and innate cells with a distinctive set of PRRs which helps in mounting a unique tailored immune response [89]. This, along with site specific elements imprinted by the priming DC, allows for a tightly controlled response. All TLRs are known to induce a Th1 response while a few of them can induce a Th17 response [90]. Similarly, Dectin-1 is known to induce a Th17 response and in some cases a Th1 response has also been reported [91]. NOD receptors are also known to induce Th17 and Th1 responses along with type 1 interferon [87, 92].

In real life situations, an individual PRR is never present alone. Microbes trigger multiple PRRs and multiple cell types simultaneously. Researchers are gradually looking into the aspect of cooperation between different families of PRRs such as TLR and CLR families [93]. Given the complications in creating models for performing the studies, opposite and often confusing results are common with use of generic TLR ligands such as LPS and CpG. Another interesting angle to

examine in T helper progression is whether there is flexibility in regards to differentiation into subsets. It would seem advantageous for the immune system to be able to further differentiate a T helper subset based on need to maximise protection and win the fight. There is a growing body of evidence to suggest that there is some plasticity in the differentiated subsets. For instance, a Treg can become a Th1 or a Th17 cell in the presence of IL-2 or IL-6 respectively [94].

1.3 Cytoskeleton and vesicular trafficking in antigen presentation

A different aspect of exogenous antigen presentation is how an APC handles soluble antigens in regards to intracellular cargo movement. Extracellular material is taken up through various methods and moved along microtubules where the vesicles tend to mature enroute.

1.3.1 Vesicular trafficking

Soluble and particulate materials enter the APCs through one of several endocytic and phagocytic mechanisms. Various modes of uptake include pinocytosis, macropinocytosis, receptor based endocytosis and phagocytosis through receptors such as Fc receptors [58]. With such a constant uptake of materials, DCs and other APCs have an efficient system of sorting the cargo. A typical mammalian cell is able to cycle the equivalent of 50% of the total surface area of the cell back to the cell surface every hour [95]. Macrophages take up material that is approximately 30% of their cell volume every hour. They quickly sort out the cargo to return more than two thirds of that volume back to the immediate environment in 15 minutes [95]. Upon formation, small endocytic vesicles first fuse to become early endosomes at locations close to the plasma membrane. Early endosomes are generally identified using markers Rab5 and transferrin receptor and are characterized by low electron density [96]. The early endosomal compartment where the cargo sorting occurs is about 400 nm in diameter and has a mildly acidic

pH. To maintain surface and volume equilibrium, the majority of the endocytic contents, as well as the lipid membrane are recycled back to the surface [59, 97]. Once the cargo is sorted, there is some level of proteolysis that occurs as the trans-golgi network continuously feeds the entire endocytic system with proteases. With a very small fraction of the cargo remaining after the sorting and recycling, the early endosomes mature to become late endosomes. Late endosomes are more acidic than early endosomes and are about 250-500 nm in diameter. They do not undergo recycling of their contents and are more electron dense than early endosomes. They have multiple inter luminal vesicles and have acid hydrolases within them. With more lysosomal contents coming into the compartment, late endosomes mature into lysosomes. Lysosomes have the highest electron density and acidity [98]. Lysosomes are identified using markers LAMP1 and LAMP2 [59]. From an antigen presentation view, antigens are processed and loaded onto MHC class II molecules in a yet to be clearly defined compartment which is said to have characters of lysosomes and late endosomes [21]. For cross presentation, early endosomes have been implicated as loading centers for MHC I molecules for cross presentation. The early endosomes are also the loading center for MHC I that undergo recycling [29]. The complexes are then displayed on the cell surface.

1.3.2 The cytoskeleton

Every eukaryotic cell has a filamentous web of proteins known as the cytoskeleton. The cytoskeleton performs multiple functions such as maintaining cell shape, rigidity, and helping in vesicle trafficking, cell adhesion and cell migration. The major components of the cytoskeleton are actin and microtubules [99]. Plasma membrane proximal actin and myosin are mainly involved in uptake of external cargo during phagocytosis and macropinocytosis. In both cases inward cups are formed and resolved from the membrane. Myosin, along with other proteins like

PI3kinase, enables the vesicle resolution from the membrane that occurs during phagocytosis, macropinocytosis and clathrin mediated uptake. Actin and myosin can help in short range movements before the vesicles enter the microtubule network for appropriate trafficking [100, 101].

Continuous reorganization of the microtubule network creates a spatially dynamic grid that facilitates long range movement of these vesicles in both directions. Soluble α and β tubulins found in the cytosol polymerise to become microtubule filaments of 25 nm in diameter. Single subunits of α and β tubulin proteins form a heterodimer which then can assemble into protofilaments. Protofilaments assemble together to give rise to microtubules that have various roles in the cell. The plus end of the microtubules, which is close to the plasma membrane, is called the fast-growing end while the minus end is called the slow-growing end as it is embedded deep in the microtubule-organizing center (MTOC) near the nucleus (Illustration 2). Microtubules exist in two forms in the cell: the stable form and the dynamic form. As expected the microtubule fibers inside and close to the MTOC are stable. Stable α-Tubulin is often acetylated while the fast-growing end has dynamic tubules with no acetylation [102]. There are two families of proteins that help in the movements in opposite directions, namely dyneins and kinesins. Dyneins drive the vesicles centripetally towards the minus end and the MTOC. Kinesins on the other hand migrate along the microtubule networks towards the plus end moving closer to the plasma membrane [59, 99]. Pulling by dyneins is also critical in separating cargo into recycling and lysosome-targeting components [103]. The MTOC undergoes reorganization when microtubule remodeling is required. The small GTPase Cdc42 of the Rho family of proteins is a well-known regulator of this reorganization [104] .

The molecular motors work with the SNARE family of proteins which specialize in membrane fusion to identify and target vesicles to either recycling back towards the PM or to lysosomes [105]. Strictly controlled assembly of microtubules allows polarized transport of proteins needed to form the immune synapse between an APC and a T cell. The critical role for the cytoskeleton in immunity is evident when immune synapse formation is lost when cytoskeletal rearrangement is hindered [106]. In addition recycling MHC I molecules form a substantial part of MHC I molecules being loaded with peptides in a cell. Thus inhibition of recycling associated proteins such as Arf6 can also abrogate MHC I-peptide complex from loading [107]. Arf6 is a protein that regulates cytoskeletal changes through the Ras pathway

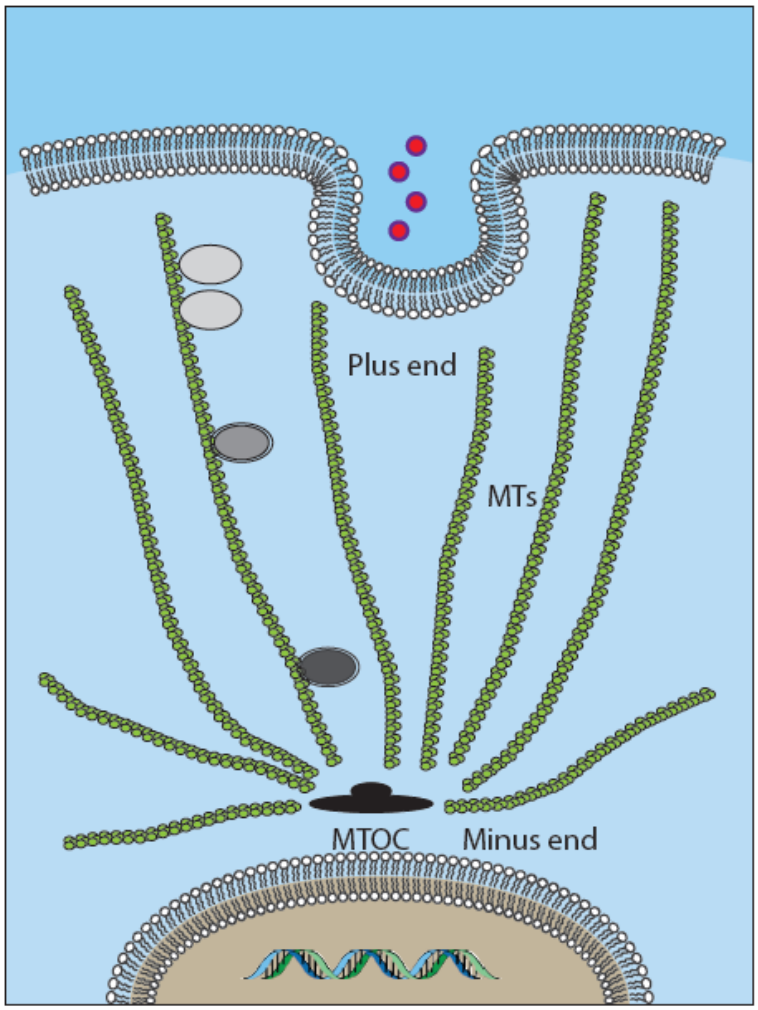

Illustration 2: Schematic of the microtubule system showing plus and minus ends.

The illustration shows a basic model of cytoskeletal dynamics. The incoming cargo is initially handled by the actin-myosin system and is later transferred to the microtubule system. The MTOC being the control center for the microtubulary system is seen near the nuclear region. While the region close to MTOC is the minus end where stable tubulin is generally found, the opposite end is the plus end where tubulin is actively rearranged.

Illustration made by Melanie Stenner.

1.4 T helper cells-Different outcomes

Ever since the Th1-Th2 paradigm was established, these cells have been under increasing scrutiny. Effector T helpers can be best characterised by the functionally distinct subsets. Table-1 shows a summary of CD4 effector T cell subsets along with associated transcription factors and cytokines.

1.4.1.1 Th1 response

Th1 cells were one of the first T helper cells to be described, producing the signature cytokine IFN-ɣ [108]. The most vital role of this group of cells is to promote cell mediated immunity whose hallmark is CTL activity. Despite being the signature cytokine, IFN-ɣ is not the critical factor in the induction of Th1 response, which is instead mainly attributed to IL-12 [109]. IL12 expression by DCs in addition initiates the transcription and translation of IL12 receptors in T cells needed to drive Th1 response. IFN-ɣ expressed in the local milieu by some cell types such as NK cells amplifies the expression of IL12 receptors in T cells thereby cementing the Th1 bias. Hence signals from cytokines IL-12, and later IFN-ɣ, solidifies and drive the expression of the transcription factor T-box transcription factor (T-bet) which is the master regulator of Th1 differentiation [89]. Other than promoting Th1 progression, these cytokines also inhibit Th2 development, which is the opposing subset in this case. The antibody isotype associated with the Th1 response in mice is IgG2a. These antibodies are potent activators of macrophages and can drive complement fixing along with antibody dependent cell killing. IFN-ɣ can induce macrophages to merge their intracellular contents with lysosomes, thereby killing any pathogen living inside vesicles [110]. Therefore, Th1 response is vital for protection against intracellular pathogens such as *Mycobacteria* and *Listeria.* IL-12, critical for Th1 response, is mainly secreted by DCs that have been stimulated by various PAMPs and is enhanced by CD40 signaling. As

noted before, TLR2, TLR4 and TLR7 are known to induce IL-12 in DCs [110]. CD8 T lymphocytes, another important effector of cell-mediated Th1 response, upon activation differentiate into mature CTLs and memory T cells[111]. The main function of CTLs is to kill infected or transformed cells directly. CTLs have an arsenal of components including granzymes and perforin that can induce apoptosis [112]. Uncontrolled activity by Th1 cells is also implicated in tissue damage and unwanted inflammation in inflammatory bowel disease and autoimmune conditions such as Diabetes mellitus [94, 110].

1.4.1.2 Th2 response

Th2 cells are the other subset that was originally discovered in the 1980s. They are defined by their ability to produce IL-4, IL-5, IL-10 and IL-13. Th2 cells are often synonymous with a humoral response and are important for the defense against extracellular pathogens. IL-4 is the most potent among the cytokines to induce Th2 phenotype through trans-acting T-cell-specific transcription factor (GATA-3) [89]. GATA-3considered the master regulator for Th2 cells, is a transcription factor that is sufficient and necessary for a strong Th2 response [94, 113]. Th2 cells are essential for the protection against nematodes and other pathogens. The typical antibody isotypes linked to Th2 response in mice are IgG1, IgA and IgE. IgA antibodies are secreted into the mucosal spaces where they prevent parasite attachment. On the other hand, IgE can activate mast cells and eosinophils that express high affinity receptors for IgE and release cytokines and other mediators upon cross linking. Eosinophils are capable of dealing with many parasites such as helminthes when activated. IL-4 secreted by Th2 cells inhibit Th1 progression similar to the action of IFN- ɣ against Th2. Exaggerated or aberrant activity by Th2 cells often leads to chronic conditions such as asthma and allergy [94].

1.4.1.3 Other T helper subtypes

Th17 cells, a newly discovered subset of T helper cells, have received a lot of attention in recent times. These cells secrete variants of IL-17 such as IL-17A, IL-17B and IL-22 when stimulated. TGF-β and IL-6 cooperate to promote Th17 induction [114]. Since Th17 cells are found in epithelial regions, barrier immunity seems to be their primary function. They are detected early during the immune response at sites of infection where they can effect additional neutrophil reinforcements and activation [89] . Th17 cells can also promote inflammatory and autoimmune diseases under certain conditions. A new subset similar to Th17 cells secreting only IL-22 but not IL-17 was discovered and named Th22 cells. A relatively new cell type reported to have functions in the skin, Th22 cell functions are relatively unknown [111]. Regulatory T cells are a subset of CD4 T cells that can originate in the thymus (natural Tregs) or be differentiated in the periphery (induced Tregs). Development of the induced Tregs is based on the presence of TGF-β. Unlike all the other T helper subsets, the main function of Tregs is to suppress the immune system and to induce tolerance. Foxp3 is the master regulator for Tregs. It is crucial in tapering off the immune response after pathogen clearance. Malfunction by Tregs can lead to several autoimmune pathologies [89, 111]. Other smaller subsets of T helpers include follicular helper T cells (Tfh) and Th9 cells. Tfh cells express IL-10 and IL-21 not expressed by any other T helper subset. Tfh cells play a role in the promotion of germinal center formation and help in B cell class switching [94, 111]. Th9 cells that produce IL-9 seem to have a role in airway hypersensitivity and anti-helminthes action [89]. This newly characterised subset is the newest addition to the Th group was discovered in 2010 [115]. As with Th22 cells, the understanding of the role of Th9 cells in the body is not complete.

Table 1: CD4 effector T cell subsets

Th subset	Transcription factor involved	Cytokines produced	Antibody associated in mice
Th1	T-bet	IFN- ɣ, IL-12	IgG2a
Th2	GATA-3	IL-4	IgG1, IgE, IgA
Th17	ROR-ɣ	IL-17, IL-22	
T regs	Foxp3	IL-10	

1.5 Rationale

In the case of particles taken up by phagocytosis, a consensus is that antigens are mostly localised in phagosomes. However this leads to a considerable debate about how they gain access to the class I pathway, which needs processing through proteasome in the cytosol or proteases in early endosomes [116]. For cell biologists, phagocytosis has been a fascinating complex and a well-organized event [58]. It triggers a long list of activation cascades, including ITAM containing receptors, Syk, PI3 kinases as well as the associated PKC and diacyl glycerol activities. Phagocytosis is known to extensively modify cytoskeletal structures, cellular morphology and influence organelle traffic [117, 118]. In previous work from our group, uric acid and alum crystals [53, 54] as well as latex beads drove phagocytosis in conjunction with cross presentation [52, 119]. Of all the reported forms of cross presentation such as cytosolic, receptor mediated and endosomal, a common factor is cell activation mediated by these receptor/membrane events. Among them, nearly all involve endo/phagocytosis. Superficially the biggest factor is the physical state of the antigens involved [120]. Identical antigen seen in its solid state is cross presented with several logs higher efficiency than its soluble counterpart [121]. Nonetheless, endocytic soluble antigens can be cross presented at a basal level although it is not very efficient [50]. Interestingly, receptors such as DEC205 and FcR that are reported to enhance cross presentation are involved in cellular uptake. The basic assumption to explain the receptor based cross presentation is that these receptors enhance antigen loading. Another possibility is that receptor based signaling targets endocytic antigens into a different compartment/pathway for cross presentation. In a recent article, Peter Creswell suggested that all the data available point to the idea that there is a general yet unidentified signaling requirement in cross presentation [44]. He went on to predict that multiple signals originating from different

pathways will ultimately determine fate of exogenous antigens that have been taken up by various ways [44].

The questions I would like to address in this thesis are the following:

- How long does it take for an antigen to be processed in MHC I and MHC II pathways for optimal loading of epitope and to be presented on the plasma membrane of the APC?
- Can we obtain a higher presentation of endocytic soluble antigens by providing a phagocytic signal simultaneously?
- What happens to the endocytic soluble antigens in this scenario of phagocytosis?
- Why does particulate antigen get presented well on MHC I and how does it compare with soluble antigens?
- How is vesicular trafficking and maturation affected during cross presentation of endocytosed antigens?
- What is the role of cytoskeleton during cross presentation of soluble antigens during phagocytic signaling?
- What are the *in vivo* implications of these questions? Does the phenomenon exist *in vivo*?

We hypothesise that soluble antigens entering with phagocytic stimuli are segregated and kept in early endosomes for processing and loading on MHC I molecules. Furthermore, this localisation and other associated events such as proteolysis are results of signals from the cell interacting with the phagocytic target at the plasma membrane. Cytoskeletal changes are an integral part of this process. We hypothesise that this phenomenon is biologically relevant *in vivo*.

Chapter Two: **Methods**

2.1 Mice and cells

C57BL/6, TAP-deficient, OT-II and OT-1 transgenic mice were purchased from Jackson Laboratories. Cathepsin S, L, B, CYBB and NCF-deficient mice were housed at University of Calgary Animal Research Centre[53, 54]. Cathepsin-deficient mice were kindly provided by Dr. Kenneth Rock of University of Massachusetts Medical School. CYBB and NCF-deficient mice were kind gifts from Dr. Robin Yates of University of Calgary. Myd88-TRIF double knockouts were kindly given by Dr. Paul Kubes of University of Calgary. All mouse experiments were approved by the Animal Protocol Committee at the University of Calgary. DC2.4, L cells (Cells that produce M-CSF) and FLT3L-transfected B16 cells (a kind gift from Dr. Glenn Dranoff of Harvard Medical School) were maintained with RPMI (Invitrogen) media containing 5% FBS.

All mice were genotyped maintained by Melanie Stenner.

2.2 Reagents

Ovalbumin (OVA), Cytochalasin B (5 µg/ml), Nocodazole (100ng) and Piceatannol (50 µM) were purchased from Sigma. Wortmannin (60 nM) was from A.G. Scientific. Nap sul lle trp Cho (10nM) and CA074Me (10µM) were purchased from Enzo lifesciences. Bestatin (10µM), Concanamycin A (100nM), Leupeptin (25µM), Pepstatin (1.5µM), Z phe leu COCHO (2.3nM), Dynasore (10µM), STLC (50µM) and MG132 (10µM) were obtained from Tocris. Cell Tak was purchased from BD. Monosodium urate, basic calcium phosphate crystals were made from materials purchased from Sigma as previously described[53, 54]. To obtain fine MSU, the crude crystal preparation was tumbled with 5 mm metal beads in a 50 ml conical tube for one week to produce crystals that were mainly between 0.5-1µm in length. 3 µm latex beads were

purchased from Polyscience Inc. OVA beads were made by passive coating of OVA on the beads by overnight incubation of OVA in borate buffer at 4^{o}C in a tube rotator. Complete Freund's adjuvant (CFA) and incomplete Freund's adjuvant (IFA) were obtained from Rockland. IL-2 ELISA ready-set-go kits were purchased from eBioscience. Alexa conjugates for OVA, Lysotracker and Alexa tagged Transferrin receptor were bought from Invitrogen.

2.3 Antibodies

Anti-mouse CD4 and anti-mouse LAMP1 antibodies were ordered from BD Pharmingen. Anti-mouse EEA1 and Rab5 antibodies, anti-clathrin, alpha tubulin and acetylated alpha tubulin were purchased from Cell Signaling Technologies. Anti-mouse antibodies for CD8, CD40, CD45.1, CD69, CD80, CD86, CD90.1, MHC I (H2Db), MHC II (Ia/Ie), 25D1.16, IL-4 and IFNγ were purchased from eBioscience Inc. Secondary antibodies Alexa- 488, -594, -633, Alexa-647 conjugated cholera toxin B subunit and Prolong® Gold Antifade with DAPI were bought from Molecular Probes (Invitrogen). Anti-rabbit Dylight 549 tagged secondary antibodies were ordered from Jackson Immunoresearch. Anti-chicken OVA antibodies were bought from Sigma.

2.4 Atomic Force Microscopy

DC2.4 cells were grown on cover slips previously washed with ethanol and distilled water. Soluble OVA (100 µg/ml) or particulate OVA (3 µm OVA beads) were added for different times of incubation. At the end of the incubation period, the glass disks were washed twice with PBS to remove any unbound antigens or particles. The Cell-hesion module of the JPK Nano-wizard AFM was used in all experiments. Cell binding experiments require the AFM module that permits the cantilever separation distance to 100µm. This was critical to achieve complete separation between interacting cells. Glass disk with DC2.4 cells was loaded onto the

microscope stage, followed by a few microlitres of the T cell suspension. The incubator chamber in which the machine is housed maintained a temperature of 37ºC with 5% CO_2. The stage was left in the machine chamber for a few minutes to allow the T cells to settle. A blank cantilever was mounted to a clean glass block that was provided with the machine and the peizo unit was placed on top the glass disk with the cells. A healthy looking T cell was glued on to the cantilever by motors that lowered the unit in small increments of 1-2 µm. The selection was based on the target cell with proper shape and absent of any apoptotic blobs. After calibration in a clear area, the T cell was positioned above a separate DC2.4 cell and the force measurement was started by repeated close contact of the two cells followed by their separation. The force of interaction was measured between a T cell and a DC using the AFM. The two cells coming into contact were given 15 seconds to interact. The cantilever was then moved upwards by 45 µm (Z length) each time to ensure complete separation of the interacting cells. A minimum of 14 force curves were collected for further analysis in all experiments. The force curves were processed using the JPK Image Processing software according to the manufacturer's instructions. Force curves were analyzed for their maximum binding force. The average force was calculated by taking a simple mean of all force curves for the given condition. A minimum of 3 repeats were performed in every condition. The same procedure was repeated in the case of inhibitors or MSU crystals where the stimuli was added with the antigen simultaneously.

This assay was done by Aswin Hari with assistance from Enaam Alghamdi.

2.5 Bone marrow cultures

Bone marrow obtained from mice were grown in RPMI media with 10% FBS supplemented with IL-4 (3ng/ml) and GM-CSF (3ng/ml) (Biosource and Gibco Inc, Invitrogen) to obtain bone marrow dendritic cells (BMDCs) [122]. To obtain FLT3L BMDCs, the bone marrows were grown using 15% FLT3L transfected B16 cell preconditioned culture media. Bone marrow macrophages were obtained by growing bone marrow in 15% L cell conditioned media. In all cases, on day 6 of cell culturing, the cells were gently washed and replaced with warm RPMI media with 10% FBS before use.

2.6 Flow cytometry

For the OVA uptake experiments, DCs were incubated for 2 hours with and without MSU crystals along with Alexa 488-conjugated OVA or Alexa OVA coated latex beads. The cells were scrapped from the wells, washed with PBS and fixed using 2% PFA to be read using an Attune® Acoustic Focusing Flow Cytometer. Apoptotic assays were performed using apoptotic detection kits based on the manufacturer's instructions (eBioscience). For epitope detection, DCs were fed with OVA in the presence or absence of MSU crystals and fixed after overnight incubation. Biotin tagged anti-mouse OVA257-264 (SIINFEKL) peptide bound to the MHC I molecule restricted to H-2Kb (25-D1.16) antibody from eBioscience was used in the assay. All analyses were done using Treestar Flowjo 10.0.

Aswin Hari performed the apoptotic assays. Melanie Stenner performed OVA uptake and 25D1 stains with assistance from Aswin Hari.

2.7 Antigen presentation assays

Antigen (soluble or 3 μm OVA beads) was added with or without phagocytic stimuli to BMDCs grown in 24-well plates. After 4 hours, cells were given fresh media. 2 million OT-1 or OT-II cells were allowed to interact with the BMDCs. After 18-24 hours, the cells were collected and stained for CD8/CD4 and CD69. The supernatant was collected at the same time and used to measure IL-2 levels. In the case of inhibitors, they were added at same time as the antigen/phagocytic stimuli. A similar protocol was followed for all gene deficient BMDCs, macrophages, FLT3 DCs and DC2.4 cells.

Aswin Hari developed and standardized the assays. The CD69 assays were performed by Aswin Hari. The IL2 ELISAs were done by Raymond Lam or Melanie Stenner.

2.8 Electron microscopy

For TEM analyses, the cultured cells were processed in situ for fixation, dehydration, infiltration and embedding in a culture dish. The cells were prefixed with 1.6 % paraformaldehyde and 2.5 % glutaraldehyde in 0.1 M cacodylate buffer, pH 7.3 for 1 hour and post fixed with cacodylate buffered 1% osmium tetroxide for 1 hour at room temperature. Cells were then dehydrated through graded ethanol and embedded in an Epon mixture. After polymerizing, the hardened Epon layer containing the embedded cells was separated from the plastic culture dish. Under a light microscope a representative area was selected, trimmed and glued to a resin stub for sectioning. Ultra-thin sections were cut with a diamond knife on an ultramicrotome (Ultracut E, Reichert-Jung, Vienna, Austria) and collected on single hole grids with Formvar supporting film. The sections were stained with aqueous uranyl acetate and Reynolds's lead citrate and observed under a Hitachi H7650 TEM at 80 kV. Images were

acquired with an AMT16000 digital camera mounted on the microscope. Unilamellar vesicles lacking electron dense contents and 300-500 nm diameter were visually counted and quantified using Graphpad Prism 6.0. For SEM, dried crystals were laid on prefabricated standard aluminum stubs with carbon tape. The samples were coated with gold (Techniques Hummer II, Anatech). The samples were then inspected under a Scanning Electron Microscope (ESEM–XL30, FEI).

All TEM sample processing and imaging was done by Wei Dong. Aswin Hari prepared the cells and did the post-acquisition analysis. SEM was done by Aswin Hari with assistance from Dr. Michael Schoel.

2.9 Electron Tomography

Thick sections (~250 nm) were cut and stained with 2 % aqueous uranyl acetate and Reynold's lead citrate. They were then placed on one side of a TEM Slot Grid (1 x 2 mm slot) that was covered with a ~40 nm thin continuous formvar film (EMS, Hatfield, Pennsylvania) and left to dry for several minutes. Colloidal gold particles (10 nm diameter) were placed on the both sides of the grid to serve as fiducial markers. Finally, a thin carbon coating was applied to both sides of the grid for mechanical stabilization and to reduce electric charging in the microscope. The images were captured on a Gatan UltraScan 4000 CCD (Gatan, Pleasanton, California, USA) at 2048x2048 pixels. Dual axis TEM tomography was carried out by taking one image every degree for a range between 120 and 130 degrees with the program Serial EM. The tomographic reconstruction was done by weighted back-projection with the IMOD software package, resulting in a tomographic dataset of approximately 4 nm resolution[123, 124]. The same software was used for visualization and analysis (3D rendering of endosome positions) by

manually tracing them on every tomographic section through the dataset. Videos were generated from tiff images using Virtualdub software.

Tobias Furstenhaupt performed all electron tomography imaging and reconstruction. Wei Dong processed the samples for the assay. Aswin Hari performed post-acquisition analysis.

2.10 Proteolysis and pH assays

These assays were performed as previously described [65, 125]. IgG- conjugated experimental particles used to evaluate phagosomal pH and proteolysis were prepared as previously described[126]. To measure endocytic proteolysis, DQ OVA (Molecular Probes) was used as the substrate. Relative fluorescent units (RFUs) were obtained from the equation: $RFU = \frac{SFRT}{CF}$ where SFRT is substrate fluorescence in real time, while CF represents average calibration fluorescence and was represented relative to time expressed in minutes. Hydrolytic capacities were evaluated by plotting the slopes (as described by the equation $y = mx + c$, where y=RFU, m=slope and x=time) of the linear portion of the relative substrate fluorescence against time, and were calculated relative to an internal control fluor added simultaneously. Experimental groups were plotted and compared by one-way Analysis of Variance (ANOVA) with Sidak's multiple comparisons test.

For measurements of phagosomal pH, fatty acid-free bovine serum albumin (BSA) (Calbiochem) and human IgG (Sigma) were covalently coupled to 3 μm carboxylated silica experimental particles (Kisker Biotech), followed by fluorescent labelling with CFSE (Molecular Probes) as previously described [126]. Quenched and washed experimental particles were added to DC monolayers at a ratio of 1–2 particles per cell prior to fluorescent measurement. Fluorescence emission at 520nm was measured using FluorStar Optima plate reader (BMG

Technologies) every 60 seconds with two alternating excitation wavelengths of 450 and 485 nm. Phagosomal pH was determined using the calculated excitation ratio between the pH-insensitive excitation at 450 nm and the pH-sensitive excitation at 485 nm. Conversion of excitation ratios to phagosomal pH was achieved through third-order polynomial regression to a standard curve generated using excitation ratios of beads in buffers of known pH. Excitation values generated in this way were equivalent to those generated using particle-containing BMDCs in standard buffers containing ionophore nigericin (10 ng/ml).

These assays were done by Aswin Hari with technical help from Dale Balce and Joanna Rybicka of the Yates lab.

2.11 Immunostaining

The Delta vision microscope (a wide field microscope with deconvolution capacity) was used to study Lysotracker- transferring interaction and for epitope bound MHC I stain. LAMP1 and Rab5 imaging was done on a Leica SP5 confocal microscope to measure colocalization between the two. The Elyra super resolution microscope was used for microtubule and actin imaging.

2.11.1 Lysotracker-Transferrin

DCs were plated at ~60% confluency on sterile cover slips and grown overnight. 1 µl/ml of Alexa 594- tagged Transferrin receptor and 1 µl/ml of LysoTracker® Green DND-26 from the original factory packaging were added to cells in the presence and absence of crystals. After 1 hour of incubation, the cells were washed twice with PBS. The cells were fixed in 2% PFA in PBS for 20 minutes and mounted with DAPI in the media. All imaging was done on a Delta Vision microscope, followed by deconvolution of the images with the following setup: Objective

60X, NA-1.4, pixel size-110nm, Z stack distance- 0.2 µm, image resolution- 1024*1024. Image J was used for the correlation of Lysotracker and Transferrin. More than 50% overlap was documented as a positive correlation.

Anutosh Ganguly performed image acquisition and analysis with assistance from Aswin Hari.

2.11.2 Microtubule and actin stain

For microtubule staining, cells grown to 50–70% confluence were incubated with and without MSU crystals for 1 hour, rinsed in PBS, and fixed in methanol at −20°C for 20 minutes. Fixed cells were washed in PBS, incubated with α-Tubulin antibody (DM1A) for 1 hour at 37°C, then washed again in PBS and incubated with goat anti-mouse IgG that included 1 µg/ml DAPI. For microtubule and actin staining, cells were fixed in 2% PFA for 15 minutes and then permeabilized with 0.5% Triton® x-100 (10 minutes) and washed with 0.1% Triton® x-100. Cells were also counterstained with goat antimouse IgG that included DAPI and rhodamine labeled phalloidin (Invitrogen). For clathrin staining, DC2.4 cells with or without treatment of MSU (100 µg/ml) for 2 hours were fixed with 4% PFA for 20 minutes. 10% FBS containing 0.1% saponin was used as a blocking buffer. After incubation with Anti-clathrin antibody, Alexa 488-conjugated secondary antibody was used for visualization. The cover slips were mounted on Prolong® Gold mounting media and incubated overnight. The clathrin images were acquired by Nikon's Structured Illumination Microscopy (N-SIM) Super-Resolution Microscope Systems. All other SIM imaging was carried out on the ELYRA Superresolution Microscope from Zeiss with the following parameters: Objective 63X with 1.6 magnification, NA-1.4, pixel size-70nm, Z stack distance- 0.1 µm, image resolution- 2048*2048. The grid size was used in the default

setting recommended by the vendor and the number of rotations was three. For calculation and movie conversion, all raw images were incorporated in image J with LOCI bio-format importer plugin. All movies were 5 FPS. The crystals in in 3D projections were manually grafted. Ortho slices were made using the ortho slice function in ImageJ.

Sample preparation was standardized by Anutosh Ganguly and Aswin Hari with input from Shevaun Davis. Shevaun Davis performed all the SIM image acquisition. Aswin Hari and Anutosh Ganguly performed the post-acquisition analysis. Clathrin imaging was done by Libing Mu with assistance from the core facility in Tshingua University.

2.11.3 Endo-lysosomal measurement

To determine the overlapping of endosomal cargo with vesicular maturation markers, OVA was given to DC2.4 cells with or without MSU crystals simultaneously. After 2 hours, the cells were washed with PBS and fixed with 3.5% PFA for 10 minutes. The cells were permeabilized using a buffer containing PBS, 0.2% Tween® 20 and 0.5% saponin. After 2 washes, anti-OVA antibody and either LAMP1 or Rab5 antibody were added to the cells and incubated for 1 hour. After washing twice appropriate secondary antibodies were added and incubated for 45 minutes. Consequently samples were mounted on glass slides using Prolong® Gold antifade agent and left to dry overnight. The samples were imaged under a Leica SP5 confocal microscope (objective 63X, NA-1.4, pixel size-70nm, Z stack distance- 0.2 µm, image resolution- 512*512). The data was analyzed using Volocity image analysis software to quantify colocalization between the fluorescent signals. A Pearson's correlation was gathered from the analysis of each image to determine the colocalization of OVA and Rab 5 or LAMP 1 for each

data set. The Pearson's correlation was averaged over each data set. The figure generated was one of at least 3 independent images acquired under each condition.

Aswin Hari developed and standardized the protocol. Fay Munro performed the image acquisition and analysis.

2.11.4 Stain for epitope bound MHC I

For epitope bound MHC I antibody staining, DC2.4 cells were incubated with 5 mg/ml OVA overnight. The cells were washed and treated with Transferrin receptor in the presence or absence of MSU crystals for 1 hour. The cells were washed twice with PBS and fixed using 2% PFA for 15 minutes, then permeabilized with 0.5% Triton® X-100 (10 minutes). APC tagged Anti-Mouse OVA257-264 (SIINFEKL) peptide bound to H-2Kb (25-D1.16) antibody from eBioscience was added and incubated for 1 hour. The cover slips were washed and mounted with Prolong® Gold antifade agent and visualized under the Delta Vision microscope (objective 60X, NA-1.4, pixel size-110nm, Z stack distance- 0.2 µm, image resolution- 1024*1024).

This experiment was done by Anutosh Ganguly with assistance from Aswin Hari and Melanie Stenner.

2.12 Total Internal Reflection Fluorescence Microscope (TIRFM)

To check the mobility of the endosomes aligning against the plasma membrane, single molecule imaging experiment by TIRFM was performed as previously described[127]. All images were acquired at 37°C on a heating stage. The acquisition was controlled by Metamorph

(Molecular Devices, Sunnyvale, CA) and the exposure time was 100 ms for a 512 x 512 pixels image. The acquired images were analyzed and processed with Imaris 7.2.3. The DC2.4 cells in the chamber were treated with 20 µg/ml Alexa 488-conjugated ovalbumin for 3 hours. Then 100 µg/ml MSU was added and thoroughly mixed. After another 1 hour incubation, the ovalbumin was removed and the TIRF images were acquired immediately after washing.

Libing Mu performed TIRF image acquisition with assistance from Chenguang Xu.

2.13 *In vivo* assays

200 µg OVA with or without 1 mg MSU crystals was injected subcutaneously in footpads and thighs of C57BL/6 and Cathepsin S-/- mice. BL6 control mice were injected with CFA admixed with 200 µg OVA. After 24 hours, isolated T cells from OT-1 and OT-II T mice (using kits from Stemcell Technologies.) labeled with CFSE (Invitrogen) were injected intravenously. Local draining lymph nodes and the spleen were collected on day 6 and analyzed for CFSE proliferation. The populations were selected based on congenic markers (C57BL/6: CD45.2, OT-1-: CD90.1, and OT-II: CD45.1). The data was collected on a BD LSR-II flow cytometer and analyzed with Flowjo 10.0. Intra-cellular staining was done with a similar protocol: the mice were injected with 200 µg OVA with or without 1 mg MSU crystals subcutaneously in footpads and thighs. After 24 hours, isolated CD4 cells from OT-II mice were injected intravenously. The mice were boosted with the same regimen 1 week after initial injections. At the end of two weeks from first injections, the spleen and draining lymph nodes were collected and CD4 cells were isolated. The isolated CD4 T cells were restimulated by BMDCs for 24 hours in presence of brefeldin A for the last 20 hours of incubation. The cells

were processed with permeabilization buffer and IC fixation buffer from eBioscience according to manufacturer's instructions. The cells were then stained with CD4, CD45.1, IL-4 and IFNγ and read with BD LSR II.

Antibody induction was performed as previously described[54]. 200 µg OVA, with or without 1 mg MSU crystals, was injected subcutaneously in footpads and thighs of C57BL/6 mice. The mice were boosted after 2 weeks with the same regimen, except incomplete Freund's adjuvant was used instead. Two weeks after the final immunization, sera was collected and OVA specific antibody titers were determined using ELISA. IgG1 titers were analyzed as described[54], IgG2a titers were measured using a kit from Alpha Diagnostics International.

For the Balb/c-gp120 assay, the antigen preparation was performed as previously described [52]. 100 µl of 4% polystyrene beads (1 µm) (Polysciences Inc.) were washed and resuspended in 0.1 N boric acid buffer (pH 7.2). The beads and 200 µg of gp120 were mixed in 1 ml of boric acid buffer and rocked overnight at 4^{o}C. 100 µl of the total suspension was injected subcutaneously into each Balb/c mouse. Balb/c BMDCs were prepared in 12-well plates. On day 6, these DCs were treated with 20 µg/ml gp120 in the presence or absence of 100 µg/ml MSU. The immunized mice were sacrificed (after 10 days) and 5 million splenocytes were restimulated in each well of Balb/c BMDCs culture. Staining for CD4 and CD8 markers was done by FACS.

The CFSE assay was done by Aswin Hari with assistance from Ailian Yang in injecting cells. Intra cellular staining was standardized and performed by Aswin Hari. Yei Ping at the FACS facility performed FACS data acquisition, with assistance from Laurie Kennedy. Aswin Hari performed the injections for the antibody experiment. Melanie Stenner performed the ELISAs for antibody titers.

2.14 Statistical Analyses

All statistical analyses were done using Graphpad Prism 6.0. A one way ANOVA was done to compare all data sets when there were more than 3 sets. Sidak's multiple comparisons test was done as a post test on select columns. In cases where there are only 2 sets of data, student T test was used. Legend for abbreviations: P value legend * <0.05, ** <0.01, *** <0.001 and **** <0.0001. SEM- standard error of the mean.

All statistical analyses was done by Aswin Hari.

Chapter Three: **Results**

3.1 Design a system to investigate the time needed for optimal epitope appearance on the surface of an APC by measuring cell-cell interaction.

Since the early 1980s, researchers studying antigen presentation and T cell activation have used IL-2 levels and activation marker expression, among others, to measure effector T cell function [128, 129]. They were trying to understand T cell signaling and priming by measuring events occuring 24-48 hours after initial stimulation. Although the data was usable, the period of incubation with the antigen was always set in an arbitrary fashion. Sometimes antigens were left with the APCs all through the incubation period with the T cell. Thus there was never a time when the actual epitope appearance was measured in a time dependent manner. During the interaction between a DC and a T cell (Figure 3.1-1), binding is mostly transient in the absence of an appropriate epitope bearing MHC. This interaction becomes stabilized if the T cell is cognate to the epitope being presented. From the time of its invention, the Atomic Force Microscope (AFM) has been used in a variety of applications in imaging and force spectroscopy modes [130]. The technique is unique with real-time measurements of living cells and forces detected are as low as a few Pico-Newtons (10^{-12}). Our lab tried to measure the time needed for antigen processing and optimal epitope appearance for both MHC I and II molecules, to set the period of incubation and removal of excess antigen for T cell activation assays. For this we used the AFM in SCFS (Single Cell Force Spectroscopy) (Illustration 3 A) mode to study the speed of OVA class I and class II epitope appearances on the DC surface [131-133]. During a typical AFM experiment in this mode, a DC adhering to a glass disk is allowed to interact with a T cell that is glued to a cantilever. When a DC is allowed to bind with a T cell for few seconds and

separated, the force needed for separation is measured as the maximum binding force. Illustration 3 B shows a typical force curve generated along with different stages in adhesion. A minimum of 14 consecutive such force curves are collected and the average of maximum binding force is plotted in the data panels. From this assay, we concluded that soluble OVA needed a minimum of two hours of processing for a MHC class II epitope to reach sufficient density for CD4 T cell activation while presentation of bead bound OVA for class I antigen presentation (Figure 3.1-2 and 3.1-3) requires 4 hours. Piceatannol inhibits Syk kinase while cytochalasin B and wortmannin inhibit actin remodelling and PI3 kinase respectively. They can potentially influence the antigen processing and these inhibitors have been used in our laboratory previously [53, 54]. We noticed that DCs fed with soluble OVA antigen showed enhanced binding force with OT-II T cells if Syk, a factor generally believed to be irrelevant in class II antigen processing, was inhibited (Figure 3.1-4). This observation, even though not statistically significant, is potentially biologically relevant as it raises the possibility that phagocytic signalling may be involved in this scenario. While inhibiting actin or PI3 kinase yielded results on predicted outcomes, given their involvement in cytoskeletal remodeling and membrane resolution, the effect of inhibition of Syk kinase was not foreseen (Figure 3.1-4). This seemed to suggest that the class II antigen processing was affected by a component of phagocytosis. We sought to study the reverse: would antigen entering endocytic/class II pathway be driven into the class I cross presentation if signaling events associated with particulate antigen uptake/phagocytosis were triggered? To trigger phagocytic processes we used monosodium urate (MSU) crystals which are known to activate Syk kinase dependent signals [53]. DC2.4 cells were incubated with soluble OVA in the presence/absence of MSU crystals. We observed that the binding between DC and OT-1 T cells increased following the treatment (Figure 3.1-5).

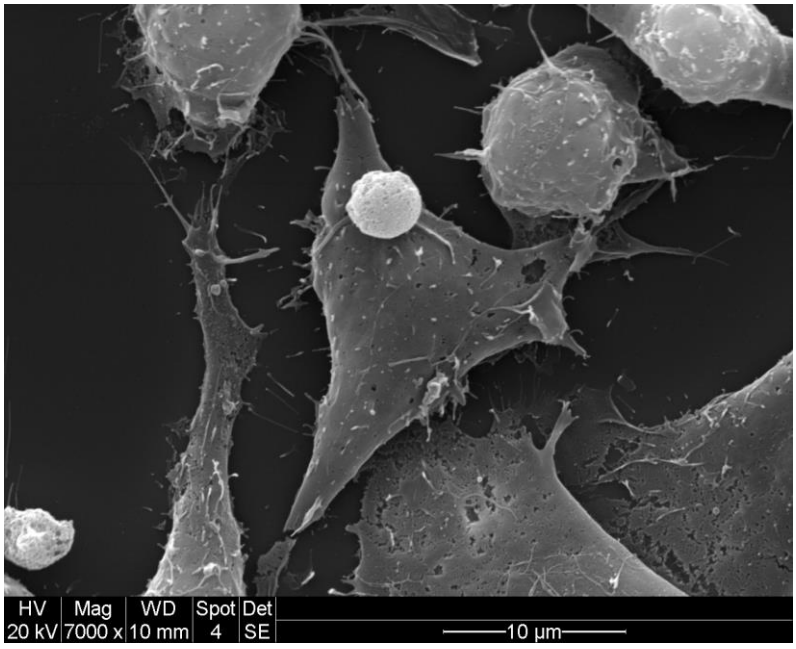

Figure 3.1-1: Scanning electron microscope image of a DC interacting with a T cell.

DCs plated on coverslips were allowed to interact with T cells for an hour. Following fixation using gluteraldehyde and dehydration with ethanol gradient, the samples were coated with colloid gold and inspected under SEM.

Images were acquired by Aswin Hari with assistance from Michael Schoel.

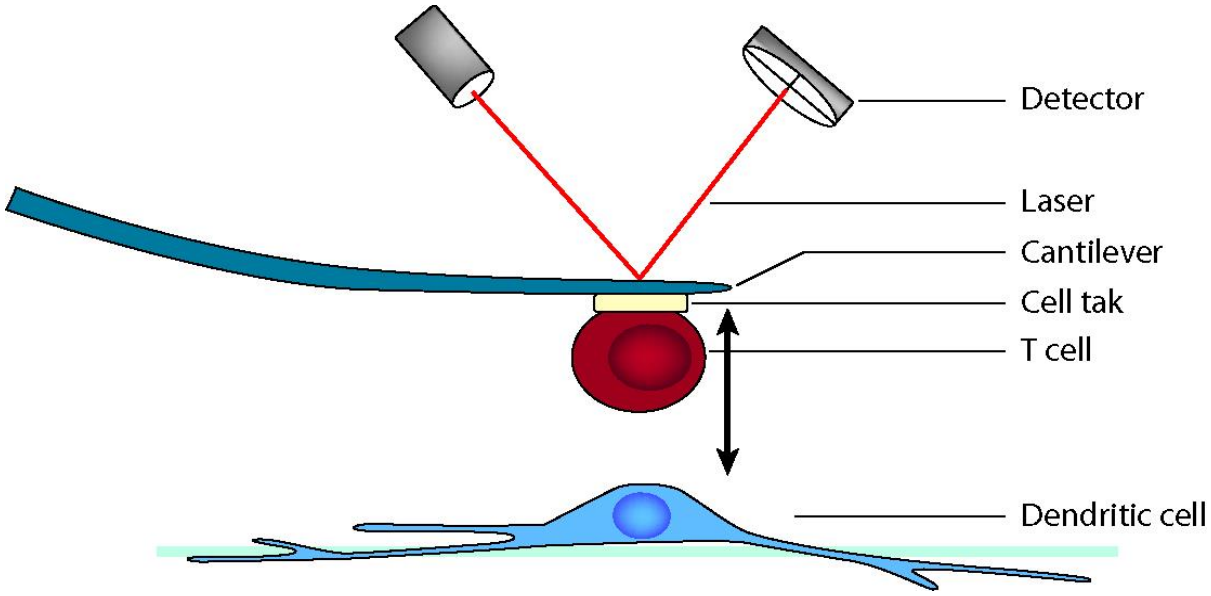

Illustration 3 A: A model of the cell-cell binding assay conducted using the AFM.

The 2-way arrow denotes the upward and downward motion of the cantilever that allows measurement of the maximum force needed to separate the interacting cells.

Illustration was made by Jennifer Tran.

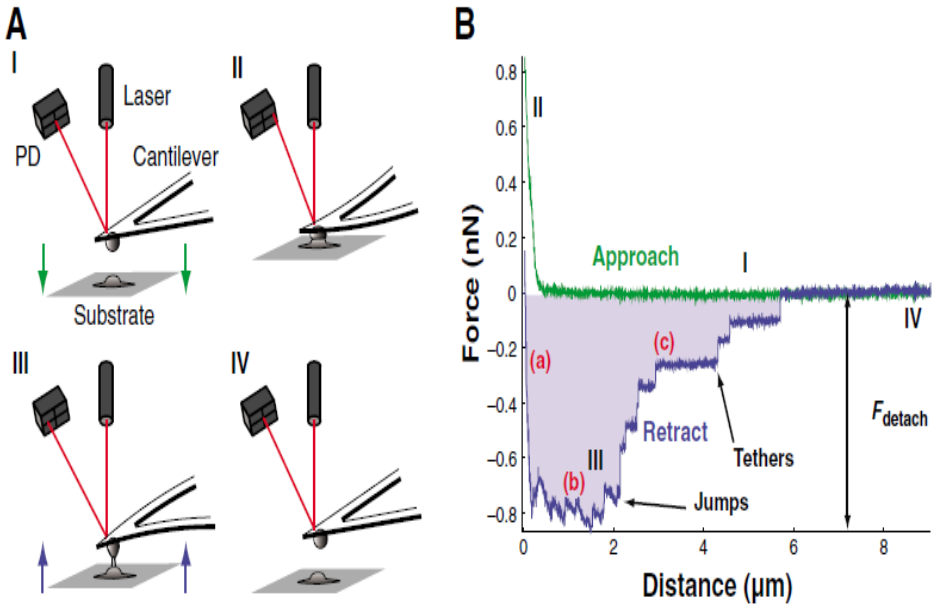

Illustration 3 B: A model of the cell-cell binding assay conducted using the AFM and a representative force curve showing various stages in adhesion.

The force curve on the right is a typical data point obtained from a measurement from the AFM in SCFS mode [134]. The green approach curve correlates with the 1st panel on the left showing the cantilever's movement towards the substrate. The blue curve is the retraction curve that is generated when the cantilever pulls away from the substrate it is bound to. The jumps in the curve occur when the cells are still in contact fully, as shown in 2nd panel on the left. The tethers are seen when the 2 cells try to stretch when separating from each other, as shown in the 3rd panel. The last stage is when the cells detach completely whereby the maximum force needed for detachment can be measured.

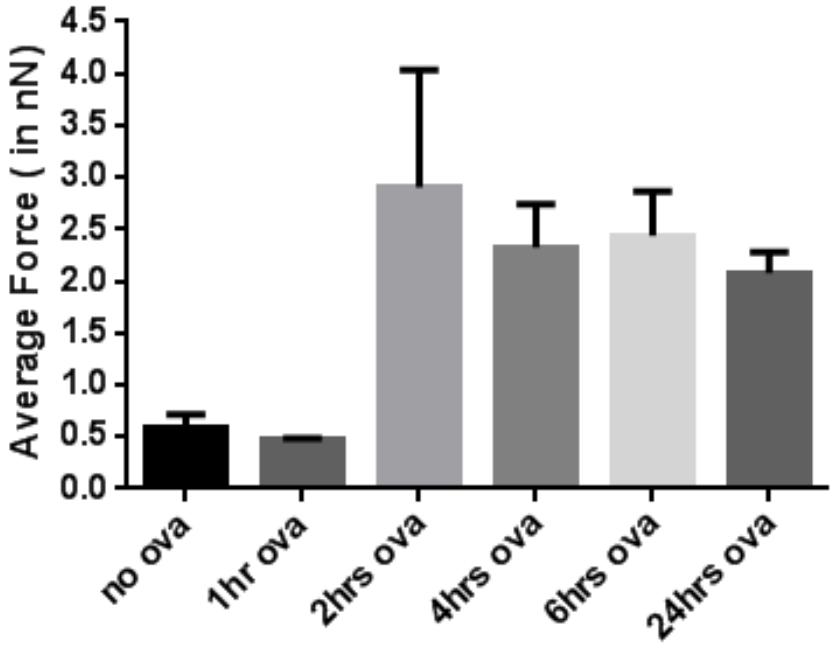

Figure 3.1-2: Average of maximum binding force between DCs fed with soluble OVA and OT-II T cells.

The force of interaction between OT-II T cell sand DC 2.4 cells fed with soluble OVA was measured.

Panel represents the average of minimum three independent experiments with SEM.

A one way ANOVA was done followed by post hoc test (Sidak's multiplicity test) to compare the selected columns.

P value: No ova vs. 2hr ova- ***, No ova vs. 4hr ova-**, No ova vs. 6hr ova-**.

This assay was performed by Aswin Hari.

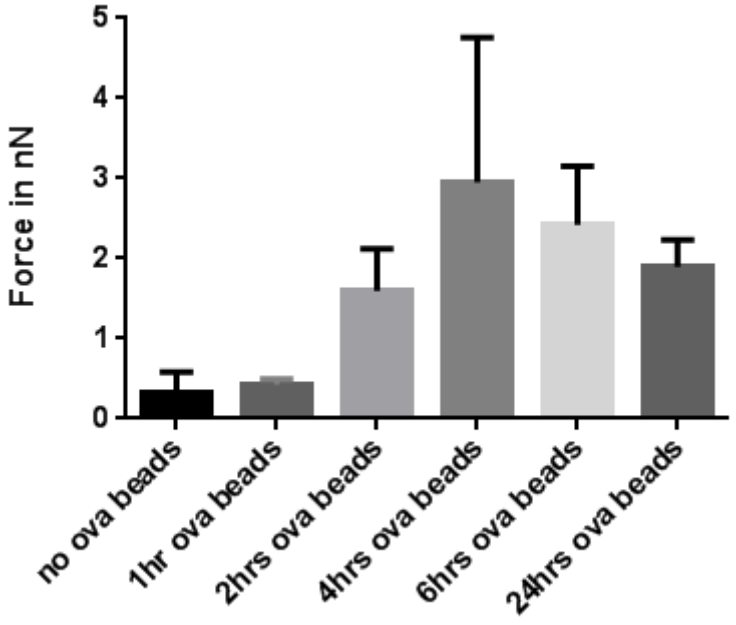

Figure 3.1-3: Average of maximum binding force between OVA bead fed DCs cells and OT-1 T cells.

The force of interaction between OT-I T cells and DC 2.4 cells fed with bead bound OVA was measured.

Panel represents the average of minimum three independent experiments with SEM.

A one way ANOVA was done followed by post hoc test (Sidak's multiplicity test) to compare the selected columns.

P value: No ova vs. 2hr ova- N.S., No ova vs. 4hr ova-*, No ova vs. 6hr ova-*.

This assay was performed by Aswin Hari.

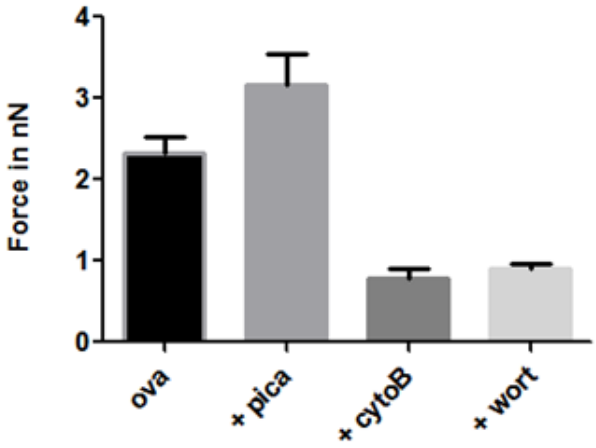

Figure 3.1-4: Force of interaction between OT-II T cell and DCs in the presence of soluble OVA with the additional indicated inhibitors.

The force of interaction between OT-II T cells and DC 2.4 cells fed with soluble OVA was measured in the presence or absence of the listed inhibitors. The incubation period was 4 hours. Panel represents the average of three independent experiments with SEM.

A one way ANOVA was done followed by post hoc test (Sidak's multiplicity test) to compare the selected columns.

P value: ova vs. piceatannol- N.S., ova vs. cytochalasin B- *, ova vs. wortmannin- *

This assay was performed by Aswin Hari.

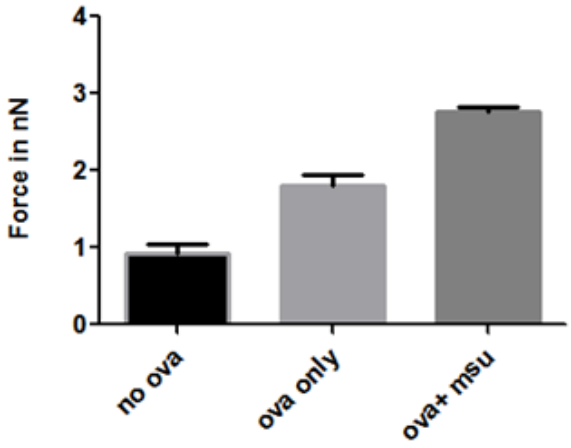

Figure 3.1-5: Average of maximum binding force between DCs and OT-1 T cells in the presence and absence of MSU crystals.

The force of interaction was measured in DC 2.4 cells fed with soluble OVA in the presence or absence of MSU crystals. The incubation period was 4 hours.

Panel represents the average of three independent experiments with SEM.

A one way ANOVA was done followed by post hoc test (Sidak's multiplicity test) to compare the selected columns.

P value: ova only vs. ova + MSU- ***.

This assay was performed by Aswin Hari with assistance from Enaam Alghamdi.

3.2 Phagocytosis enhances cross presentation independently of endocytosed soluble antigen

The AFM data implied that the antigen may be diverted into MHC I pathway as measured by increased adhesion between the DC and T cell. To assess this altered antigen presentation with conventional immunological assays; we used the OT-1/OT-II system for our readouts. While the OT-II mouse has a transgenic TCR that is specific for chicken ovalbumin 323-339 in the context of I-A b, the OT-1 mouse has a transgenic TCR that is designed to recognize ovalbumin residues 257-264 in the context of H2Kb. The epitope for OT-1 TCR is also called SIINFEKL based on its sequence. Using DC2.4 cells, it was evident that presentation to OT-1 T cells was enhanced significantly when soluble OVA was given in the presence of MSU (Figure 3.2-1). In Figure 3.2-1, the upper panel shows a representative dot plot and a histogram obtained during a typical assay. Since this study involves multiple sets of data from Fluorescence-Activated Cell Sorting (FACS) and Enzyme-Linked Immunosorbent Assay (ELISA), we normalized all the mean channel fluorescence intensity (MFI) intensities and ELISA readings against SIINFEKL-pulsed DCs henceforth for simpler presentation (Figure 3.2-2).

OT-1 T cell stimulated by C57BL/6 BMDCs that were treated with soluble OVA in the presence of MSU showed enhanced levels of CD69 expression and IL-2 production (Figure 3.2-3). One of the common concerns in antigen presentation assays is whether the antigen being given binds non-specifically to the solid structure. To rule out this type of non-specific binding of OVA to MSU, MSU was added before or after OVA incubation, with washings in between. This did not change the outcome (Figure 3.2-4), ruling out any non-specific binding. Throughout our imaging experiments, we did not detect any binding of OVA to MSU visually even when they were mixed (data not shown). To ascertain if the addition of a phagocytic signal such as MSU altered presentation on MHC II molecules, a similar protocol was used to measure OT-II T cell

activation. MSU treatment marginally decreased OT-II T cell activation. Even though the reduction was not statistically significant it may be? biologically relevant as it suggests that presentation on MHC II molecules is not affected significantly (Figure 3.2-5). In addition, we tested other solid structures, including BCP (basic calcium phosphate) and latex beads that are known not to drive DC activation. Both of them enhanced the ability of class I presentation of soluble OVA as shown by the CD69 and IL-2 levels measured (Figure 3.2-6). We also analyzed the enhanced epitope presence with 25-D1.16 antibody that detects the K^b/SIINFEKL complex. This method requires approximately 100 times higher soluble OVA concentration to display positive staining, out of our normal working range of concentrations. While we used OVA at the 5-100μg/ml range for antigen presentation, we had to increase the OVA concentration to the 5-10mg/ml range to obtain a signal. Nonetheless, an elevated 25-D1.16 staining was seen in the presence of MSU stimulation (Figure 3.2-7, upper panel). Immunofluorescence stain using 25-D1.16 antibody shows a similar trend where more epitope loaded MHC I is seen in presence of MSU crystals (Figure 3.2-7, lower panels).

Using fluorescently tagged OVA, we show that adding solid structures did not alter the amount of OVA uptake by DCs (Figure 3.2-8, left panel). To demonstrate that our MSU crystals or other preparations were not contaminated by microbial products, we performed the cross presentation assay with Myd88/Trif double KO BMDCs. Myd88/Trif double KO BMDCs lack TLR signaling. The enhanced cross presentation in response to the MSU crystal remained intact despite these deficiencies (Figure 3.2-8, right panel). DCs stimulated with MSU did not show enhanced activation in general. First, OT-II response was not greater with MSU (Figure 3.2-5). Second, we used a new preparation of fine MSU crystals (Figure 3.2-9) that had a much milder DC stimulation capacity and showed reduced cell death (Figure 3.2-10). Thus, this preparation,

in the duration of our assays, did not cause any change in DC rate of apoptosis (Figure 3.2-10) or MHC class I, MHC class II CD40, CD80, or CD86 expression (Figure 3.2-11). To probe if the enhanced crosspresentation is associated with only BMDCs, we also tested FLT3L stimulated splenic DCs and cultured primary macrophages (differentiated with L cell supernatant). FLT3L DCs are known to be more like resident DCs in contrast with the inflammatory DC like phenotype of GMCSF-IL4 derived DCs. While FLT3L DCs behaved similarly to that of GM-CSF/IL-4 BMDCs and DC2.4 cells (Figure 3.2-12), macrophages on the other hand showed high variable results in response to MSU (Figure 3.2-13). We plotted all the data from IL-2 and CD69 experiments and found that the ability of soluble OVA to be presented as a class I antigen increased by at least 40 times in the presence of MSU (Figure 3.2-14). The calculation was based on the fact that 5μg/ml OVA in the presence of MSU was presented at the same efficiency as 200 μg/ml OVA. MSU and uncoated latex beads themselves did not lead to any T cell activation (Figure 3.2-14).

It remained possible that this type of enhanced antigen presentation was limited to certain assay systems, such as the ovalbumin model commonly used in C57BL/6 mice. To this end, we performed HIV gp120 antigen presentation assay in Balb/c mice. As we reported previously, when soluble and latex bead coated gp120 were injected subcutaneously into Balb/c mice, a typical mixed CD4 and CD8 response against the antigen was detected after 10 to 14 days[52] (and our own observation). Balb/c mice were subcutaneously injected with soluble /latex bead coated gp120. After 10 days, we isolated the T lymphocytes from lymph nodes and the spleen, and challenged them with Balb/c BMDCs fed with gp120 in the presence and absence of MSU crystals. Remarkably, while DCs fed with gp120 alone induced an expected CD4/CD8 mixed response; DCs simultaneously treated with MSU induced a nearly complete CD8 response

(Figure 3.2-15). This result indicated that the particle induced cross presentation of the soluble antigen maybe at work in other assay systems.

These results suggest that, instead of being sources of antigen for cross presentation, the solid particles trigger phagocytic signaling which itself enhances soluble antigen cross presentation to CD8 T cells.

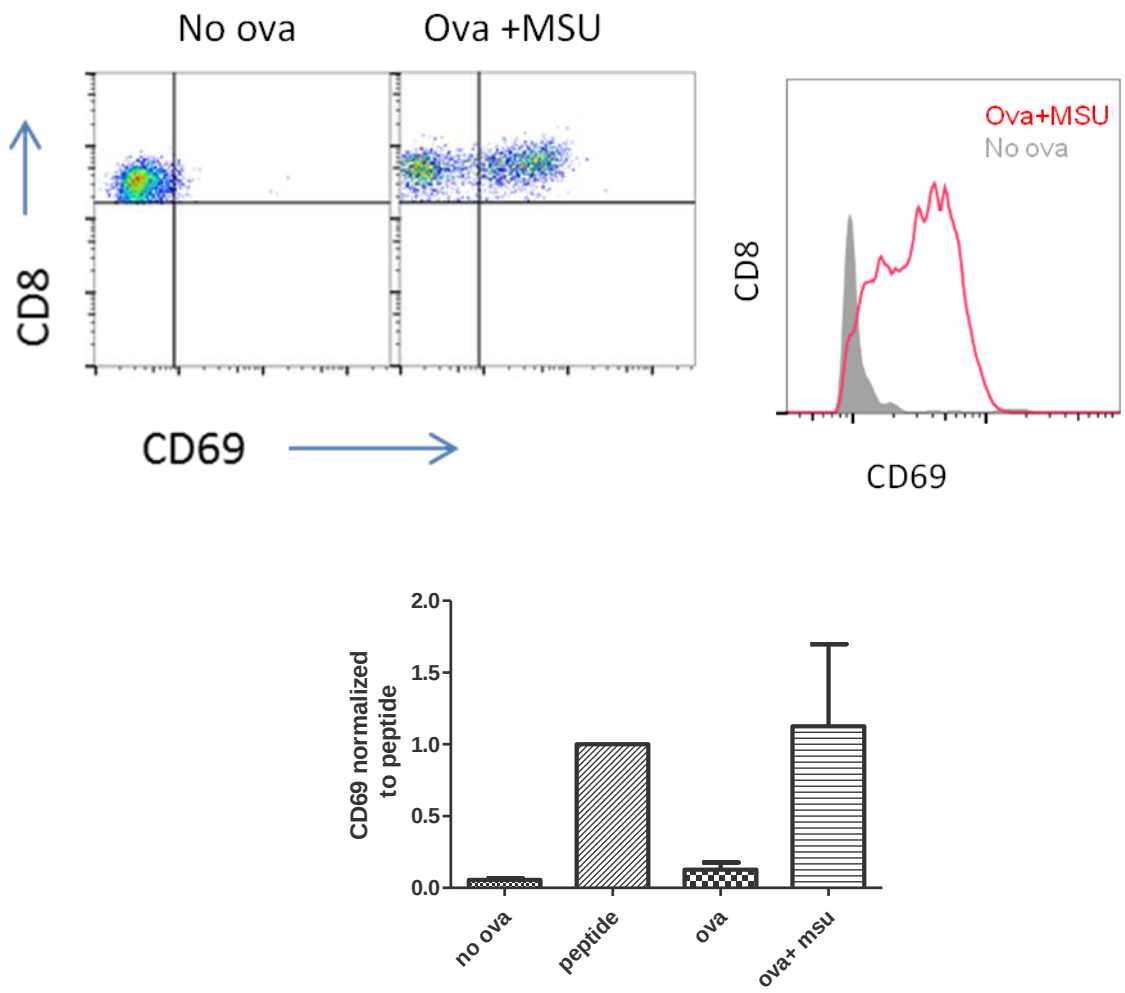

Figure 3.2-1: Representative data plots showing the method of analysis used in the thesis.

Representative histogram of CD69 expression by OT-1 T cells upon activation with OVA and MSU (upper right panel). Illustrative dot plots for quantification throughout the thesis (upper left panel). Expression of activation marker CD69 by OT-1 T cells upon stimulation by DC2.4 cells (lower panel).

Panel represents average of three independent experiments with SEM. A one way ANOVA was done followed by post hoc test (Sidak's multiplicity test) to compare the selected columns.

P value: ova vs. ova+ MSU - *.

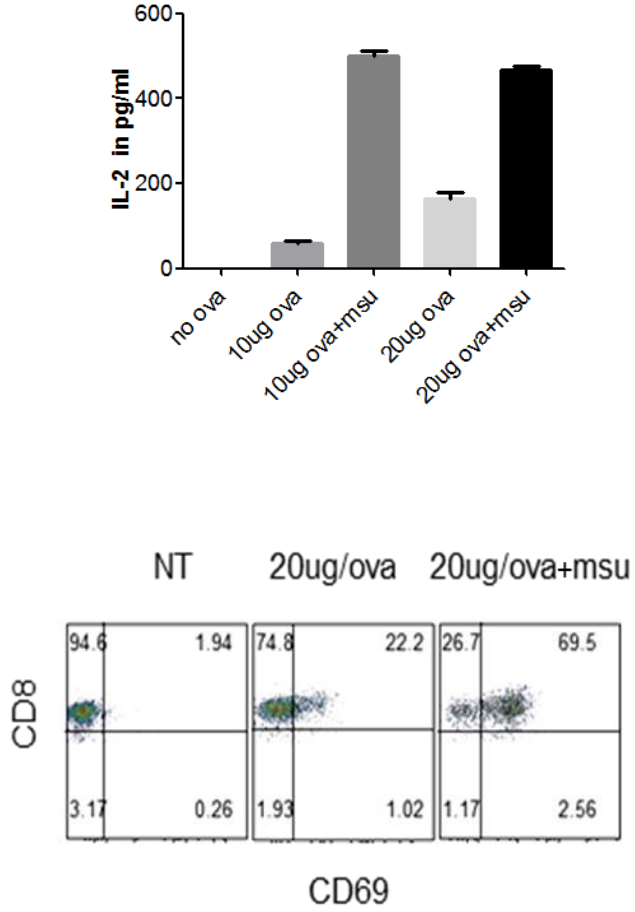

Figure 3.2-2: Representative plot of IL-2 (upper panel) and CD69 expression (lower panel) by OT-1 T cells after being stimulated by DCs fed with OVA.

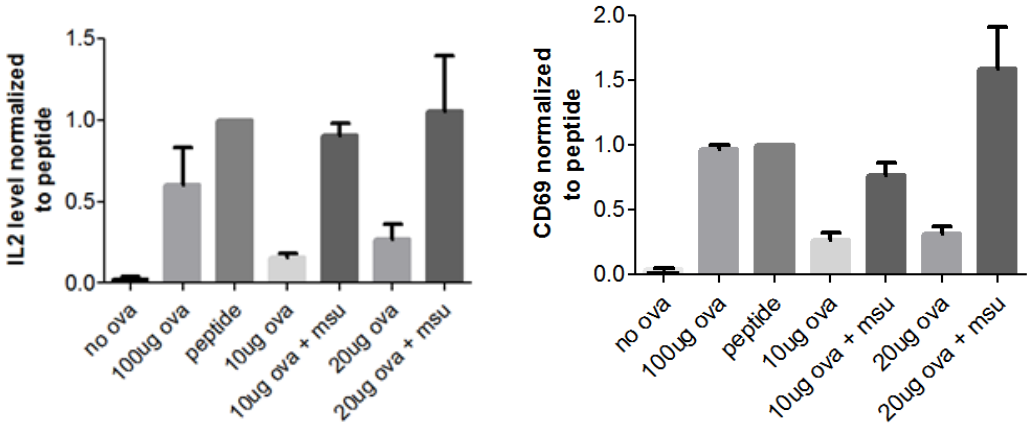

Figure 3.2-3: Addition of MSU crystals at the same time as soluble antigen enhances presentation on MHC I molecules.

Left panel: Production of IL-2 by OT-1 T cells upon stimulation by C57BL6 BMDCs mixed with soluble OVA in the presence or absence of MSU. Right panel: as in the left panel, the expression of activation marker CD69. CD69 expressed as mean fluorescence intensity, MFI. A one way ANOVA was done followed by post hoc test (Sidak's multiplicity test) to compare the selected columns.

IL-2- Panel represents average of minimum four independent experiments with SEM. P value: no OVA vs. peptide -****, 10µg OVA vs. 10µg OVA + MSU -**, 20µg OVA vs. 20µg OVA + MSU-*.

CD69-Panel represents average of minimum three independent experiments. P value: no OVA vs. peptide- ***, no OVA vs. peptide- ****, 10µg OVA vs. 10µg OVA + MSU-*, 20µg OVA vs. 20µg OVA + MSU- ****.

This assay was done by Aswin Hari with assistance from Raymond Lam.

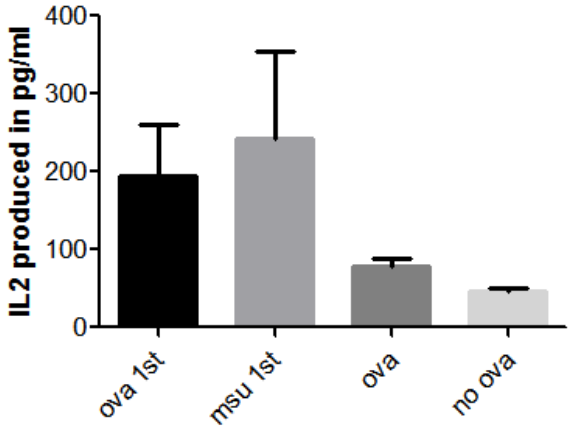

Figure 3.2-4: Production of IL-2 by OT-1 T cells upon stimulation by DC2.4 cells.

IL2 production from OT-1 T cells was measured using ELISA. Stimuli/antigen or vice versa were given 20 minutes apart, with washing steps in between. OVA was added either 1st or after 20 minutes of treatment with MSU.

The figure is a representative of three control experiments.

This experiment was done by Aswin Hari with assistance from Raymond Lam.

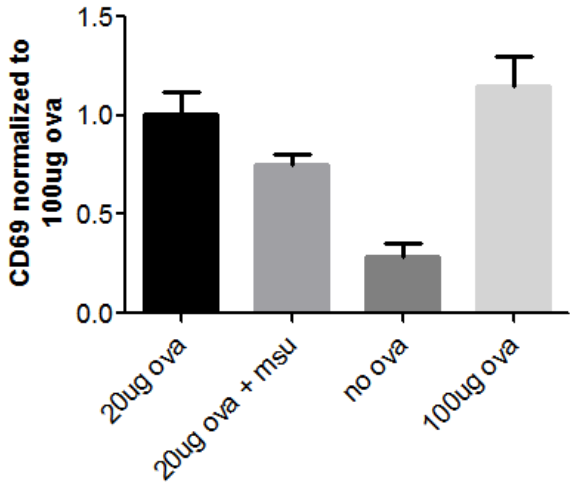

Figure 3.2-5: Expression of activation marker CD69 by OT-II T cells upon stimulation by BL6 BMDCs mixed with soluble OVA in the presence of MSU.

Production of IL-2 by OT-II T cells upon stimulation by C57BL6 BMDCs mixed with soluble OVA in the presence or absence of MSU.

The panel represents the average of a minimum of four independent experiments with SEM.

A one way ANOVA was done followed by post hoc test (Sidak's multiplicity test) to compare the selected columns.

P value: 20µg OVA vs. 20µg OVA + MSU -N.S.

This assay was done by Aswin Hari.

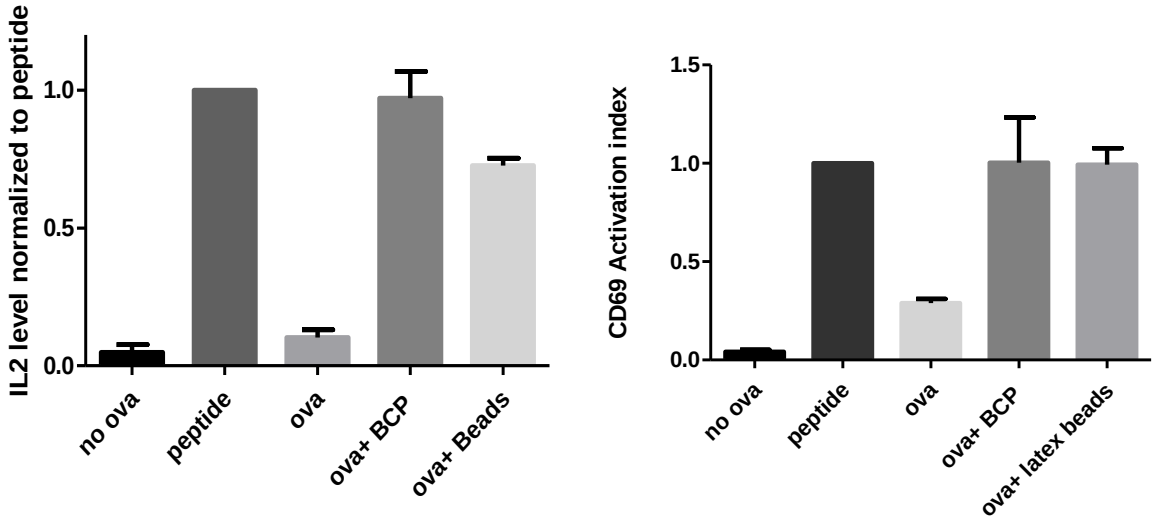

Figure 3.2-6: IL-2 (left) and CD69 (right) expression by OT-1 T cells upon stimulation by C57BL6 BMDCs in the presence of other receptor independent phagocytic stimuli.

Left panel: Production of IL-2 by OT-1 T cells upon stimulation by C57BL6 BMDCs mixed with soluble OVA in the presence or absence of beads/ BCP. Right panel: as in the left panel, the expression of activation marker CD69.

A one way ANOVA was done followed by post hoc test (Sidak's multiplicity test) to compare the selected columns.

IL-2- Panel represents the average of a minimum four independent experiments with SEM. P value: OVA vs. OVA + BCP-***, OVA vs. OVA + latex beads- *.

CD69-Panel represents the average of a minimum three independent experiments with SEM. P value: OVA vs. OVA + BCP-***, OVA vs. OVA + latex beads- **.

This assay was done by Aswin Hari with assistance from Melanie Stenner.

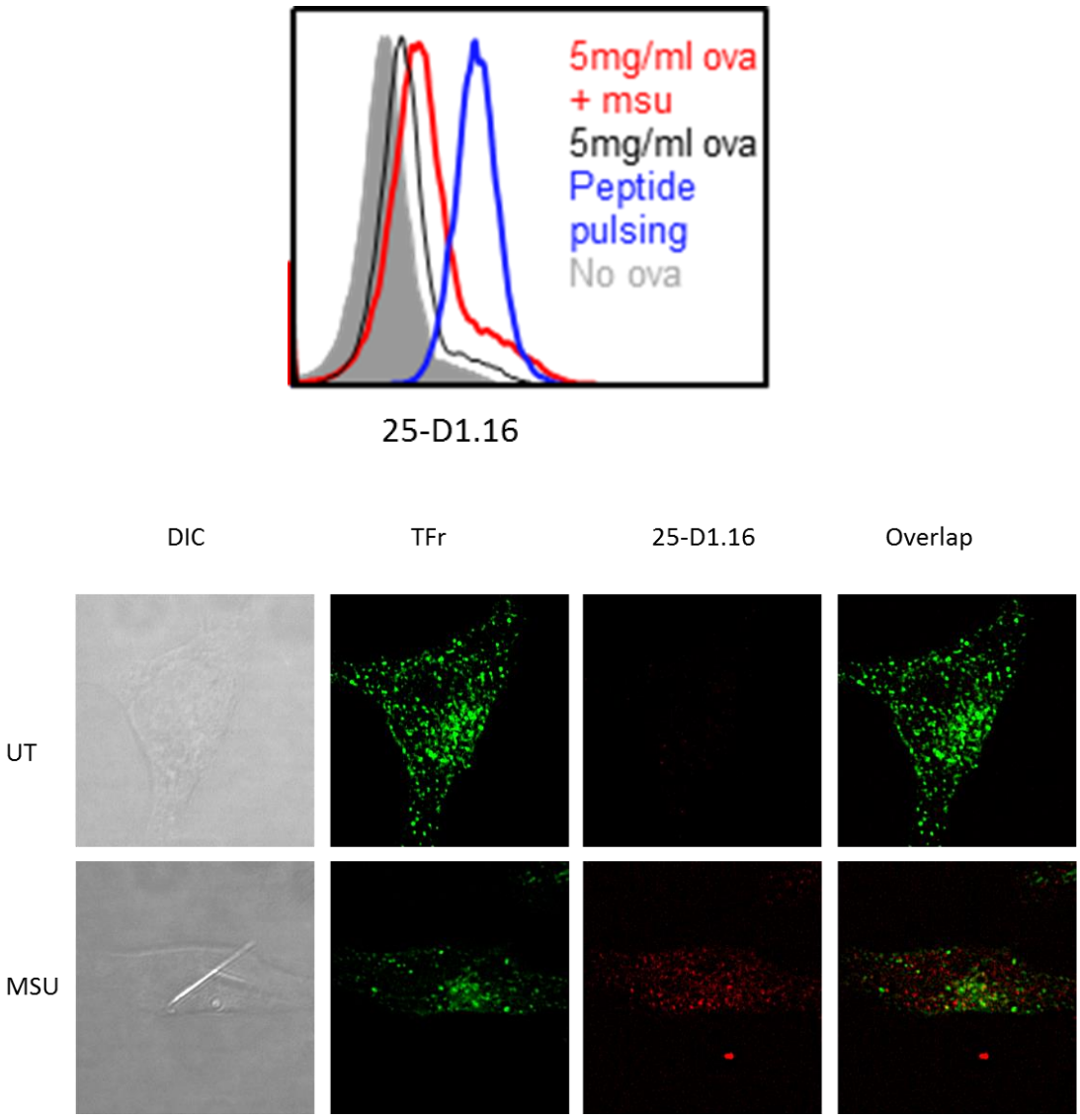

Figure 3.2-7: Expression of SIINFEKL epitope on MHC I measured using 25-D1.16 antibody in the presence and absence of MSU crystals.

Epitope appearance as measured by FACS (upper panel). DC2.4 cells treated with and without MSU crystals were stained for transferrin receptor (TFr) and Kb/SIINFEKL complex in the cell (lower panels). TFr was stained for sake of reference. Both experiments are representative images from three independent experiments. This experiment was done by Aswin Hari with assistance from Melanie Stenner and Anutosh Ganguly.

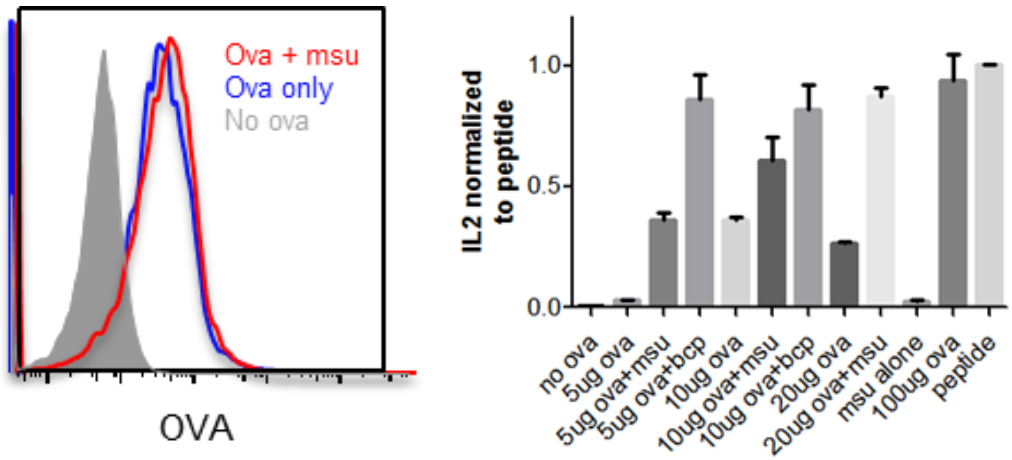

Figure 3.2-8: Analysis of amount of OVA uptake by DC2.4 cells and Myd88-Trif Double KO BMDCs stimulation of OT-1 T cells.

Uptake of Alexa conjugated OVA after 2 hours by DC2.4 cells measured by FACS with or without MSU stimulation (left panel). Production of IL2 by OT-1 T cells upon stimulation by Myd88-Trif Double KO BMDCs mixed with soluble OVA in the presence or absence of MSU (right panel).

Both panels are representative of minimum of two control experiments.

These experiments were done by Melanie Stenner with assistance from Aswin Hari.

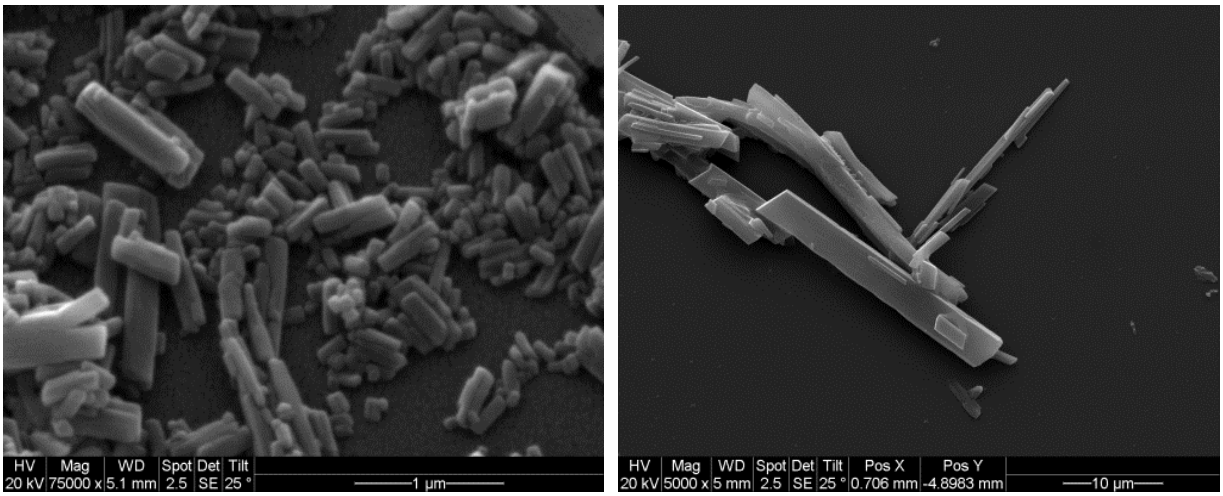

Figure 3.2-9: Scanning electron microscope images of fine MSU crystals (left) and crude MSU crystals (right).

In both cases, the crystals were coated on to carbon tape on pre-fabricated aluminum stubs. The samples were coated with gold and inspected under an SEM. Note the difference in scale.

Images were acquired by Aswin Hari with assistance from Michael Schoel.

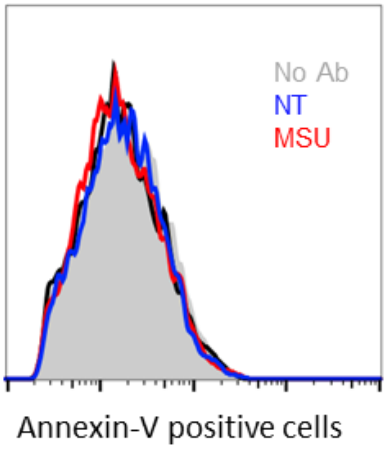

Figure 3.2-10: Histogram of Annexin V positive cell population in BMDCs treated with fine MSU crystals.

DC2.4 cells treated with crystals for 6 hours or left untreated for same amount of time. The cells were scraped and stained using Annexin V labelling antibody and propidium iodide. The samples were analyzed using FACS.

This panel is representative of three control experiments.

This experiment was done by Aswin Hari.

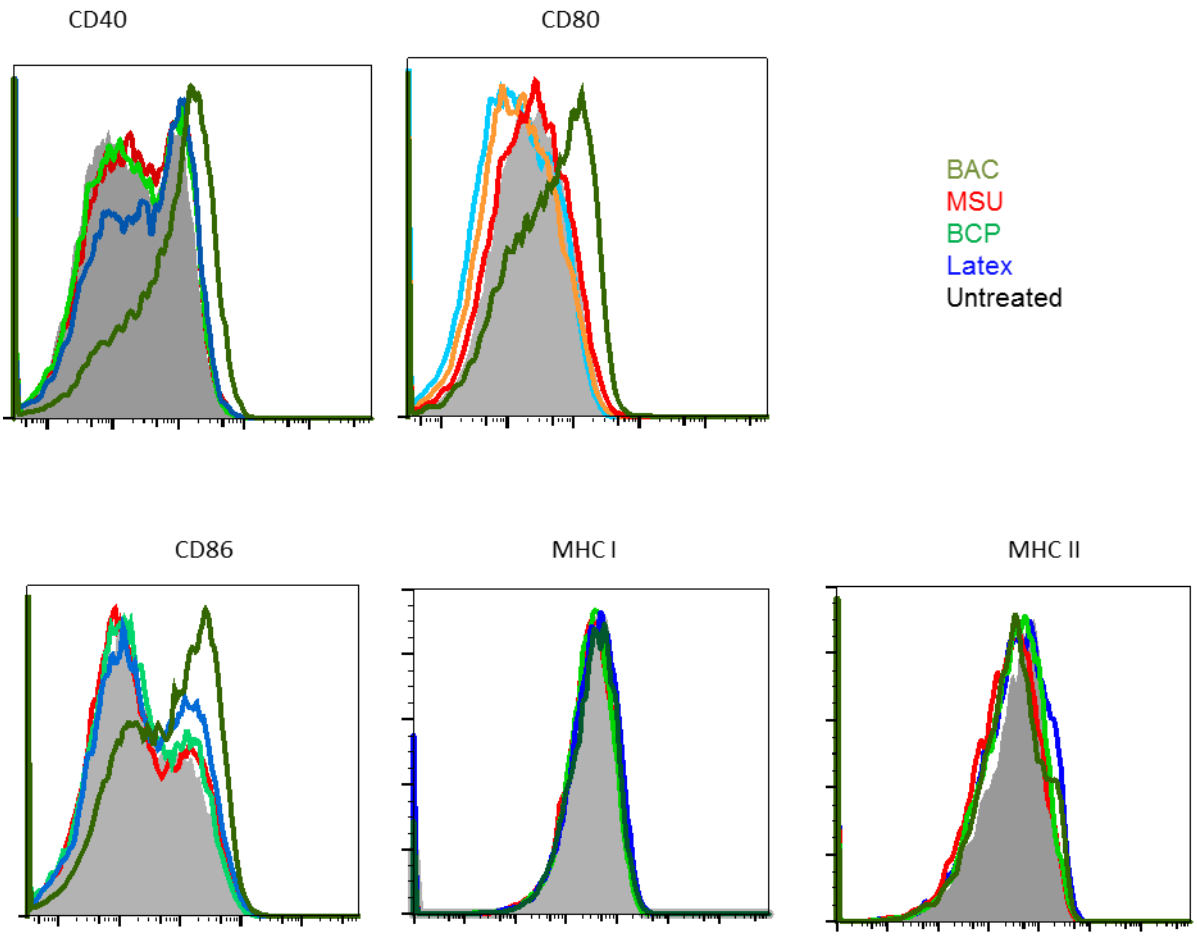

Figure 3.2-11: MHC I, MHC II, CD40, CD80 and CD86 expression in the presence of MSU crystals, latex beads and BCP.

C57BL6 BMDCs were treated with different crystals or beads as listed for 6 hours. The cells were scraped and stained for different markers and analyzed using a FACS analyzer.

All panels are representative of three control experiments.

This experiment was done by Aswin Hari with assistance from Melanie Stenner.

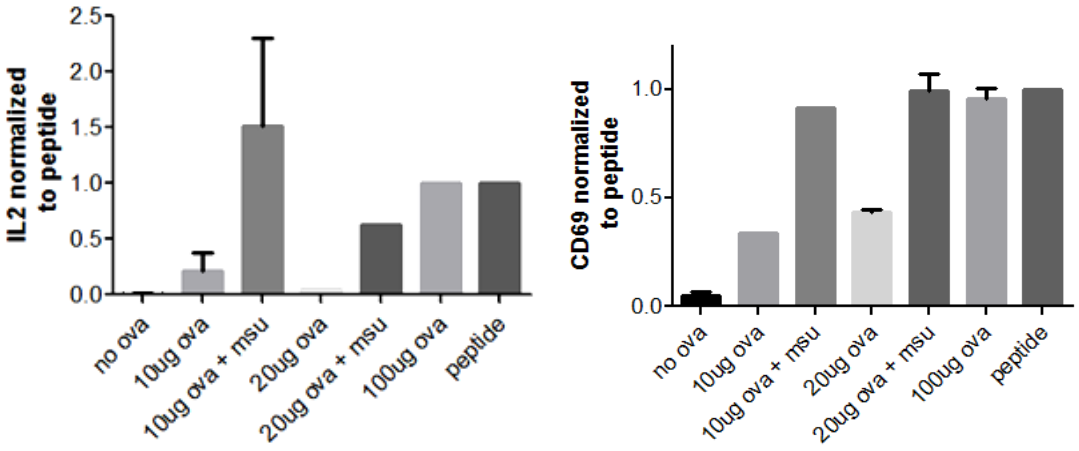

Figure 3.2-12: Expression of activation marker CD69 (right panel) and production of IL-2 (left panel) by OT-1 T cells upon stimulation by FLT3L BMDCs.

FLT3L BMDCs were fed with different concentrations of OVA with or without MSU as indicated. Cells were collected for CD69 measurement (right panel) and supernatants were used for measuring IL-2 using ELISA (left panel) after 24 hours.

This figure is representative of three experiments with SEM.

These experiments were done by Aswin Hari with assistance from Raymond Lam.

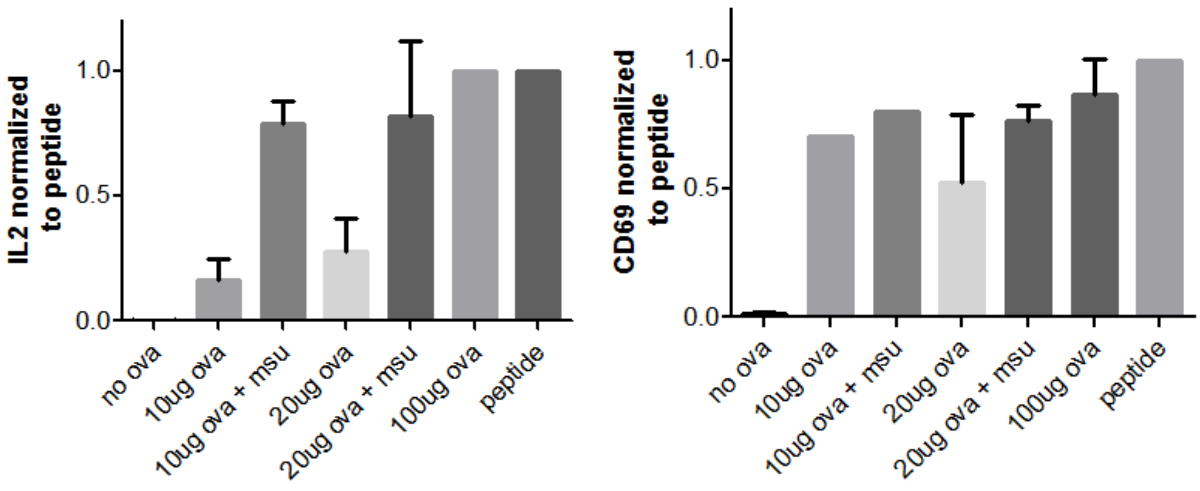

Figure 3.2-13: Expression of activation marker CD69 (right panel) and production of IL-2 (left panel) by OT-1 T cells upon stimulation by bone marrow derived macrophages.

BM derived macrophages were washed on day 6 of culturing and were fed with different concentrations of OVA with or without MSU as indicated. Cells were collected for CD69 measurement (right panel) and supernatants were used for measuring IL-2 by ELISA (left panel) after 24 hours.

This figure is representative of three experiments with SEM.

These experiments were done by Aswin Hari with assistance from Raymond Lam.

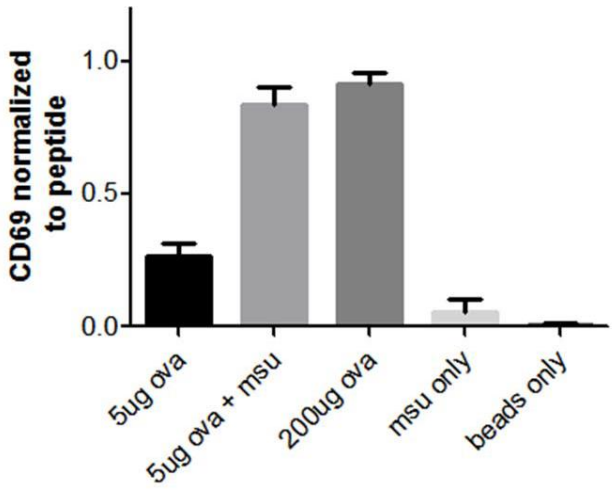

Figure 3.2-14: Average data from 3 independent OT-1 CD69 expression experiments.

Expression of CD69 by OT-1 T cells upon stimulation by C57BL6 BMDCs mixed with soluble OVA in the presence or absence of MSU crystals.

Bars are SEM.

This figure is representative of three experiments with SEM.

These experiments were done by Aswin Hari

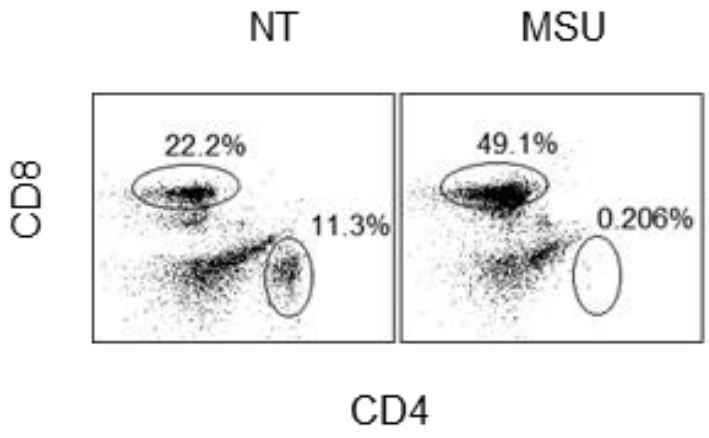

Figure 3.2-15: Cross presentation during phagocytic signaling using BALB/c system.

Balb/c mice were immunized with gp120 antigen in the presence or absence of MSU subcutaneously. T cell populations were isolated from lymph nodes and spleens on day 10. The dot plot shows CD4 versus CD8 population ratio obtained upon restimulation with Balb/c BMDCs pulsed with soluble gp120 in the presence or absence of 100 µg/ml MSU.
This experiment had a minimum of three mice in each group.

3.3 Cross presentation of endosomal antigen is efficient

The observations from the previous section raised another question: how efficient is the endosomal cross presentation compared with its phagosomal variant? While any particle above 0.5-1μm in length is considered to be taken up by phagocytosis, any substance less than 0.5 μm is viewed to be taken up by endocytosis. We loaded DCs with either soluble or 3 μm latex bound Alexa OVA. Considering these two routes of antigen uptake may have different efficiencies, we titrated both preparations instead of measuring incoming amounts of antigen. At certain points, soluble and latex bound OVA achieved similar mean channel fluorescence by FACS (Figure 3.3-1). We concluded that 200 μg/ml soluble OVA was approximately equivalent to 15 μl of OVA beads. Using these doses as the next starting points, we fed them to DCs for OT-1 activation assays. Using CD69 and IL-2 as readouts, the same amount of OVA was cross presented approximately 40 times more efficiently via endosomes than via phagosomes (Figure 3.3-2). In this assay, the particles used to deliver the antigen and for phagocytic stimulation were of different nature (latex vs. MSU), and were therefore imperfectly controlled. Coating MSU and many other rigid crystalline structures (such as basic calcium phosphate and silica) with proteins is not efficient and often results in unpredictable quality (our own observation). We therefore studied latex beads, both as phagocytic target carrying OVA and as solid structure that stimulated phagocytosis, when OVA was used separately. Figure 3.3-3 shows that latex beads were fully capable of stimulating the soluble antigen cross presentation with similar efficiency. Other crystalline structures, such as silica-induced robust DC activation (our own observation), and therefore may potentially upregulate costimulatory markers independent of antigen processing. BCP is another crystalline structure that does not induce DC activation [52]. We

therefore repeated experiments described in Figure 3.3-3 with this structure and found it had a similar ability to enhance cross presentation of soluble antigen (Figure 3.3-4).

Whether with phagocytic signaling, endosomal antigens are always more efficiently cross presented than phagocytosed antigens needs to be tested under biological settings. Nonetheless our results (Figure 3.2-14 and all Figures in 3.3 series) suggest that endosomes can be a potentially important source for cross presenting antigens.

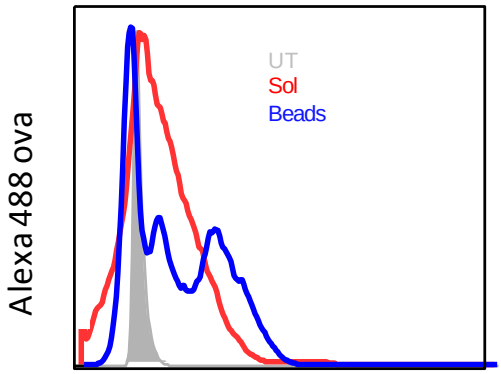

Figure 3.3-1: Titration of amount of antigen taken up by DCs in soluble and particulate form.

DC2.4 cells fed with 200 µg/ml Alexa 488-OVA or 15 µl Alexa 488-OVA latex beads were analyzed by FACS after 2 hours of incubation, and determined to have similar MFIs (soluble-2053, beads-2690).

This figure is representative of three control experiments.

These experiments were done by Aswin Hari.

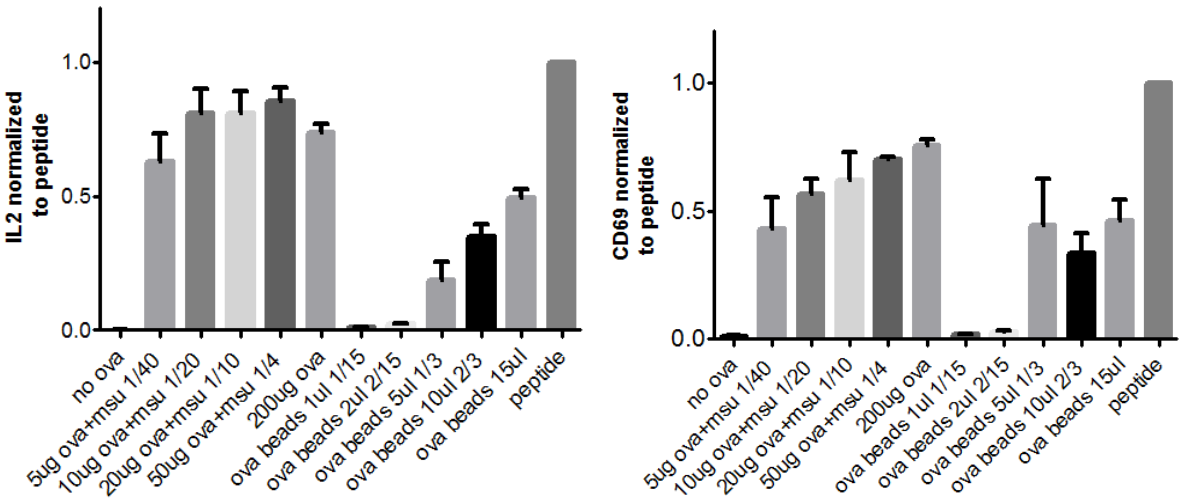

Figure 3.3-2: Comparison of efficiency of epitope loading between soluble in the presence of MSU and particulate forms of the same antigen.

Similar to other OT-1 stimulation assays, levels of IL-2 and CD69 expression by OT-1 cells were measured after stimulation with DC2.4 cells treated with OVA along with MSU or with latex/OVA beads alone at the indicated concentrations.

A one way ANOVA was done followed by post hoc test (Sidak's multiplicity test) to compare the selected columns.

IL-2- Panel represents the average of four independent experiments with SEM. P value: all concentrations of OVA + MSU vs. OVA coated latex beads-N.S.

CD69- Panel represents average of four independent experiments with SEM. P value: all concentrations of OVA + MSU vs. OVA coated latex beads-N.S.

The experiments were done by Aswin Hari with assistance from Melanie Stenner.

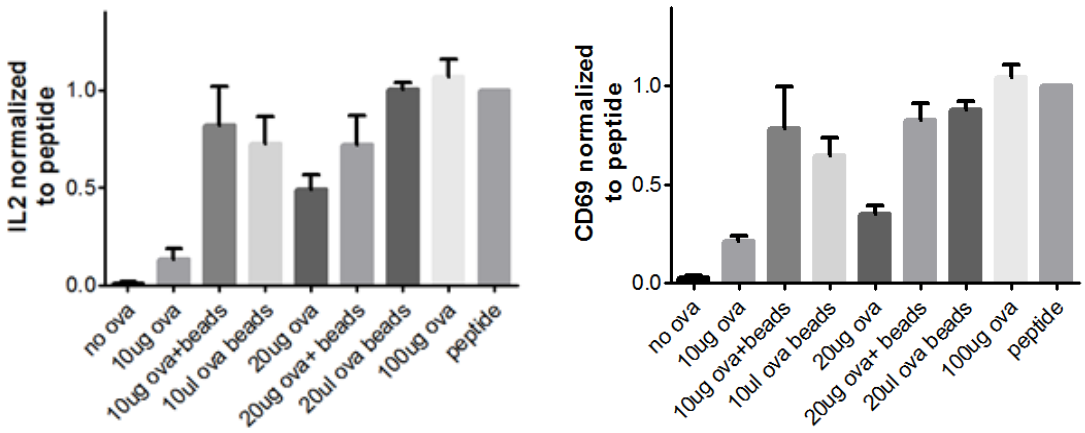

Figure 3.3-3: Comparison of efficiency of epitope loading between soluble in the presence of latex beads and particulate forms of the same antigen.

Similar to other OT-1 stimulation assays, levels of IL-2 and CD69 expression by OT-1 cells were measured after stimulation with DC2.4 cells treated with OVA along with uncoated latex beads or with OVA coated latex beads alone at the indicated concentrations.

A one way ANOVA was done followed by post hoc test (Sidak's multiplicity test) to compare the selected columns.

IL-2- Panel represents average of four independent experiments with SEM. P value: 10 µg OVA vs. 10 µg OVA + latex beads-***, other comparisons-NS

CD69- Panel represents average of five independent experiments with SEM. P value: 10 µg OVA vs. 10 µg OVA + latex beads-***, 20 µg OVA vs. 20 µg OVA + latex- **, other comparisons-NS.

The experiments were done by Aswin Hari with assistance from Melanie Stenner.

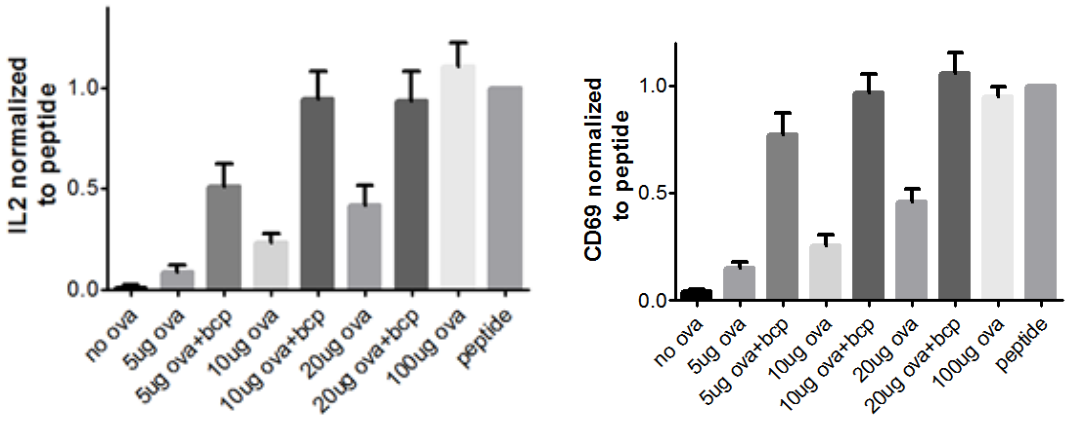

Figure 3.3-4: Use of BCP as the phagocytic signal to achieve strong MHC I presentation.

Similar to other OT-1 stimulation assays, levels of IL-2 and CD69 expression by OT-1 cells were measured after stimulation with DC2.4 cells treated with OVA along with or without BCP crystals at the indicated concentrations.

A one way ANOVA was done followed by post hoc test (Sidak's multiplicity test) to compare the selected columns.

IL-2- Panel represents average of five independent experiments with SEM. P value: 5 µg OVA vs. 5 µg OVA + BCP-**, 10 µg OVA vs. 10 µg OVA + BCP-***, 20 µg OVA vs. 20 µg OVA + BCP- **.

CD69- Panel represents average of five independent experiments with SEM. P value: 5 µg OVA vs. 5 µg OVA + BCP-****, 10 µg OVA vs. 10 µg OVA + BCP-****, 20 µg OVA vs. 20 µg OVA + BCP- ****

The experiments were done by Aswin Hari with assistance from Melanie Stenner.

3.4 Phagocytosis arrests endocytic maturation

It is generally believed that phagocytosis is a triggered event, either receptor-dependent or –independent. Endocytosis, although inducible, happens at basal levels, as endosomes form constitutively even in "resting" cells. The maturation processes and proteolytic activities in both cases are similar, given the extensive cross talk and shared cellular machinery between the two vesicular systems [57]. It is therefore possible that phagocytosis influences endosomal behavior. When a vesicle resolves from the PM upon cellular uptake, the early endosome formed generally takes the road to the lysosome on its maturation process in the absence of other signals. Endosomes and lysosomes are traced by transferrin receptor (TFr) and Lysotracker respectively. Figure 3.4-1a shows that in the presence of MSU, endosome/lysosome overlapping was reduced by about 70%, suggesting a lack of progression in endosomal maturation (Figure 3.4-1b). Normal endosomal maturation can also be identified by the loss of early endosome markers Rab5 and EEA1 and the acquisition of lysosomal markers LAMP-1 and LAMP-2. Fluorescence imaging shows that in the presence of phagocytic signals (Figure 3.4-3a), soluble OVA mainly overlapped with early endosomal marker Rab5, and less so in the absence of MSU. On the other hand OVA was localized less efficiently with LAMP-1 when treated with MSU in contrast with the untreated cells. The colocalization bar graph is shown in Figure 3.4-3b.

Endosomes emerge from the plasma membrane at a given rate under steady state conditions. The lack of maturation suggests that there could be an accumulation of these organelles at certain cytosolic locations. Using high resolution Electron Tomography (Figure 3.4-5) and TEM (Figures 3.4-6 and 3.4-7) we studied their morphology and distribution in the cytoplasm. Interestingly, with MSU stimulation, a large quantity of unilamellar early endosomes remained closely aligned with the plasma membrane while untreated DCs showed multilamellar

late endosomes deep inside the cells. All TEM figures (3.4-6 and 3.4-7) were used to quantify such a change in distribution. In the presence of MSU, early endosomes were over represented, in comparison with late endosomes (Figure 3.4-8).

Proteolytic activities are modulated in the vesicular system in different ways such as by reactive oxygen species. To understand how phagocytosis altered intracellular proteolysis, we used standard fluorescent probes (DQ OVA) to measure protease activity. To study proteolysis in phagosomes, we used DQ OVA coated onto silica beads and for endocytic measurements soluble DQ was used. Figure 3.4-9 demonstrates that in the presence of MSU, phagocytic (time plot and lower left panel) and endocytic compartments (lower right panel) had reduced proteolysis particularly in the linear range of the slope. The linear range is defined as the region of the slope where the rate of proteolysis increases exponentially. The acidification progression was less affected in such cases as shown by Figure 3.4-10 with concanamycin A (acidification blocker) used as a control. Endosome accumulation and weak/delayed proteolysis are believed to be associated with strong cross presentation due to limited epitope destruction. These traits are also regarded as a hallmark of DCs in comparison with macrophages and neutrophils [116].

Our results indicate that the “arrested” early endosomes have features that favor cross presentation, potentially providing answers to why DCs are the best cross presenting APCs

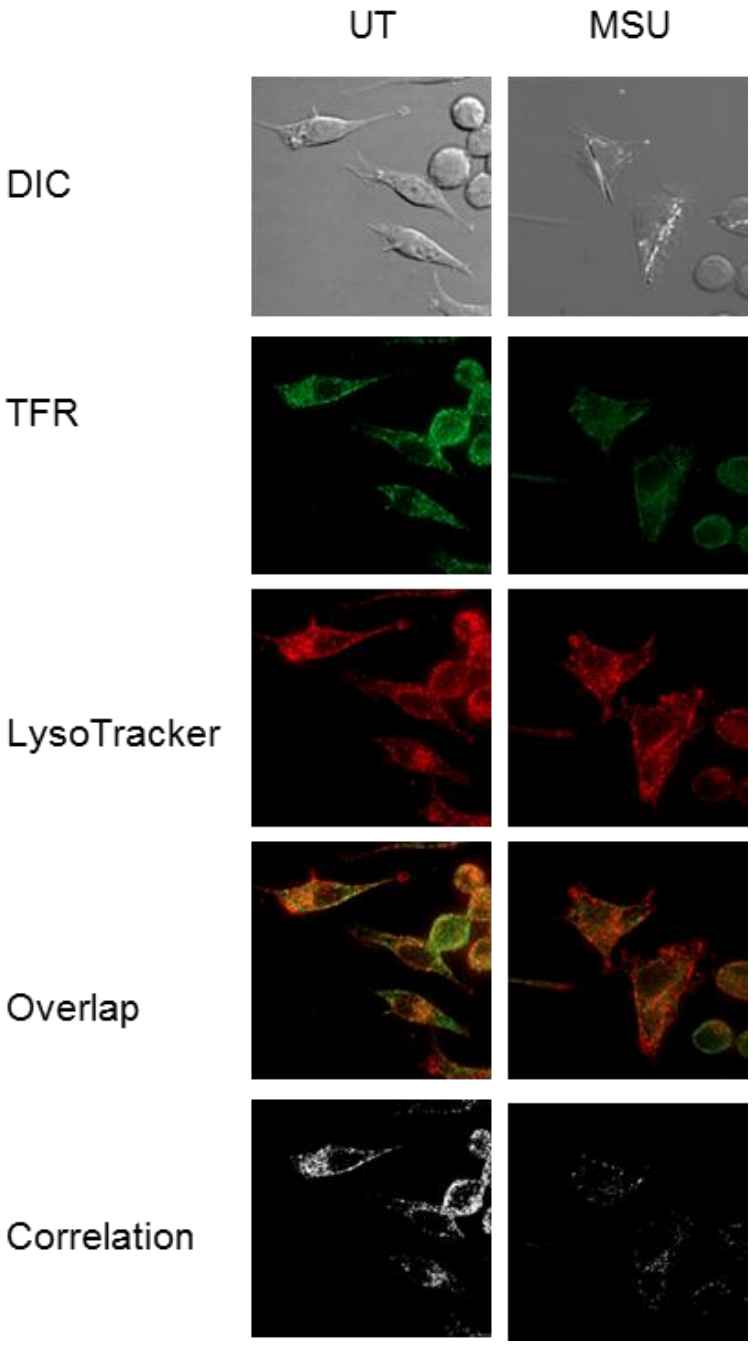

Figure 3.4-1a: Distribution of Lysotracker (red) and transferrin receptor (green) in the presence and absence of crystals with a correlation plot generated by ImageJ.

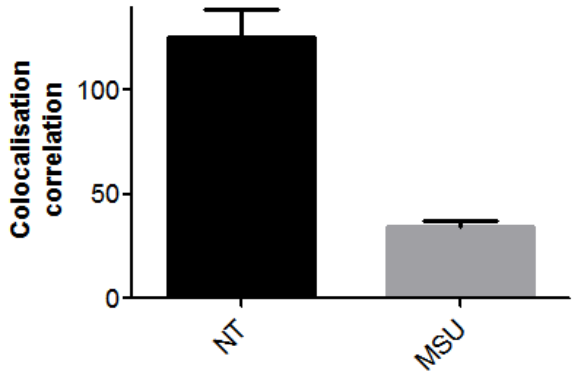

Figure 3.4-1b: Quantification of the colocalisation correlation generated by ImageJ for the two conditions.

This panel represents an average of 10 different fields of view from three different cover slips with SEM.

A students T test was done to compare the 2 columns. P value- ****.

This experiment was done by Anutosh Ganguly with assistance from Aswin Hari.

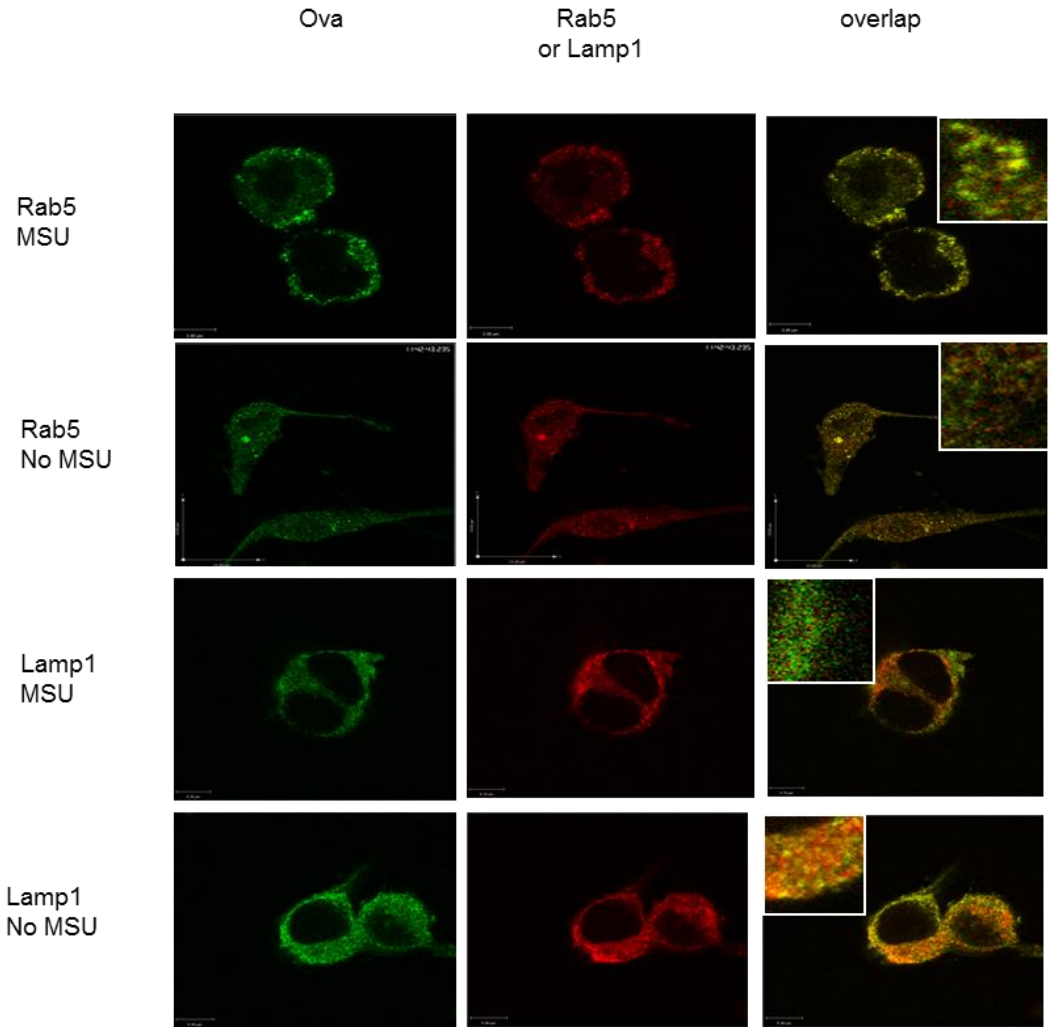

Figure 3.4-3a: Confocal images of DCs showing distribution of Rab5/LAMP-1 in relation to OVA.

Distribution of Rab5 or LAMP1 (red) in the absence and presence of stimuli with respect to ingested soluble ovalbumin (green) in DC2.4 cells. The right panels are overlaps. Inserts are magnified to show the detailed degree of overlapping.

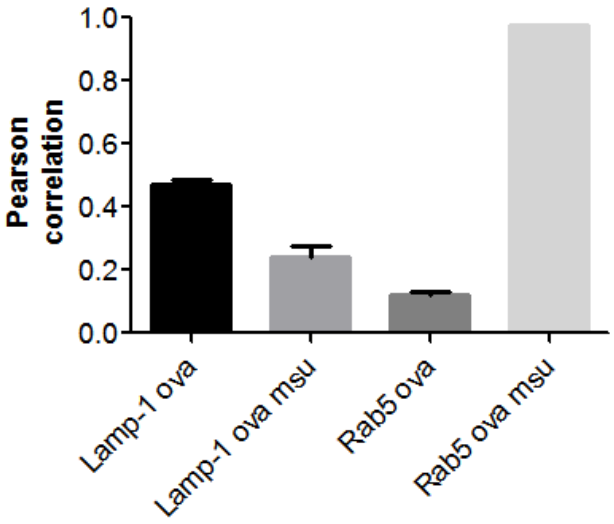

Figure 3.4-3b: The bar graph shows the Pearson correlation of the respective green and red channels of other three experimental conditions normalized to Rab5/OVA.

This panel represents an average of 3 different fields of view with SEM.

P value-LAMP1 NT vs. MSU- **, RAB5 NT vs. MSU-***.

This experiment was done by Aswin Hari and Fay Munro.

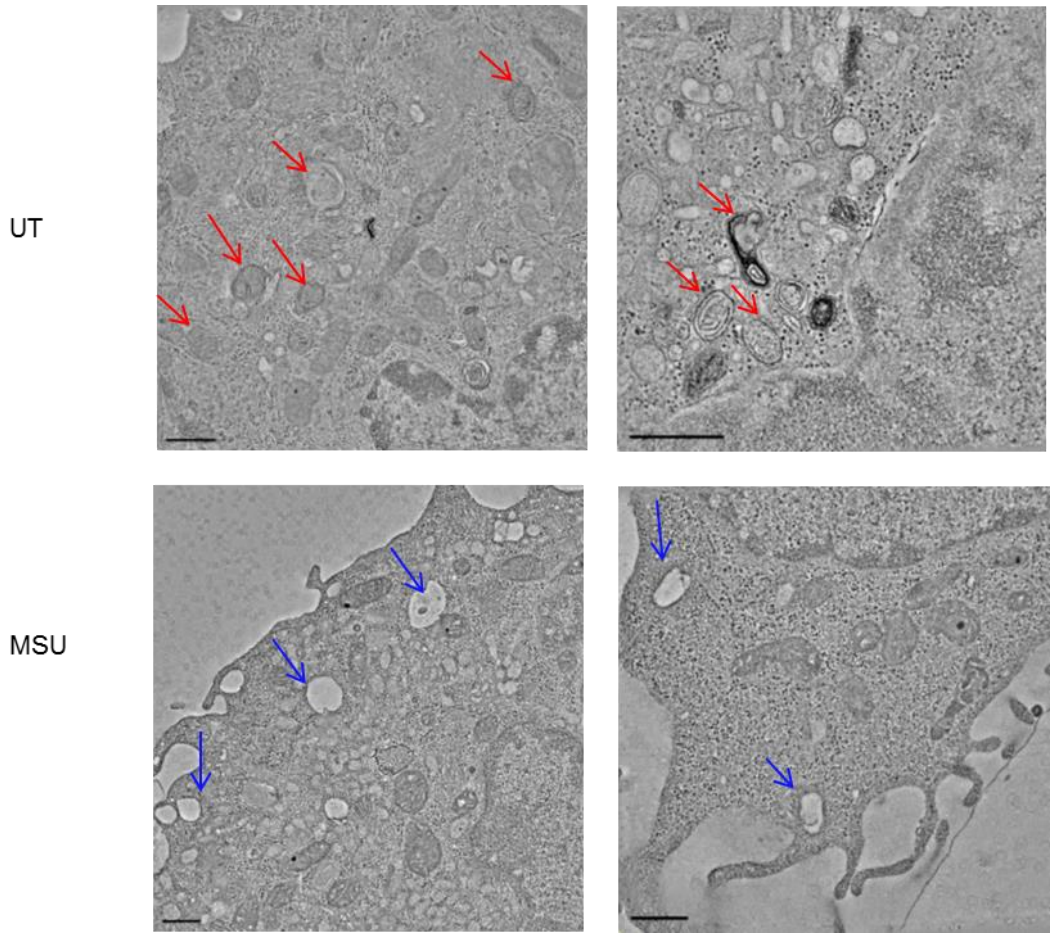

Figure 3.4-5: Electron tomography sections of DCs.

Tomography sections of DCs showing distribution of early endosomes (unilamellar, empty vesicles, blue arrows) and late endosomes (multilamellar, electron dense vesicles, red arrows) in treated and untreated cells.

This experiment was done by Tobias Fürstenhaupt with assistance from Aswin Hari and Wei Dong.

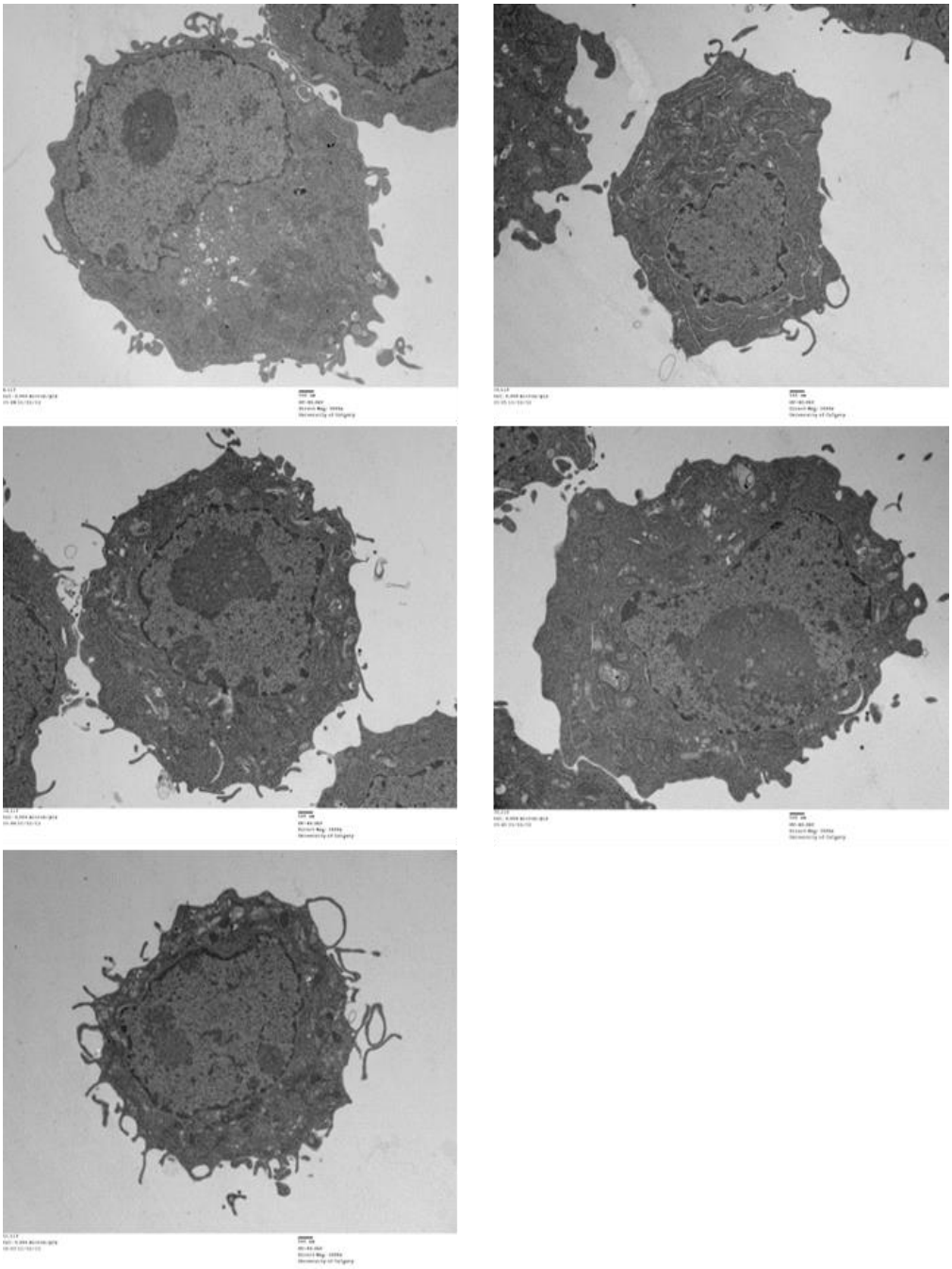

Figure 3.4-6: TEM images of untreated DC2.4 cells.

Untreated DC2.4 cells were fixed and processed as described in the TEM section of the methods chapter. Five different cells were used in the quantification.

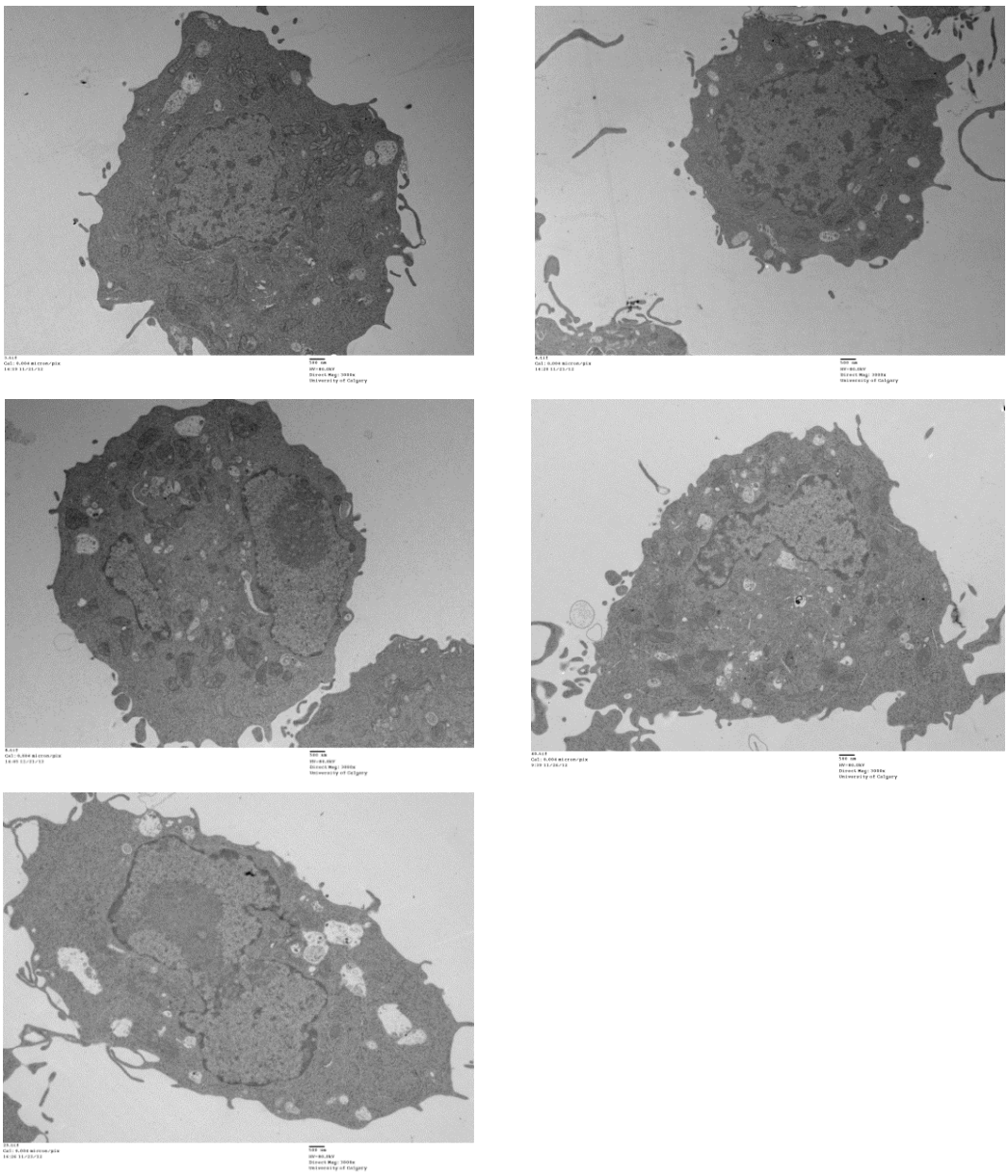

Figure 3.4-7: TEM images of DC2.4 cells treated with MSU crystals.

MSU treated DC2.4 cells were fixed and processed as described in the TEM section of the methods chapter. Five different cells were used in the quantification.

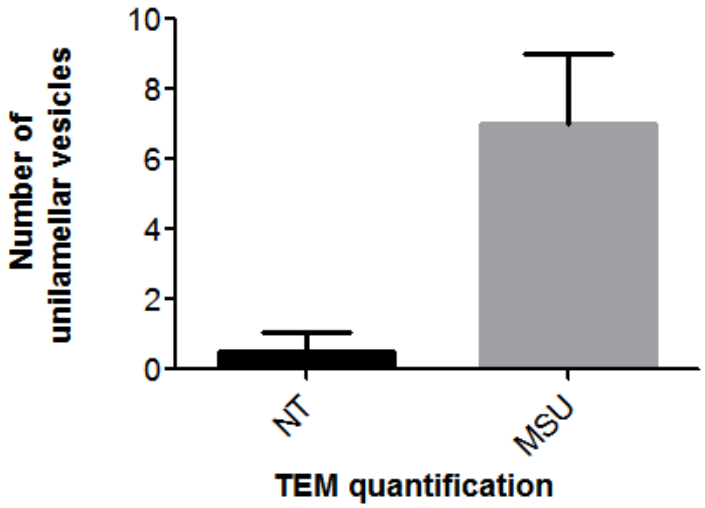

Figure 3.4-8: Quantification of the number of vesicles seen at the same magnification and resolution in both conditions.

Plot was generated from all TEM images shown in Figure 3.4-6 and 3.4-7.

This panel represents an average of five different cells with SEM.

A students T test was done to compare the 2 columns. P value- ****.

This experiment was done by Wei Dong with assistance from Aswin Hari. Aswin Hari performed data analysis.

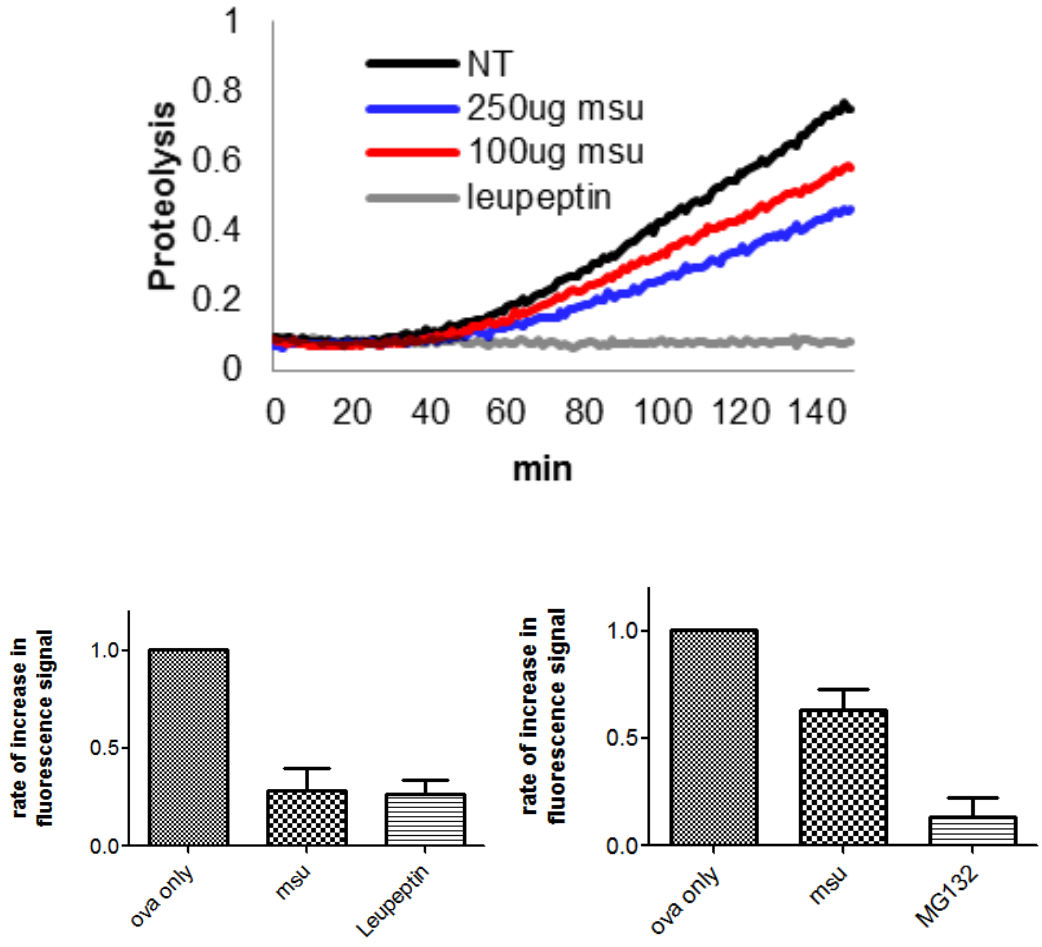

Figure 3.4-9: Proteolysis is slowed down in presence of MSU.

Upper panel: relative fluorescence units obtained to measure phagosomal proteolytic activity over time as described in the methods. Lower panels: quantification of the linear range of the curve for phagocytic (left) and endosomal (right) proteolysis assays. Leupeptin and MG132 are general protease inhibitors used as controls. These panels represent an average of five independent experiments with SEM.

A one way ANOVA was done followed by post hoc test (Sidak's multiplicity test) to compare the selected columns. Phagocytic proteolysis- OVA only vs. MSU- ***, OVA only vs. leupeptin- ***. Endocytic proteolysis- OVA only vs. MSU- **, OVA only vs. MG132-***.

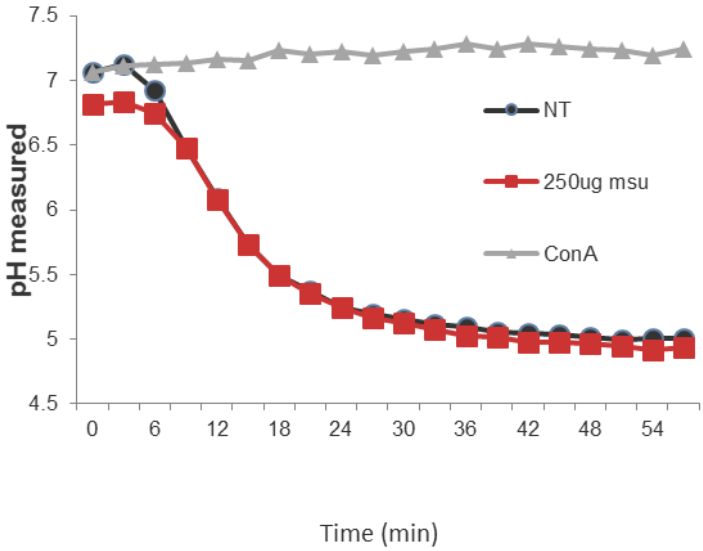

Figure 3.4-10: Phagocytic probe showing pH levels over time measured as relative fluorescence units.

IgG opsonised beads were used in this assay with concanamycin A as a control.

This graph is a representative plot from three independent repeats showing similar trends.

The proteolytic and pH assays were done by Aswin Hari with assistance from Dale Balce and Joanna Rybicka.

3.5 The MT system is modified during phagocytosis

To map the connections between phagocytosis, enhanced cross presentation of soluble antigens and the nature of the "arrested endocytosis", we analyzed the change in the molecular motors that drive both phagosomes and endosomes during their maturation. The molecular motors use the microtubule (MT) system to navigate in the cytoplasm. We first tested the acetylation state of α tubulin. The acetylation state of α tubulin is linked to its stability. A high degree of acetylation indicates a stable MT system with a relatively low turnover rate. Upon MSU treatment, there was essentially no acetylated filamentous α tubulin in the cells (Figure 3.5-1). This is consistent with the hyperactive state of the MTs during phagocytosis revealed by extensive literature showing rearrangements accompanying phagocytic uptake. Since conventional imaging cannot resolve the details of MTs, we used Structural Illumination Microscopy (SIM) to analyze the distribution of MTs with and without a phagocytic target. In the absence of phagocytosis, the MT labels showed a 3D web like presence, essentially permeating the entire cytoplasmic volume (Movie 1 & 2). The fibrous structures consisted mostly of thin threads. Microtubule organising centers (MTOCs) in this case were less focused. In a sharp contrast, with MSU, the fibers became much more robust and appeared to involve multiple threads. The overall density however was reduced. MTOCs were more punctual and intense. Most of cells have lost the 3D web-like distribution of the MTs in presence of the crystals (Movie 3 & 4). The MT staining showed a pattern of "wrapping" on the crystals (Figure 3.5-2). We then looked into the detail of this "coating" of MT fibers on the crystals. Ortho views from several cross-sections of a 3D cell image were analyzed. With sections before and after the crystals, MT fibers showed a continuous pattern in the region. However, with a MSU

crystal in the middle, MT fibers showed double solenoid patterns that both went cross the crystal and pulled from the other side, creating a locking mechanism on the crystal (Figure 3.5-2).

Phagocytosis involves two steps. A phagocytic target is first engulfed by pseudopods that are driven by a continuous extension of actin filaments and myosin lying immediately below the membrane of those pods. After the secession of early phagosomes from the membrane, the vesicles are hauled along the MT transports, mainly driven by dynein that is attached to the phagosome as a part of multiple protein complex, towards the minus end of MT fibers (centripetal). We studied how the distribution of actin and MTs were altered with respect to each other and to the crystal during phagocytosis. In a resting cell, actin staining was mostly restricted to the cell periphery and in membrane protrusions. Upon phagocytosis, most DCs lost those extensions and became more spherical. Most actin filaments remained close to the cell membrane with some dotting the crystal. MT network was essentially focused on the crystal with a reduced presence in the cytoplasmic volume (Figure 3.5-3). This unique pattern is consistent with the altered distribution of MT in response to the crystal.

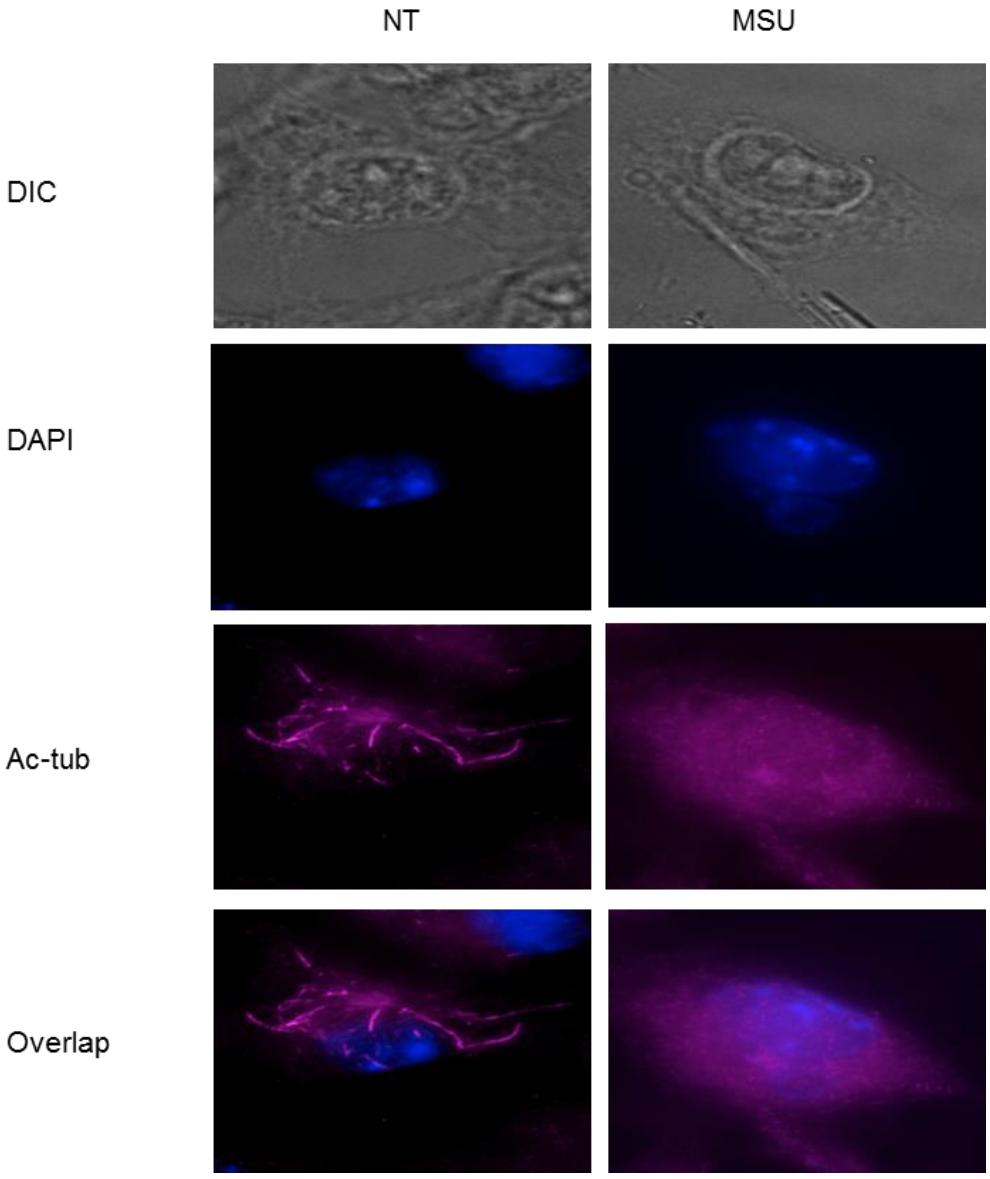

Figure 3.5-1: Comparison of acetylated tubulin distribution in the presence and absence of crystals.

DC2.4 cells were treated with MSU or untreated. Two hours later, the cells were fixed and stained for acetylated α tubulin (magenta) and the nucleus (blue, DAPI).

This panel was done by Anutosh Ganguly with assistance from Aswin Hari.

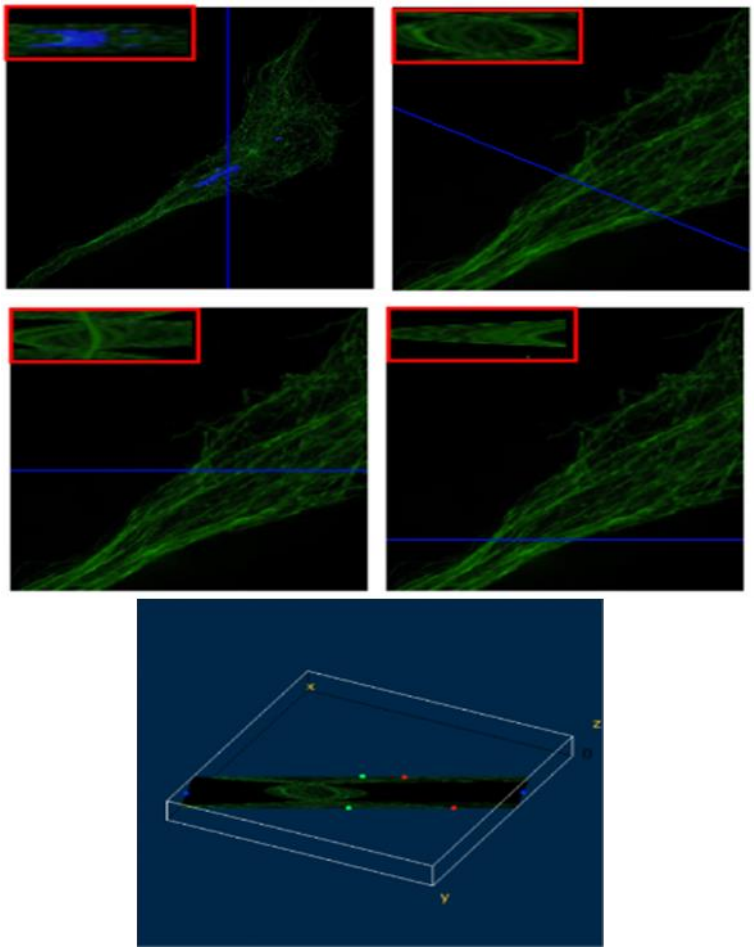

Figure 3.5-2: Ortho slices of a high resolution image generated by SIM.

Top left: Ortho slice in YZ plane indicated by the blue line. The inset shows the view of the slice. It is evident that the microtubules surround the crystal (blue color in the cell). Top right: similar to the top left except that the slice is at XY (45^0) in Z plane showing the microtubules form a tunnel or solenoid like structure surrounding the crystal. Middle left: Ortho slice in a position away from crystal (XZ plane) shows the tunnel of microtubule is closed. Middle right: Ortho slice in a position away from crystal (XZ plane) showing that there is no tunnel. Bottom: a schematic representation of the tilted angle of the ortho slice in the top right, to arrange the view so that it is perpendicular to the axis of the tunnel.

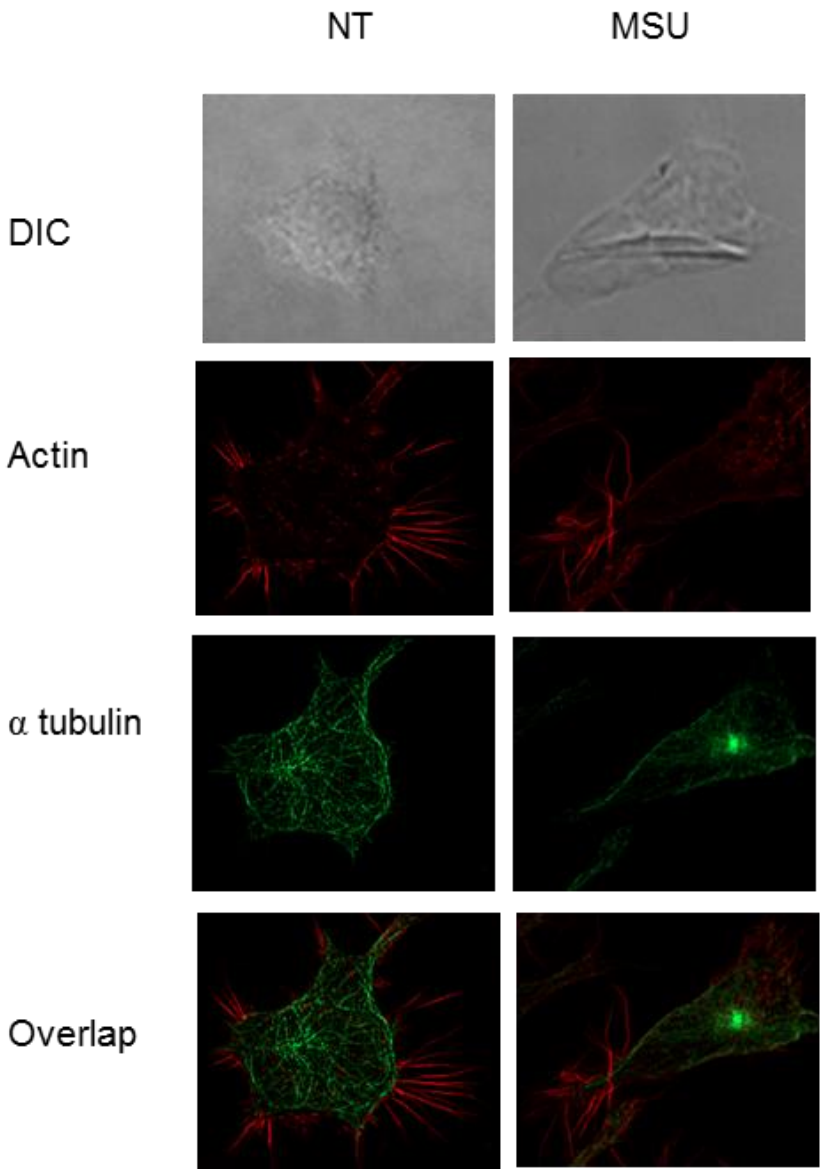

Figure 3.5-3: Actin and tubulin double stain of DCs in presence and absence of MSU.

DC2.4 cells treated with MSU and untreated cells were fixed and stained for the distribution of actin (red) and microtubule (green) in the presence or absence of the stimulus, as described in the methods.

SIM imaging was done by Shevan Davies with assistance from Aswin Hari and Anutosh Ganguly

3.6 Endocytic antigens during phagocytosis have reduced access to the MT transportation

Endocytoic and phagocytic vesicles share the molecular motors for their transportation. The extensive use of this system to handle phagocytic cargos may impact the endosomal transport and/or processing of antigens associated with endosomes. To test this possibility, we traced Alexa-488-OVA by Total Internal Reflection Fluorescence Microscopy (TIRFM). While the overall antigen uptake was not affected by the presence of MSU crystals (Figure 3.2-8), the Alexa-488 pattern was more scattered, creating a hue around the cell while undergoing phagocytosis (Figure 3.6-1 and Movie 8-10). The number of labelled objects in motion was also low. Without phagocytosis, the Alexa-488 staining was overall more punctual and well defined (Figure 3.6-1 and Movie 5-7). Since Alexa-488 is stable from pH 4 to 10, it should label both early and late stage compartments in the endosomal maturation (4 hours of incubation time). Thus the observation represented by an overall reduced degree of vesicular motion and an inability for the label to reach lysosomes imply retardation of endosomal progression. The result was consistent with earlier observations that more endosomes developed into late endosome/lysosome without phagocytic signaling (Figure 3.4-8).

To further verify that the capacity of MT system was inversely associated with cross presentation of soluble antigens, we altered the MT traffic by inhibitors. Dynasore is a dynamin blocker that is essential in closing up the endocytic cup and the secession of endocytic vesicles from the plasma membrane (Figure 3.6-2). It is therefore expected to inhibit the endocytic antigen uptake and prevent any traffic of vesicles on MTs. This was indeed the case as OT-1 T cell activation was inhibited byDynasore, (Figure 3.6-3). Blocking kinesin with STLC had little effect on the cross presentation (Figures 3.6-2 and 3.6-3). This was expected as endocytic recycling towards the cell surface does not require MTs. Since there is no specific inhibitor for dynein, we tested

the general importance of MTs in this type of cross presentation. Nocodazole depolymerizes the MTs and creates a cell devoid of MTs compared to untreated controls (Figure 3.6-4). Our model would predict that a lack of MTs for the minus end movement would accumulate endosomes near cell surface in DCs and should lead to stronger cross presentation as incoming OVA was recycled to the plasma membrane. This was indeed the case (Figure 3.6-5).

Phagocytosis is known to affect endocytosis in a clathrin dependent manner, and entry of solid structures may reduce cell surface availability of clathrin that is critical for some subtypes of endocytosis. To explore whether MSU uptake by DCs had any effect, we performed clathrin staining on MSU treated and untreated DCs. Figure 3.6-6 (and Movie 11 & 12) shows that the overall distribution of clathrin on the DCs was not affected by the concomitant phagocytosis, suggesting that modifications to endosome traffic were the most likely mechanism regulating cross presentation.

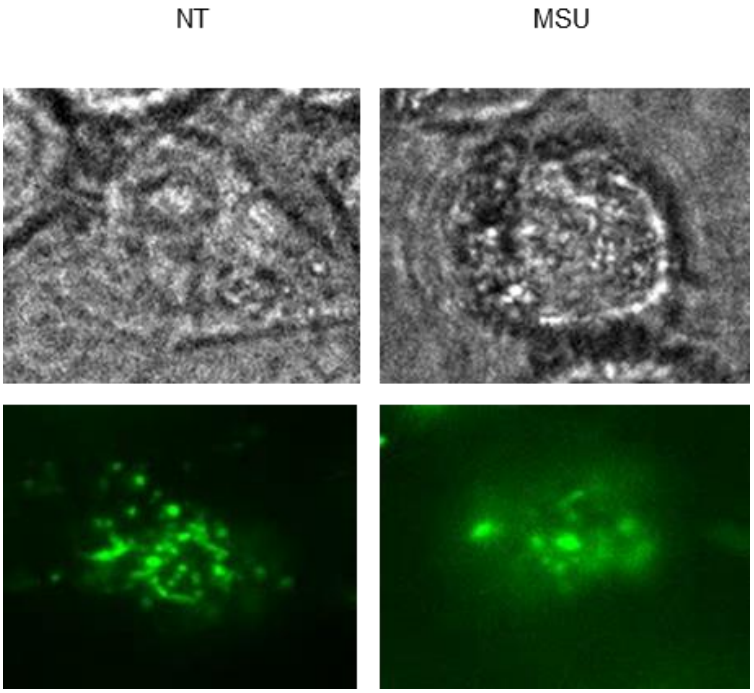

Figure 3.6-1: Live cell imaging of fluorescent OVA uptake by TIRF microscopy.

Top: DIC images taken from DC2.4 cells fed with Alexa 488 labeled OVA, either treated or untreated with MSU crystals for 1 hour described in the methods. Bottom: the same image showing Alexa fluorophores instead from a TIRF microscope. In the supplemental movies, notice the differences in overall numbers of defined bright spots in untreated DCs and the increased background hue in treated DCs.

This experiment was done by Libing Mu with assistance from Chenguang Xu.

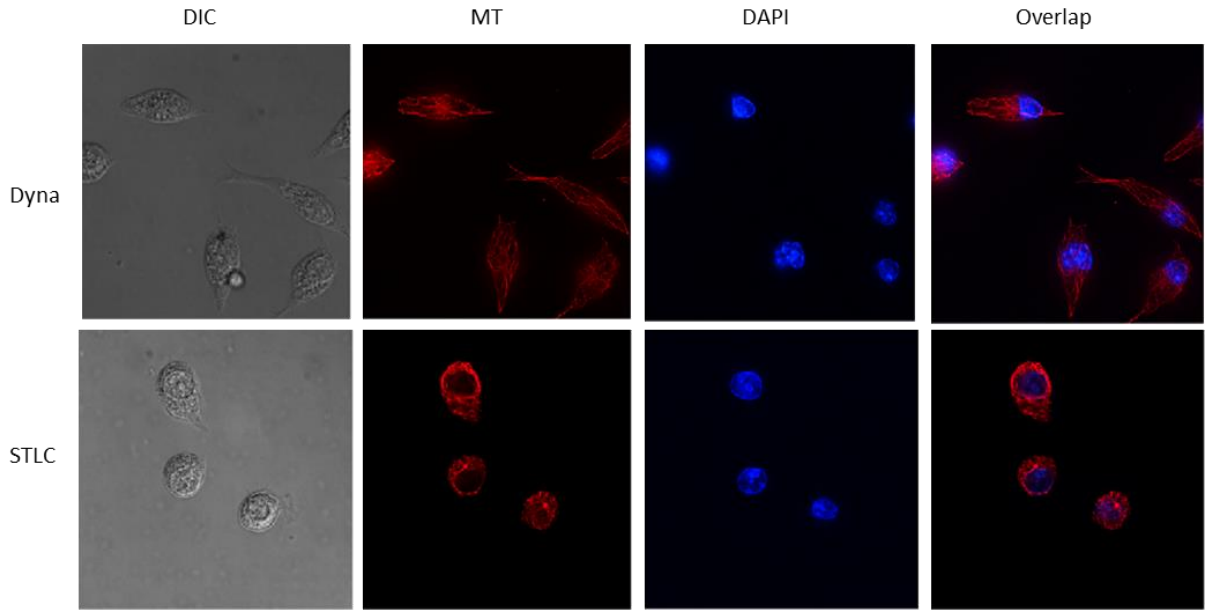

Figure 3.6-2: Images showing DCs in the presence of inhibitors of tubulin function.

DC 2.4 cells were treated with Dynosore, STLC and stained for Tubulin.

These images are representative of three independent fields of view showing similar trends.

Imaging was done by Anutosh Ganguly with assistance from Aswin Hari.

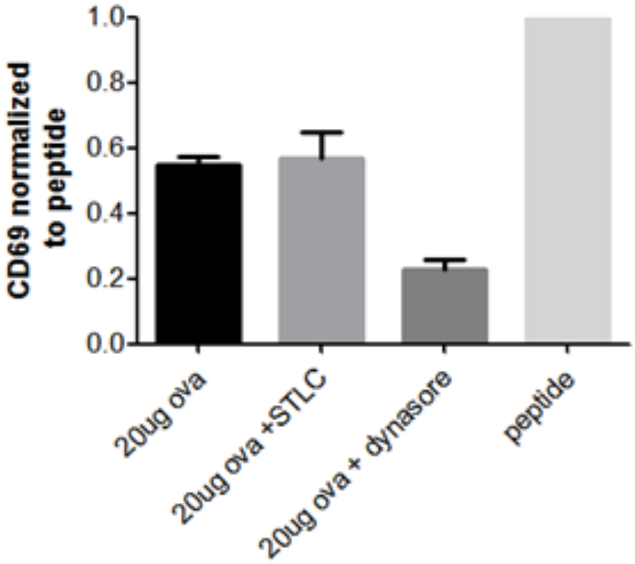

Figure 3.6-3: Cross presentation in the presence of inhibitors of tubulin function.

DC2.4 cells were used as in other cross presentation assays using OT-1 T cells except that STLC and Dynasore were used at the indicated concentrations in place of MSU to mimics the effect on the MTs. The medium with inhibitor was exchanged for fresh medium before T cell addition. The data is average of three independent experiments with SEM.

A one way ANOVA was done followed by post hoc test (Sidak's multiplicity test) to compare the selected columns.

P value- 20 µg OVA vs. 20 µg OVA + STLC- N.S. 20 µg OVA vs. 20 µg OVA + Dynasore- **.

Experiments were done by Aswin Hari.

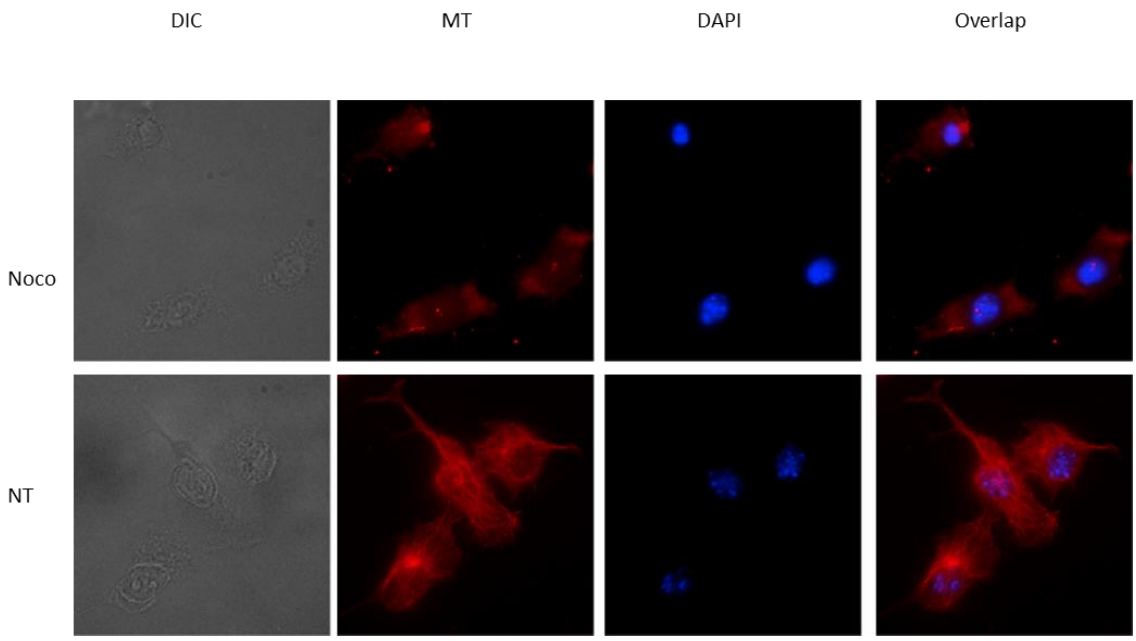

Figure 3.6-4: Images showing DCs in presence of inhibitor that depolymerizes tubulin.

DC 2.4 cells were left untreated and treated with Nocodazole and stained for Tubulin as described in the methods.

These images are representative of three independent fields of view showing similar trends.

Imaging was done by Anutosh Ganguly with assistance from Aswin Hari.

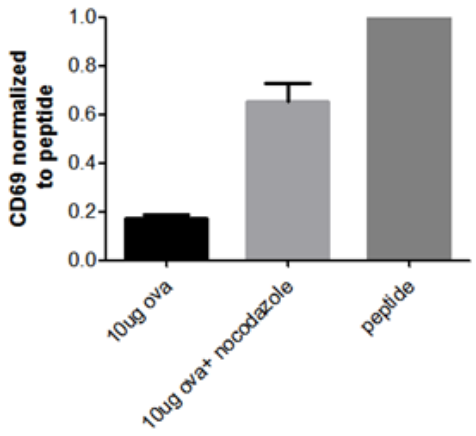

Figure 3.6-5: Cross presentation in the presence of inhibitor that depolymerizes tubulin.

DC2.4 cells were used as in other cross presentation assays using OT-1 T cells except Nocodazole at the indicated concentration was used as the treatment. The medium with Nocodazole was exchanged for fresh medium before T cell addition.

The data is the average of three independent experiments with SEM.

A one way ANOVA was done followed by post hoc test (Sidak's multiplicity test) to compare the selected columns.

P value- 10 µg OVA vs. 10 µg OVA + Nocodazole- ****

Experiments were done by Aswin Hari.

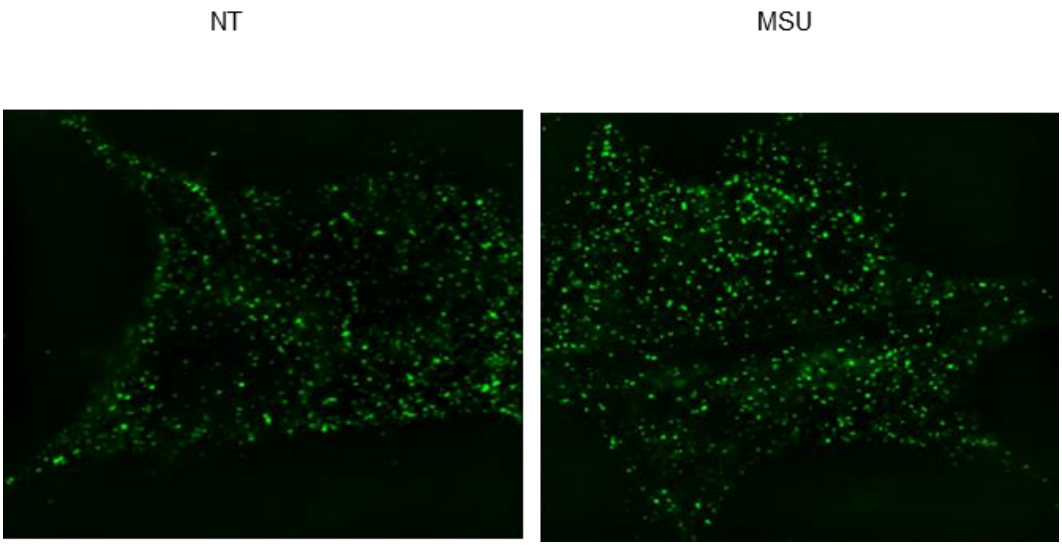

Figure 3.6-6: Images showing clathrin distribution in DCs in the presence and absence of MSU.

DC2.4 cells with or without treatment of MSU for 2 hours were fixed with PFA, blocked and stained for Clathrin. Stack images from the same SIM were used to generate the supplemental movies of clathrin distribution (see movies-11-12).

These images are representative of three independent fields of view showing similar trends.

This experiment was done by Libing Mu.

3.7 ROS and Cathepsin S are involved in soluble antigen cross presentation

Our data suggested that OVA can be processed in the endocytic compartment. To rule out the possibility of antigen translocation to the cytosol, we tested whether the redirected class I antigen required TAP for presentation. Figure 3.7-1 shows that TAP deficient BMDCs sensed MSU crystals and showed enhanced cross presentation, suggesting that cytosolic antigen processing was not essential for the soluble antigen cross presentation. In DCs, phagocytosis activates NOX2 (NADPH oxidase), and its associated ROS inhibits endosomal peptidase [65, 66]. This step is critical in protecting antigenic class I epitopes from further destruction. To explore if this mechanism was employed here, we generated DCs from CYBB (cytochrome B β chain) and NCF (Neutrophil cytosolic factor 1) deficient mice. While CYBB mice lack the gp91 subunit, NCF mice lack phox41, one of the smaller subunits of the NOX2 enzyme complex. CYBB- and NCF-deficient DCs failed to mediate the cross presentation (Figure 3.7-2 and Figure 3.7-3 respectively). These DCs when pulsed with OVA peptide showed no defect in activating OT-1 cells. This suggests that ROS generation during phagocytosis is important in dampening the proteolysis for better cross presentation.

To confirm that endosomal proteolysis was critical here, we tested general aspartic and amino peptidase inhibitors. Figure 3.7-4 shows that while both aspartic and amino peptidase inhibition stunted the OT-1 activation to some extent, the general proteolysis inhibitor (MG132) blocked it to a greater extent, suggesting another category of proteases might control the relevant epitope generation. From endosomes, there are several proteases that can process antigens for loading on MHC class I molecules. This led us to search for specific protease activities responsible for the cross presentation. Cathepsin L- and B- deficient DCs had no reduction in this mode of antigen presentation as both CD69 expression and IL-2 production by OT 1 T cells

were intact in response to MSU (Figures 3.7-5 and 3.7-6). However, Cathepsin S deficiency led to reduced IL-2 production by OT 1 cells (Figure 3.7-7). Importantly, Cathepsin S deficient cells no longer responded to particle stimulation for higher levels of cross presentation (Figure 3.7-7). Similar results were obtained with a specific Cathepsin S inhibitor (Figure 3.7-8). In some experiments and for unknown reasons, Cathepsin S-deficient DCs stimulated slightly stronger CD69 but not IL-2 activities at the basal level, yet they failed to show an enhanced response to MSU stimulation in both cases. Other than adding additional trials, we compared CD69 levels between C57BL/6 BMDCs and Cathepsin S -deficient BMDCs at lower OVA concentrations. As shown in Figure 3.7-9, Cathepsin S-deficient showed significant reduction in CD69 levels and the baseline was comparable to wild type. In all those assays, peptide loaded Cathepsin B-, L- and S-deficient DCs showed no intrinsic defect in antigen presentation with peptide pulsing (Figures 3.7-5, -6, -7, all Cathepsin assays). The result was consistent with the understanding that cathepsin S is the only major protease active in early endosomes that is known to play a role in antigen processing (pH range 6.0-7.5) [29]. Therefore, it appeared that the main cross presenting epitopes from endocytic sources were processed by Cathepsin S.

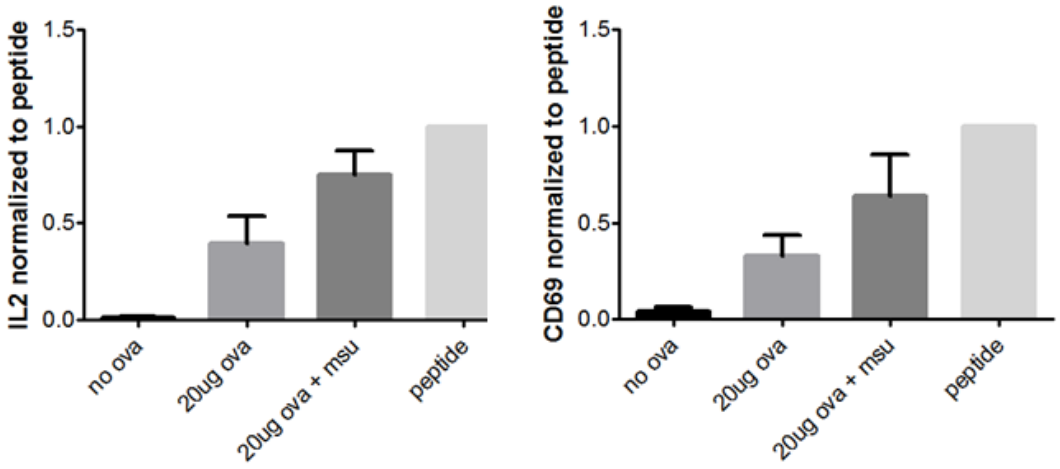

Figure 3.7-1: Use of TAP-deficient BMDCs to study involvement of the cytosolic contribution to antigen processing.

Expression of CD69 and IL-2 levels as in other cross presentation assays by OT-1 T cells upon stimulation by TAP-deficient BMDCs.

A one way ANOVA was done followed by post hoc test (Sidak's multiplicity test) to compare the selected columns.

CD69- Panel represents average of three independent experiments with SEM. P value – 20 µg OVA vs. 20 µg OVA + MSU- **.

IL-2- Panel represents average of three independent experiments with SEM. P value – 20 µg OVA vs. 20 µg OVA + MSU- *.

These assays were done by Aswin Hari with assistance from Raymond Lam.

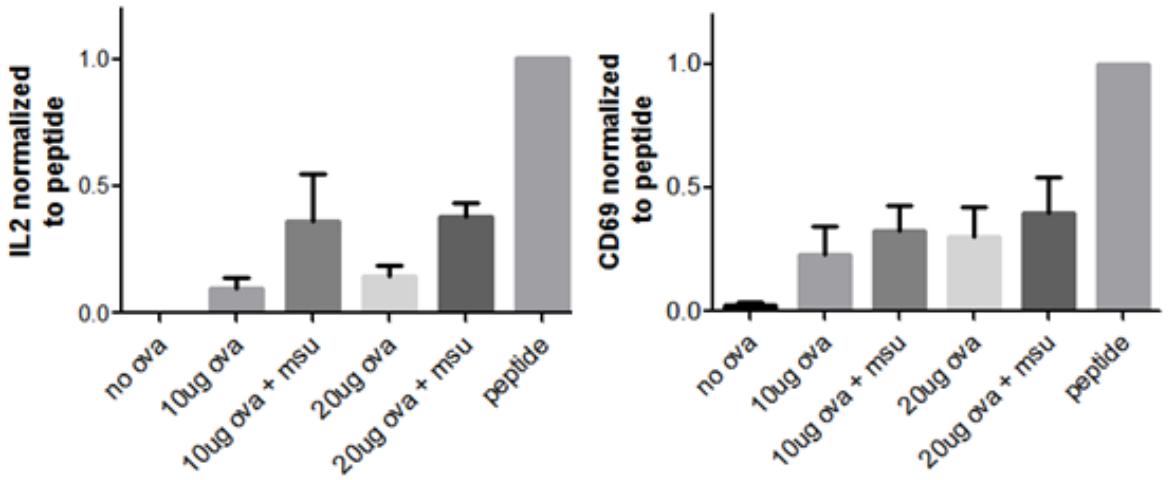

Figure 3.7-2: Production of IL-2 (left panel) and Expression of CD69 (right panel) by OT-1 T cells were stimulated by CYBB-deficient BMDCs.

Expression of CD69 and IL-2 levels as in other cross presentation assays by OT-1 T cells upon stimulation by CYBB-deficient BMDCs.

A one way ANOVA was done followed by post hoc test (Sidak's multiplicity test) to compare the selected columns.

CD69- Panel represents average of four independent experiments with SEM. P value -20 µg OVA+ MSU vs. peptide- ***, other comparisons -N.S

IL-2- Panel represents average of three independent experiments with SEM. P value -20 µg OVA+ MSU vs. peptide- ***, other comparisons -N.S

These assays were done by Aswin Hari with assistance from Raymond Lam.

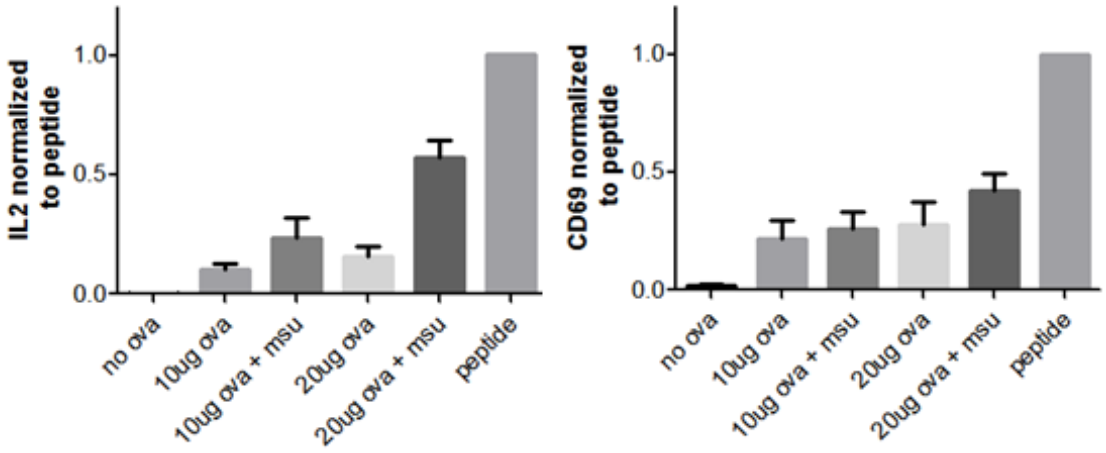

Figure 3.7-3: Production of IL-2 (left panel) and Expression of CD69 (right panel) by OT-1 T cells were stimulated by NCF-deficient BMDCs.

Expression of CD69 and IL-2 levels as in other cross presentation assays by OT-1 T cells upon stimulation by NCF-deficient BMDCs.

A one way ANOVA was done followed by post hoc test (Sidak's multiplicity test) to compare the selected columns.

CD69- Panel represents average of three independent experiments with SEM. P value -20 µg OVA+ MSU vs. peptide - *, other comparisons - N.S

IL-2- Panel represents average of three independent experiments with SEM. P value -20 µg OVA+ MSU vs. peptide - *, other comparisons - N.S

These assays were done by Aswin Hari with assistance from Raymond Lam.

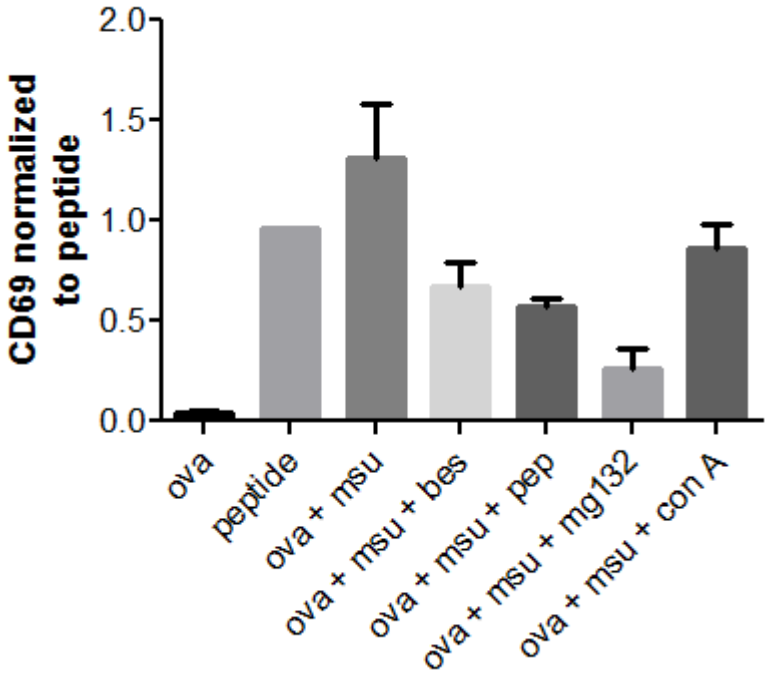

Figure 3.7-4: Levels of CD69 expressed by OT-1 T cells upon stimulation by C57BL/6 BMDCs in the presence of indicated inhibitors.

Expression of CD69 as in other cross presentation assays by OT-1 T cells upon stimulation by C57BL/6 BMDCs except with indicated inhibitors.

A one way ANOVA was done followed by post hoc test (Sidak's multiplicity test) to compare the selected columns.

CD69- Panel represents average of three independent experiments with SEM. P value - OVA + MSU vs. OVA+ MSU +bestatin (Aminopeptidase inhibitor) -*, OVA + MSU vs. OVA+ MSU +pepstatin (Aspartic protease inhibitor) -**, OVA + MSU vs. OVA+ MSU +MG132 (general protease inhibitor) -****, OVA + MSU vs. OVA+ MSU +concanamycin A (V-ATPase inhibitor)- N.S

This experiment was done by Aswin Hari.

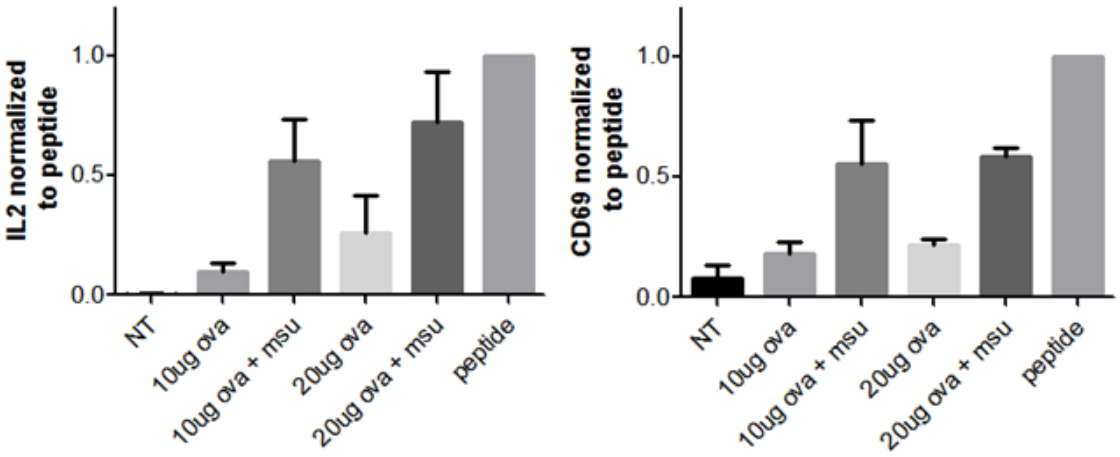

Figure 3.7-5: Production of IL-2 (left panel) and expression of CD69 (right panel) by OT-1 T cells were stimulated by Cathepsin L-deficient BMDCs.

Expression of CD69 and IL-2 levels as in other cross presentation assays by OT-1 T cells upon stimulation by cathepsin L-deficient BMDCs.

A one way ANOVA was done followed by post hoc test (Sidak's multiplicity test) to compare the selected columns.

CD69- Panel represents average of four independent experiments with SEM. P value -10 µg OVA vs. 10 µg OVA + MSU - *, 20 µg OVA vs. 20 µg OVA + MSU -**.

IL-2- Panel represents average of three independent experiments with SEM. P value -10µg OVA vs. 10 µg OVA + MSU - *, 20 µg OVA vs. 20 µg OVA + MSU -**.

This experiment was done by Aswin Hari with assistance from Raymond Lam.

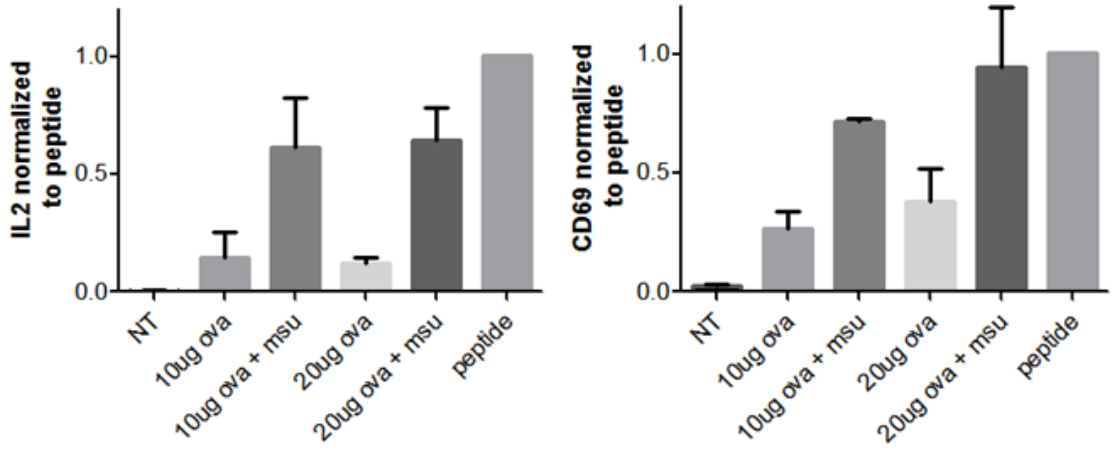

Figure 3.7-6: Production of IL-2 (left panel) and expression of CD69 (right panel) by OT-1 T cells were stimulated by Cathepsin B-deficient BMDCs.

Expression of CD69 and IL-2 levels as in other cross presentation assays by OT-1 T cells upon stimulation by cathepsin B-deficient BMDCs.

A one way ANOVA was done followed by post hoc test (Sidak's multiplicity test) to compare the selected columns.

CD69- Panel represents average of three independent experiments with SEM. P value -10 µg OVA vs. 10 µg OVA + MSU - *, 20 µg OVA vs. 20 µg OVA + MSU -**.

IL-2- Panel represents average of three independent experiments with SEM. P value -10 µg OVA vs. 10 µg OVA + MSU - *, 20 µg OVA vs. 20 µg OVA + MSU -**.

This experiment was done by Aswin Hari with assistance from Raymond Lam.

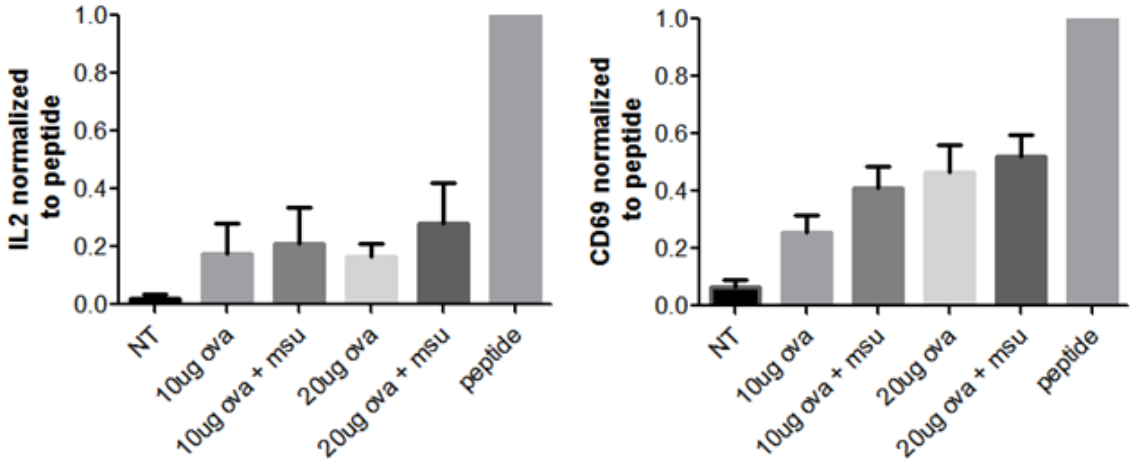

Figure 3.7-7: Production of IL-2 (left panel) and expression of CD69 (right panel) by OT-1 T cells were stimulated by Cathepsin S-deficient BMDCs.

Expression of CD69 and IL-2 levels as in other cross presentation assays by OT-1 T cells upon stimulation by cathepsin S-deficient BMDCs.

A one way ANOVA was done followed by post hoc test (Sidak's multiplicity test) to compare the selected columns.

CD69- Panel represents average of nine independent experiments with SEM. P value –none of the OVA vs. OVA + MSU comparisons were significant.

IL-2- Panel represents average of four independent experiments with SEM. P value - none of the OVA vs. OVA + MSU comparisons were significant.

This experiment was done by Aswin Hari with assistance from Raymond Lam.

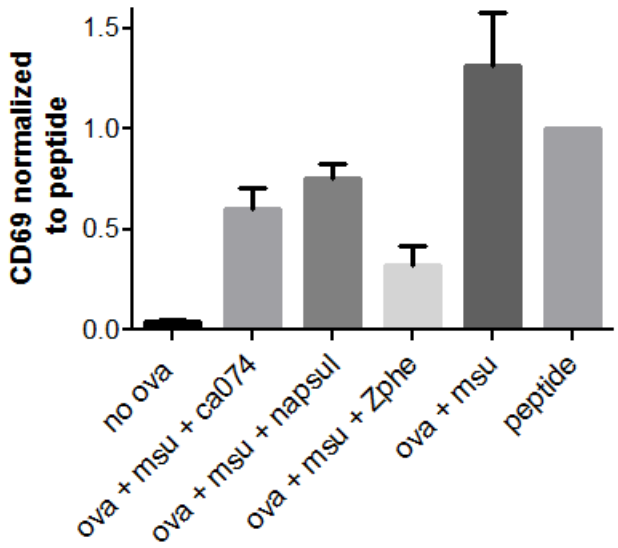

Figure 3.7-8: Expression of CD69 by OT-1 T cells upon stimulation by C57BL/6 BMDCs in the presence of indicated inhibitors.

Expression of CD69 as in other cross presentation assays by OT-1 T cells upon stimulation by C57BL/6 BMDCs except with indicated inhibitors.

A one way ANOVA was done followed by post hoc test (Sidak's multiplicity test) to compare the selected columns.

CD69- Panel represents average of three independent experiments with SEM. P value- OVA + MSU vs. OVA+ MSU +Zphe (Cathepsin S inhibitor) -****, OVA+ MSU vs. OVA+ MSU +CA074a (Cathepsin L inhibitor)-**, OVA + MSU vs. OVA+ MSU +napsul (Cathepsin B inhibitor) -*

This experiment was done by Aswin Hari.

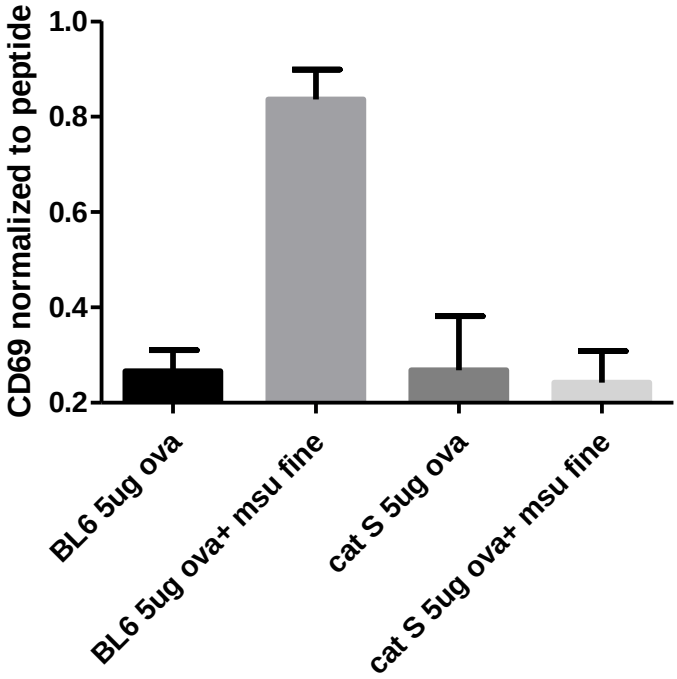

Figure 3.7-9: Expression of CD69 by OT-1 T cells upon stimulation by OVA fed C57BL/6 and Cathepsin S -deficient BMDCs in the presence of MSU.

Expression of CD69 as in other cross presentation assays by OT-1 T cells upon stimulation by C57BL/6 and cathepsin S-deficient BMDCs.

A one way ANOVA was done followed by post hoc test (Sidak's multiplicity test) to compare the selected columns.

CD69- Panel represents average of three independent experiments with SEM. P value- C57BL/6 5 μg OVA + MSU vs. 5 μg OVA+ MSU- **. Cathepsin S -deficient- N.S.

This experiment was done by Aswin Hari.

3.8 Phagocytosis triggers class I cross presentation of soluble antigen *in vivo*.

To study the *in vivo* relevance of our findings, we tested this phenomenon in mice. C57BL/6 mice were injected with CFA or MSU and OVA subcutaneously to drive the antigen into the class I pathway. Separately, CFSE labelled OT-1 and OT-II cells (isolated from spleens and lymph nodes) were intravenously injected and their proliferation was analyzed six days later. Injection of MSU triggered strong proliferation of OT-1 cells (Figure 3.8-1). OT-II activation was not altered, as it was possible that OVA could still reach most DCs that had not been encountered by MSU, thus still maintained the class II presentation (Figure 3.8-1). CD8 activation on the other hand, would require only a small population of DCs to be turned on by MSU. To study how Cathepsin S-deficiency affected this phenomenon, we used Cathepsin S-deficient mice to conduct the same assay. Figure 3.8-2 shows that as in the *in vitro* setting, Cathepsin S-deficient mice had a slightly higher basal OT-1 proliferation, however adding MSU did not result in a higher response, similar to the in vitro observation. We also tested whether antibody production, a result of CD4 T cell activation, was affected by MSU. Figure 3.8-3 shows that in the presence of MSU, IgG1 antibody production was reduced. Interestingly, IgG2a response remained intact. To test this change in CD4 T cells directly, we injected OT-II cells intravenously into congenic marker mismatched B6 recipient mice and delivered OVA with or without MSU subcutaneously. After two weeks the OT-II cells were isolated and stained for intracellular IL-4 and IFN-γ production. With MSU injection, while IFN-γ expression was slightly higher, the overall number of positive cells remained very small. The IL-4 positive cells were reduced by about 80% (Figure 3.8-4). This shift away from a dominant Th2 phenotype was in line with the notion that CD8 activation was in place.

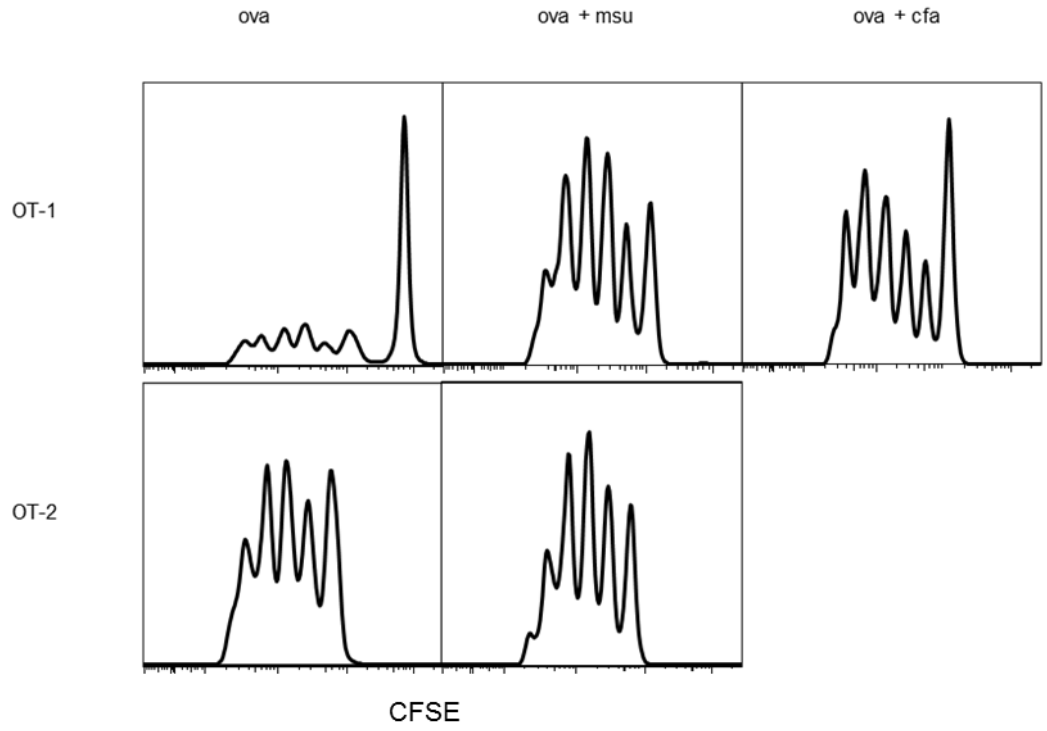

Figure 3.8-1: CFSE proliferation assay of co-injected OT-1-OT-II cells in C57BL/6 mice.

As described in the methods, CFSE labeled OT-1 (top panels) and OT-II (bottom panels) were infused intravenously into C57BL/6 recipients while MSU crystals and soluble OVA were injected subcutaneously the day before. Splenic and lymph node CD4 T cells bearing congenic markers for OT-1 and OT-2 cells were gated and analyzed for division after six days. OT-II + CFA was over divided at day 6 (not shown).

Each representative plot is from a group of four mice in each condition.

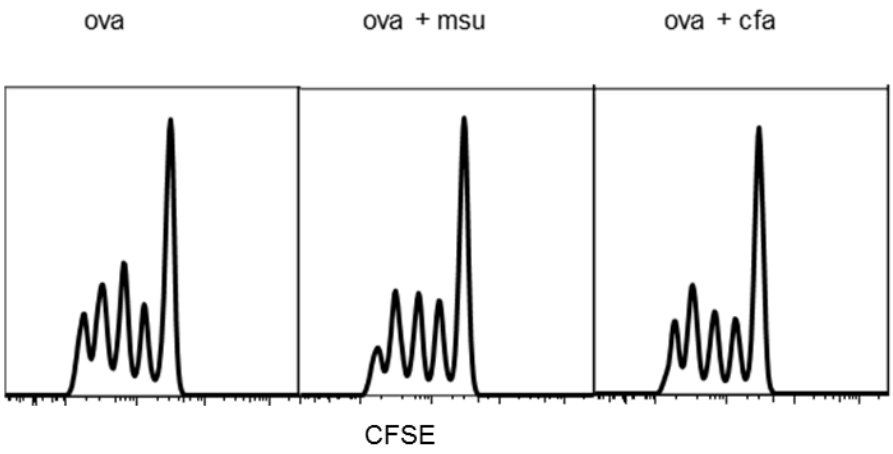

Figure 3.8-2: CFSE proliferation assay of co-injected OT-1-OT-II cells in Cathepsin S-deficient mice.

Identical to previous panels except that cathepsin S deficient mice were used as recipients. Each representative plot is from a group of four mice in each condition.

CFSE assays were done by Aswin Hari with assistance from Aileen Yang, Yie Ping and Laurie Kennedy.

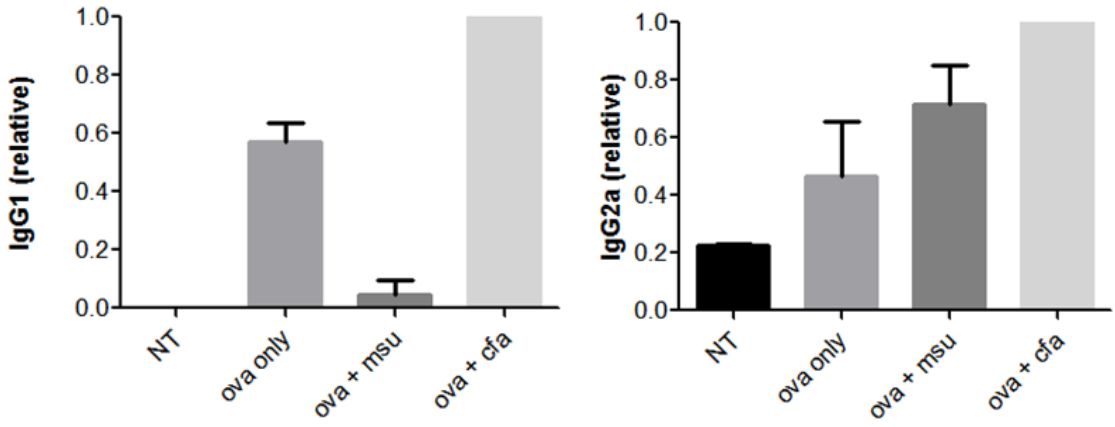

Figure 3.8-3: Antibody titers from immunizations conducted to study the phenomenon *in vivo*.

C57BL/6 mice were immunized with OVA alone, with MSU or CFA as described in the *in vivo* assays section of the methods. Anti-OVA IgG1 (left panel) or IgG2A titers (right panel) were determined after 4 weeks. All antibody levels are expressed in I.U/ml normalized against CFA mouse levels.

Panels are an average from a minimum of four mice in each group with SEM.

A one way ANOVA was done followed by post hoc test (Sidak's multiplicity test) to compare the selected columns.

IgG1- P value -NT vs. OVA + CFA ****, OVA + CFA vs. OVA + MSU ****, OVA only vs. OVA + MSU ****.

IgG2a- P value - all comparisons N.S.

These assays were done by Aswin Hari and Melanie Stenner.

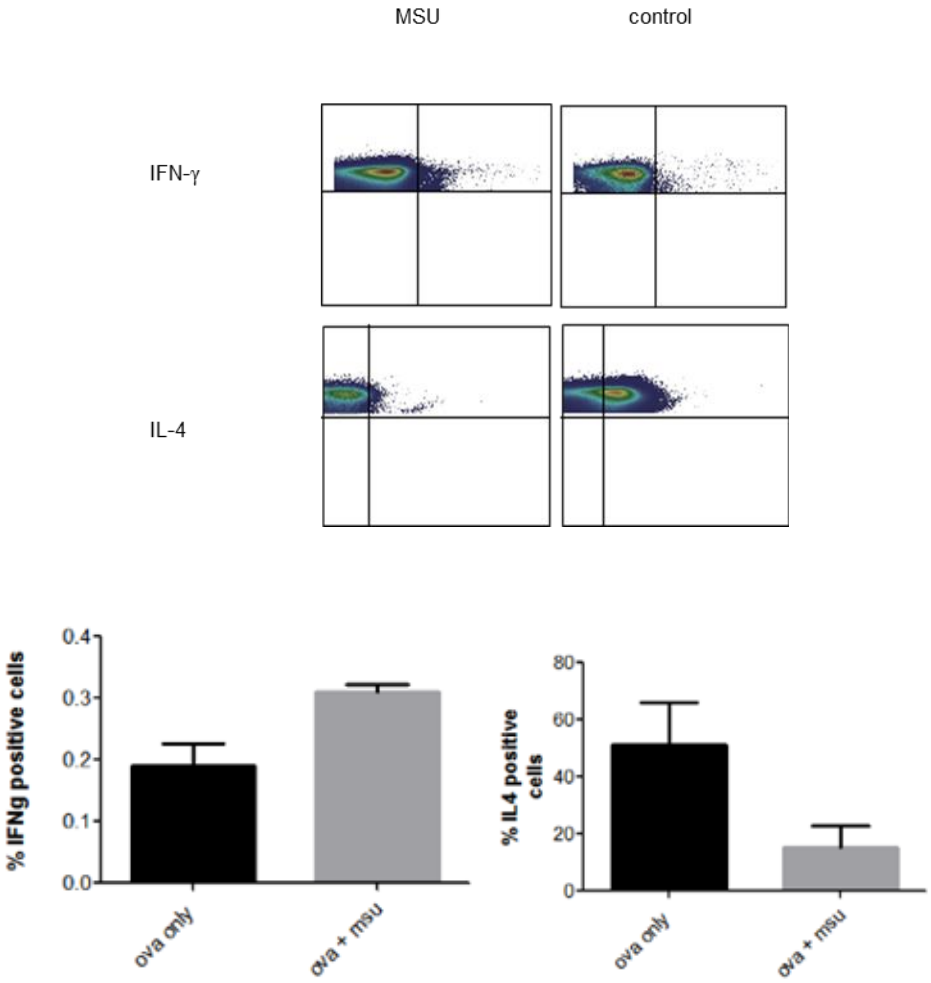

Figure 3.8-4: Intracellular staining to demonstrate a skew away from Th2 profile *in vivo*.

C57BL/6 recipients of OVA/MSU injection in the foot pads as described were boosted with the same regimen after 1 week of initial injections. At the end of two weeks, draining lymph nodes were collected and CD4 cells were isolated as described. The intracellular staining for IFN-γ and IL-4 was performed. Only gated CD4 + cells are shown in the panel. Bar graphs were created with the percentages of IFN-γ and IL-4 positive cells from the plots. Panels are an average from four mice in each group with SEM. Student t test was used. IL4- P value- *.

These experiments were done by Aswin Hari with assistance from Yie Ping and Laurie Kennedy.

Chapter Four: **Discussion**

4.1 Discussion

Cross presentation was first discovered using antigens that were cell associated. Cell associated antigens taken up through phagocytosis were localized in the early phagosomes before undergoing partial degradation by resident proteases. This partial degradation allows them to undergo cytosolic transfer where they are cleaved by proteasomes. The antigenic peptides are believed to be sent into the ER for loading on MHC I molecules. The transport of antigenic peptides was demonstrated to be dependent on TAP in a model that used OVA coated latex beads [46, 119, 135]. A variant of the cytosolic cross presentation pathway was discovered later by Shen et. al. and became known as vesicular cross presentation [29]. The relative contribution of either type of presentation *in vivo* is under considerable debate. However one thing remains constant in those discussions. When it comes to cell-associated antigens or other particulate antigens, phagocytosis was considered to be merely the means of delivering antigens to the relevant compartments, in this case early phagosomes. Thus it is not surprising that for the last two decades extensive work done on cross presentation was based on phagosomes as the model. This has led to extensive investigation on how phagosomal contents are processed and transferred into the MHC I system [6, 31].

The main proposal of this thesis is to suggest that phagocytosis is not just a means of antigen delivery, but that there is a signaling aspect that has been underestimated. The events leading from these signals include retarded endosomal maturation and modulation of proteolysis. Arrest of early endosomes close to the plasma membrane occurs through interference of the normal progression of vesicles and the modulation of proteolysis by ROS that prevents excessive antigen degradation. These two factors along with accumulation of cathepsin S in the early

endosomes lead to epitope generation, given cathepsin S is the only protease known to be active at a higher pH [136]. In addition cathepsin S is known to be expressed at higher levels in DCs [136, 137]. The main underlying mechanism by which this arrest of endosomal maturation is achieved seems to be structural remodeling of the cytoskeleton during phagocytosis.

Our hypothesis to test phagocytic signal based cross presentation arose from AFM experiments where inhibition of Syk kinase enhanced presentation on MHC II molecules. Other than testing MSU crystals, we also tested BCP crystals and latex beads. All the three stimuli showed enhanced presentation on MHC I molecules. We found that antigens given in the presence of phagocytic stimuli became retained in the early endosomes. With the processing not dependent on cytosolic processing, as shown by the relatively normal crosspresentation in the absence of TAP, the cleavage is dependent on proteases that are located in the compartment. The antigen is processed by cathepsin S in the compartment with ROS modulating the level of proteolysis. We have found that other cathepsins such as cathepsin L or B, aminopeptidases and aspartic proteases play minimal or dispensable roles. This phenomenon was shown to exist *in vivo* where we have demonstrated enhanced proliferation of CD8 T cells in the presence of phagocytic stimuli. Lower IgG1 levels and IL-4 staining in cells support the notion that a CD8 T cell response is in effect in the presence of phagocytic stimuli.

One of the aspects of cross presentation that remains unknown is the source of MHC I molecules. The presence of MHC I molecules and related apparatus in early endosomes is controversial and there are a few schools of thought to explain the mechanism of action. These include retrotranslocation of antigen from the phagosome to the cytosol through Sec61 transporter [138] and ER fusion with phagosome [139]. Another potential explanation for their presence in early endosomes is the role of constantly recycling cell surface MHC I molecules

[140, 141]. How MHC I molecules intersect with the phagocytic cargo for epitope loading is currently unclear. None of the proposals stated above fully explain the process or have proven to be the dominant mechanism. The difficulty in part comes from the established observation that phagosomal maturation proceeds only in one direction towards lysosomes and that redirection or recycling of components from a phagosome has never been shown in the literature. Thus for phagocytosis-based cross presentation, a cytosolic escape route is essential for epitope processing. Since early endosomes recycle to the plasma membrane routinely for homeostatic reasons, proposals of endosome-based cross presentation do not need to invoke an escape route to the cytosol for epitope processing [97].

Cathepsin dependent proteolysis and its regulation by ROS induced by phagocytosis fits well with the narrative of known DC characteristics that favor cross presentation [116, 142]. In our model, the involvement of ROS was studied using two strains of knock-out mice, CYBB and NCF, which lack different subunits of the NADPH oxidase enzyme complex. It is clear from the data that in the absence of proteolytic modulation by ROS the epitopes are not presented to OT1 T cells properly. ROS generated during vesicular maturation is known to block extensive proteolysis in these organelles [143-146]. This is also in line with the previously stated observation that reduced proteolysis in DCs is critical for preservation of antigenic epitopes. One interesting observation, as shown in figure 3.7-4, was that addition of concanamycin A did not affect presentation to OT1 T cells significantly. This supports the earlier findings where milder proteolysis in DCs was not associated with a lack of acidification [65, 66] but with the redox state in the compartment. Redox state involvement is a current topic of debate and is also in contrast with another report where the pH drop was said to play a role in the process [66]. In addition, vesicular pH progression was not affected in the presence of phagocytic targets

suggesting the vacuolar membrane proton pump (V-ATPase) recruitment was not affected by phagocytosis. However, it is also possible that our pH measurement system reflected the dominant acidification events in the vesicles containing solid cargos, as our probes were not designed to precisely discriminate phagosome vs. endosome. If this is shown to be the case, then more advanced methods will be needed to measure acidification of compartments that contain the incoming soluble antigens.

The cross presentation efficiency of endosomal antigens appears to be strong. Following phagocytosis, the amount of antigen targeted into the cross presentation pathway increases by about 40 fold. Similar amounts of endosomal antigen appear to be more efficiently cross presented than the phagocytic counterpart. This raises the possibility that in physiological conditions, soluble substances in the extracellular environment may serve as an important source of cross presented antigens. Illustration 4 is a schematic of the model proposed with respect to proteolysis and its control by ROS.

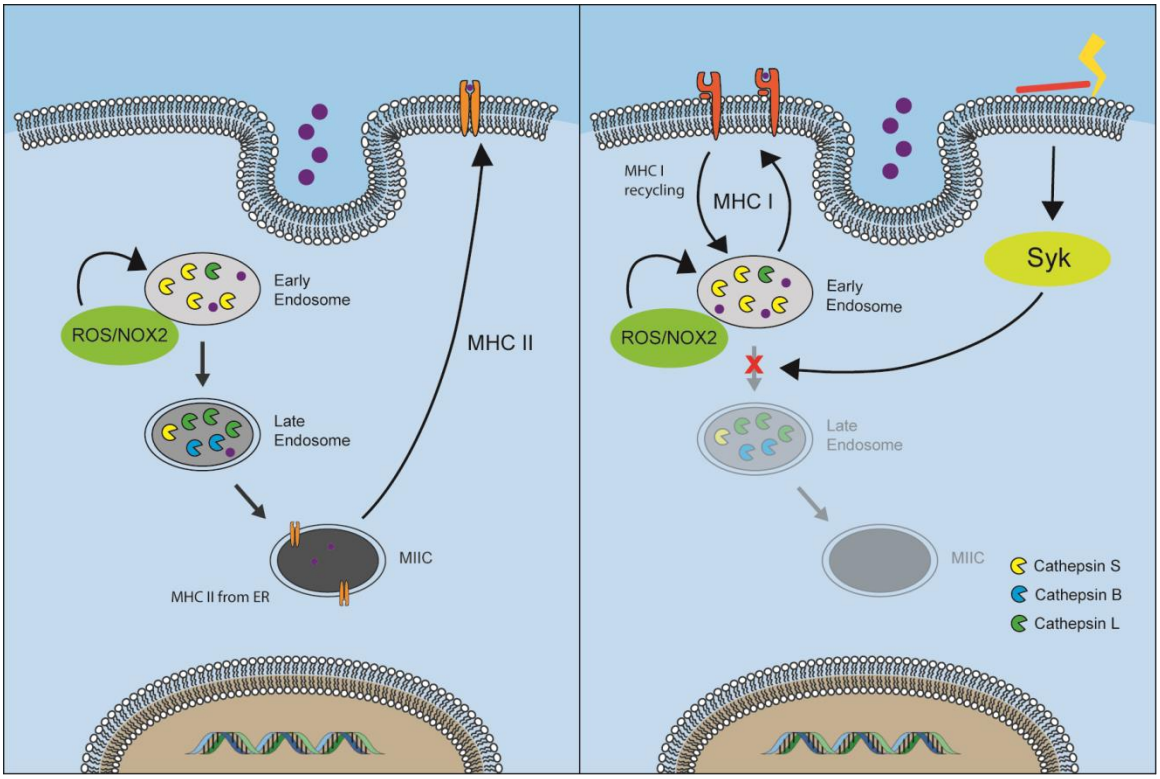

Illustration 4: Schematic of our hypothesis to illustrate our model in antigen processing.

A scheme of the hypothesis on how phagocytosis regulates DC antigen processing: endosomes typically deliver external soluble antigens into the endo/lysosomal pathway for class II antigen presentation. During phagocytosis, endosomes have reduced a ability to move to the peri-nuclear areas. Endosomes arrested for the downward migration use Cathepsin S to digest their cargos and the resulting epitope peptides bind to internalized MHC class I molecules, and return to the cell surface for class I cross presentation. The phagocytic activation also induce ROS/NOX activities that oxidize endosomal proteases, further limiting the excessive digestion of potential class I antigens.

Illustration made by Melanie Stenner.

Cross presentation can be accomplished by phagocytic and endocytosed antigens. In the case of phagocytosed antigens, the cytosolic pathway is considered active. The partially degraded antigens are sent to the proteosome for processing and transferred back into the phagosome/ER for loading. In the case of endocytosed antigens the processing occurs inside the endosomes without the need of the proteosome. Our results suggest that the phagocytic route of cross presentation may not be as efficient as antigens associated with phagocytic cargos. This is possibly due to the fact that the phagocytic route cannot utilize the recycling pathway. While our model may explain potential connections between phagosome mediated cross presentation and the use of exogenous soluble antigen in the presence of phagocytic signaling for MHC I loading, other mechanisms likely exist to explain decades of literature on phagosome-based cross presentation. Other than the scavenger activities in apoptotic cell clearance that are considered immunologically silent [147], phagocytosis of solid particles and cellular remnants induces a diverse set of DC activation events [57]. On DCs and sometimes on macrophages, phagocytosis triggers inflammatory responses. This appears to deliver concomitant solid antigens into the cross presentation pathway [142]. As discussed in the introduction, receptors reportedly involved in cross presentation, including mannose and Fc receptors, are likely to have the intrinsic ability to stimulate DC/macrophage activation, and a common denominator is that those receptors often contain an ITAM motif [148]. Of course, crystal/bead-based phagocytosis does so via aggregating cell membrane lipids and has no explicit requirement for receptors. [53, 54, 149]. With or without receptors, all these activation events may use different pathways that converge at a common point. Cytoskeletal remodeling may be a consequence to all of them, potentially triggering endosome based cross presentation [150-153]. In this study, phagocytosis

triggered endosomal antigen rerouting appears to be a DC specific event; whether the phenomenon appears in other forms of APC activation is unknown.

In the case of cross presentation of endosomal antigens in the presence of phagocytic signals, the most direct hypothesis involves volumetric considerations and competition of resources. When the phagocytic cargo is processed, enzymatic and transportation machinery, such as proteases and MTs, are not fully devoted to the endocytic processing. In this case, conventional MHC class II antigens may be rerouted through efficient recycling pathways; the antigens never reach the MHC II loading site. This would be expressed instead on MHC I molecules, which is cross presentation of external soluble antigens. Since the majority of endosomal contents and membranes are recycled to the cell surface, this proposal seems probable. Nevertheless, the implications of this potential pathway in antigen processing and presentation will be subject of long term studies.

The mechanistic insight in the altered routing of external antigens appears to be in cytoskeletal changes. The large scale of MTs used in hauling phagocytic targets inward appears to be an important phenotype during cross presentation. The main observation is the clustering of MTs around the target, robust appearance of MT fibers and the ubiquitous presence of MTOCs adjacent to the phagocytic cargo. As a consequence, the overall availability of MTs is reduced. This is consistent with the peripheral presence of early endosomes and sluggish movement of vesicles containing soluble cargos. Interestingly, depolymerizing the MTs with Nocodazole had the same effect on cross presentation as phagocytosis, suggesting that the lack of MTs transportation was the main cause of arrested centripetal movement of endosomes. Illustration 5 is a schematic representation of the proposed model in regards to cytoskeletal changes associated with the phenomenon.

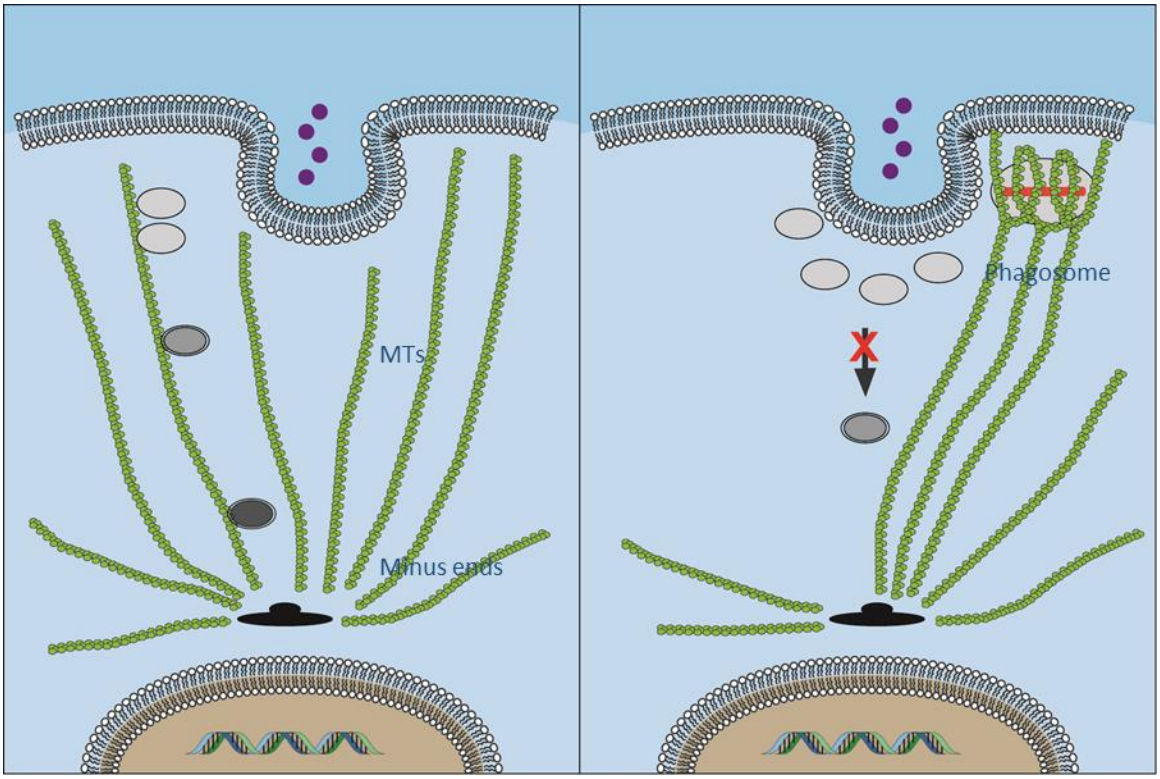

Illustration 5: Schematic of our hypothesis to illustrate our model for microtubule reorganization.

A scheme for a potential mechanism that regulates endosomal traffic during phagocytosis. During the resting state, DCs engulf external soluble substances. The endocytic vesicles fuse to form endosomes. Although the recycling of these endosome contents to the cell surface is an efficient process, some antigens are nonetheless selected for the progression to late endo/lysosomes for class I antigen presentation. This progression is critically dependent on the microtubular system for movement and fusion. During phagocytosis, the MT system is used extensively to handle the phagocytic target; the reduced availability of MTs limits the endosome maturation and centripetal movement.

Illustration made by Melanie Stenner.

As a consequence, endosomes accumulate under the plasma membrane. These endosomes contain proteases, and since they are delayed in the downward motion, cathepsin S has time to process antigens for class I cross presentation. If phagocytic antigens are not covalently attached to their solid structures, and instead have the ability to be partially released to become free antigens extracellularly, this model could provide an explanation to the phagosome based cross presentation as well.

One ramification of our results is to suggest endosomes as an important study target of cross presentation mechanisms. Since most current work focuses on phagosomes, it has been difficult to reach a consensus as to the escape mechanism of cross presenting epitopes into the class I pathway. This could have been a result of ignoring a large source of antigens. A more health relevant implication is to suggest a new method to produce elusive CTL vaccines, as most vaccines fail to take phagocytic signaling into consideration. Future vaccine development will need a holistic understanding of particle size, composition and be capable of precise targeting of the cross presentation pathway to elicit a robust MHC I response. This will enable an enhanced T cell activation and help in development of vaccines against viral diseases and potentially tumours as well. Lastly, our work modifies the classic demarcation of class I and class II antigens as soluble endosomal antigens are not destined to result in class II activation. The DC activation state at the time of their entry sets their route for antigen processing and presentation.

4.2 Future directions

- Investigate tubulin signaling that drives mobilization from the MTOC upon interaction with a phagocytic target and also study whether there is movement of the MTOC towards the phagocytic target stimulating the signal cascade.

  When a DC encounters a phagocytic target, cytoskeletal rearrangements are needed for the interaction. The MTOC being the command center for microtubules has to be prompted to achieve the rearrangements. This occurs through the Ras/Rho pathway and may involve Cdc42. We propose to study this pathway to elicit precise signaling components of the pathway. In addition, the SIM images suggest that the MTOC may be moving towards the phagocytic target. This can be ascertained only by live cell imaging to track the MTOC movement in real-time.

- Test other solid materials and adjuvants currently used in clinical studies separately and in combination to achieve the same effect.

  After testing some solid structures like latex beads, MSU and BCP that are used in basic research, we would like to test clinically used adjuvants such as MF09 or other TLR based adjuvants to study the mechanism behind their actions. These adjuvants generally contain lipid based compounds along with TLR stimulators to drive the adaptive immune system. One of the possibilities that can be probed is whether compounds like MF09 can be used along with solid structures to elicit a greater MHC I response against the antigen of interest.

- Test the lysosomal leakage hypothesis with respect to inflammasome activation by solid structures.

  Inflammasome activation is said to be critical for IL-1β production needed during inflammation. But the mechanism of how an extracellular target that may be in the vesicular system is sensed by the cytosolic NLRP3 inflammasome complex is controversial. One of the proposals is the lysosomal leakage hypothesis wherein a solid structure in the lysosome leads to leakage of the lysosomal contents. We would like to test this proposal to confirm if cathepsin B, which would escape into the cytoplasm by such leakage, was proposed to be the inflammasome activator.

Chapter Five: **Appendix**

5.1 Western blot trials for endosomal isolations.

DCs have been reported to modulate proteolysis to facilitate antigen processing and epitope preservation[44]. When it comes to vesicular cross presentation, Cathepsin S is known to be the main protease that degrades antigens and generates epitopes needed for loading on MHC I molecules[29]. In 1989, a study that characterized proteases, found that DCs in particular were enriched in cathepsin S. Their findings were validated by another study that came out more than a decade later[136, 137]. A British group found that this Cathepsin S was localized in the early endosomes and its distribution showed changes with change in antigenic particle size[120]. There has been a line of research pursued for more than two decades to study the distribution of vesicles and proteases albeit on a low profile. In the quest to isolate endosomes and lysosomes, researchers have mostly used the cell fractionation approach. It involved a tedious process of density ultracentrifugation with or without coating antigens onto gold particles[154, 155]. Recently, Hammond and his colleagues devised a novel protocol to conduct the isolation of these vesicles from brain tissue samples[156]. They used specific antibody-coated magnetic nano particles (Dynabeads, Invitrogen) to grab on to vesicles following a mild lysis of the cells. Given its importance in understanding antigen processing, we decided to pursue a modified version of protocol from Hammond et.al. to isolate endosomes. The purpose was to study differences in the distribution of proteases in presence of phagocytic stimuli. In brief, DCs were harvested after treatment with or without MSU crystals for 2 hours. After lysis under mild conditions, the endosomes were isolated using antibody-tagged magnetic nano particles in the do-it-yourself kit® from Stemcell Technologies. The magnetic beads were tagged using the anti-mouse EEA1 antibody (Santa Cruz). After the isolation process was complete, the endosomal

fractions were separated using SDS-PAGE. The protein bands were probed by western blot using specific anti-mouse antibodies (Cathepsin S: Santa Cruz, Cathepsin L: Millipore and Rab5: Cell Signaling Technologies).

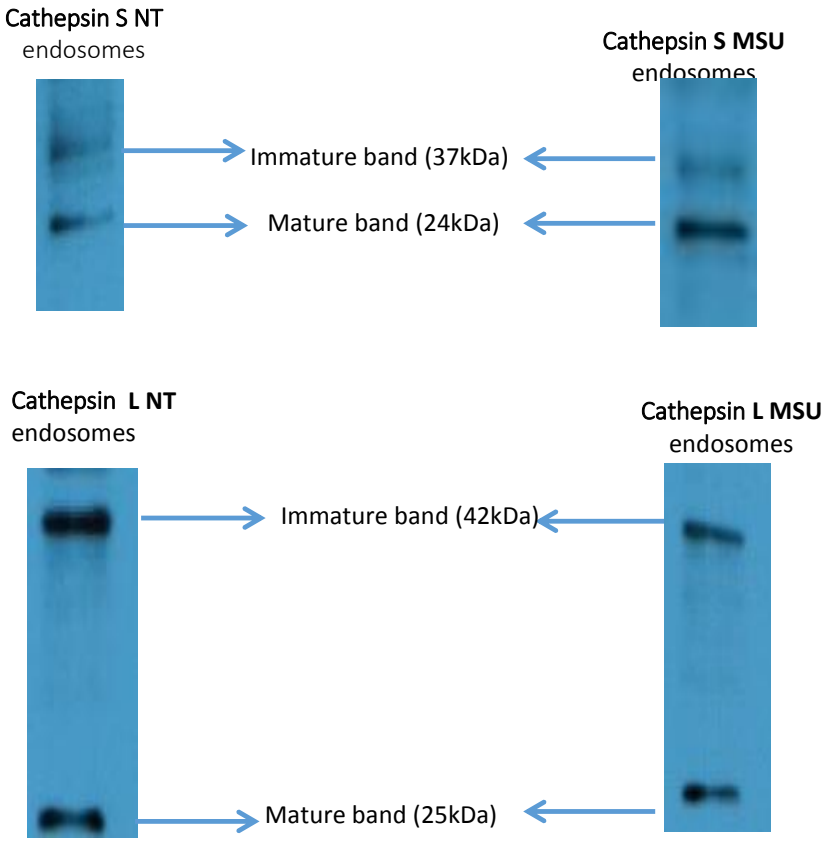

Figure 6.1: Representative western blots of vesicular isolation showing distribution of Cathepsin S and L in early endosomes with or without treatment.

The isolations yielded a pattern which seemed to suggest that Cathepsin S undergoes a shift in distribution with a stimulus compared to untreated controls (Figure 6.1). Even though we obtained an interpretable trend with both Cathepsin S and L, the variability in the results made the results unusable in its current form. The protocol needs further standardization before it can be put to use.

Chapter Six: **References**

1. F. Fenner, D.A.H., I. Arita, Z JeZek, I. D. Ladnyi, *Smallpox and its Eradication.* World Health Organisation, 1988.
2. Jenner, E., *An Inquiry into the Causes and Effects of the Variolae Vaccinae; a Disease Discovered in some of the Western Counties of England, Particularly Gloucestershire, and Known by the Name of The Cow Pox.* 1798.
3. Zinkernagel, R.M. and P.C. Doherty, *Immunological surveillance against altered self components by sensitised T lymphocytes in lymphocytic choriomeningitis.* Nature, 1974. **251**(5475): p. 547-8.
4. Janeway, C.A., Jr., *The immune system evolved to discriminate infectious nonself from noninfectious self.* Immunol Today, 1992. **13**(1): p. 11-6.
5. Mills, K.P.W.a.K.H.G., *Dendritic cells and other innate determinants of T helper cell polarisation* Trends in Immunology, 2013. **XX**(XX).
6. Vyas, J.M., A.G. Van der Veen, and H.L. Ploegh, *The known unknowns of antigen processing and presentation.* Nat Rev Immunol, 2008. **8**(8): p. 607-18.
7. Goldberg, A.L., et al., *The importance of the proteasome and subsequent proteolytic steps in the generation of antigenic peptides.* Mol Immunol, 2002. **39**(3-4): p. 147-64.
8. Kunisawa, J. and N. Shastri, *The group II chaperonin TRiC protects proteolytic intermediates from degradation in the MHC class I antigen processing pathway.* Molecular Cell, 2003. **12**(3): p. 565-76.
9. Trombetta and I. Mellman, *Cell Biology of antigen processing in vitro and in vivo.* annual reviews of Immunology, 2005. **23**: p. 975-1028.
10. Villadangos, J.A. and P. Schnorrer, *Intrinsic and cooperative antigen presenting functions of dendritic-cell subsets in vivo.* Nature Reviews Immunology, 2007. **7**: p. 543-555.
11. Wilson NS and V. JA, *Regulation of antigen presentation and cross-presentation in the dendritic cell network: facts, hypothesis, and immunological implications.* Advances in Immunology 2005. **86**: p. 241-305.
12. Harding, C.V. and H.J. Geuze, *Class II MHC molecules are present in macrophage lysosomes and phagolysosomes that function in the phagocytic processing of Listeria monocytogenes for presentation to T cells.* J Cell Biol, 1992. **119**(3): p. 531-42.
13. Inaba, K., et al., *Efficient presentation of phagocytosed cellular fragments on the major histocompatibility complex class II products of dendritic cells.* J Exp Med, 1998. **188**(11): p. 2163-73.
14. Dengjel, J., et al., *Autophagy promotes MHC class II presentation of peptides from intracellular source proteins.* Proc Natl Acad Sci U S A, 2005. **102**(22): p. 7922-7.
15. Honey, K. and A.Y. Rudensky, *Lysosomal cysteine proteases regulate antigen presentation.* Nature Reviews Immunology, 2003. **3**(6): p. 472-82.
16. Jensen, P.E., *Regulation of antigen presentation by acidic pH.* J Exp Med, 1990. **171**(5): p. 1779-84.
17. Romagnoli, P., et al., *Relationship between invariant chain expression and major histocompatibility complex class II transport into early and late endocytic compartments.* Journal of Experimental Medicine, 1993. **177**(3): p. 583-96.

18. Cresswell, P., *Invariant chain structure and MHC class II function.* Cell, 1996. **84**(4): p. 505-7.
19. Bakke, O. and B. Dobberstein, *MHC class II-associated invariant chain contains a sorting signal for endosomal compartments.* Cell, 1990. **63**(4): p. 707-16.
20. Denzin, L.K. and P. Cresswell, *HLA-DM induces CLIP dissociation from MHC class II alpha beta dimers and facilitates peptide loading.* Cell, 1995. **82**(1): p. 155-65.
21. Christopher C. Norbury, S.B., Keri B. Donohue, David C. Tscharke, Michael F. Princiotta, Peter Berglund, James Gibbs, Jack R. Bennink, Jonathan W. Yewdell, *CD8 T Cell Cross-Priming via Transfer of Proteasome Substrates.* Science, 2004. **304**: p. 1318.
22. Sigal, L.J., et al., *Cytotoxic T-cell immunity to virus-infected non-haematopoietic cells requires presentation of exogenous antigen.* Nature, 1999. **398**(6722): p. 77-80.
23. Heath, W.R., et al., *Cross-presentation, dendritic cell subsets, and the generation of immunity to cellular antigens.* Immunol Rev, 2004. **199**: p. 9-26.
24. Houde, M., et al., *Phagosomes are competent organelles for antigen cross-presentation.* Nature, 2003. **425**(6956): p. 402-6.
25. Albert, M.L., B. Sauter, and N. Bhardwaj, *Dendritic cells acquire antigen from apoptotic cells and induce class I-restricted CTLs.* Nature, 1998. **392**(6671): p. 86-9.
26. Burgdorf, S., et al., *Distinct pathways of antigen uptake and intracellular routing in CD4 and CD8 T cell activation.* Science, 2007. **316**(5824): p. 612-6.
27. Villadangos, J.A. and P. Schnorrer, *Intrinsic and cooperative antigen-presenting functions of dendritic-cell subsets in vivo.* Nat Rev Immunol, 2007. **7**(7): p. 543-55.
28. Li, M., et al., *Cell-associated ovalbumin is cross-presented much more efficiently than soluble ovalbumin in vivo.* J Immunol, 2001. **166**(10): p. 6099-103.
29. Shen, L., et al., *Important role of cathepsin S in generating peptides for TAP-independent MHC class I crosspresentation in vivo.* Immunity, 2004. **21**(2): p. 155-65.
30. Guermonprez, P., et al., *ER-phagosome fusion defines an MHC class I cross-presentation compartment in dendritic cells.* Nature, 2003. **425**(6956): p. 397-402.
31. Cebrian, I., et al., *Sec22b regulates phagosomal maturation and antigen crosspresentation by dendritic cells.* Cell, 2011. **147**(6): p. 1355-68.
32. Joffre, O.P., et al., *Cross-presentation by dendritic cells.* Nat Rev Immunol, 2012. **12**(8): p. 557-69.
33. Wiertz, E.J., et al., *Sec61-mediated transfer of a membrane protein from the endoplasmic reticulum to the proteasome for destruction.* Nature, 1996. **384**(6608): p. 432-8.
34. Hamman, B.D., et al., *The aqueous pore through the translocon has a diameter of 40-60 A during cotranslational protein translocation at the ER membrane.* Cell, 1997. **89**(4): p. 535-44.
35. Burgdorf, S., et al., *Spatial and mechanistic separation of cross-presentation and endogenous antigen presentation.* Nat Immunol, 2008. **9**(5): p. 558-66.
36. English, L., et al., *Autophagy enhances the presentation of endogenous viral antigens on MHC class I molecules during HSV-1 infection.* Nat Immunol, 2009. **10**(5): p. 480-7.
37. Levine, B. and V. Deretic, *Unveiling the roles of autophagy in innate and adaptive immunity.* Nature Reviews Immunology, 2007. **7**(10): p. 767-77.
38. Saveanu, L., et al., *IRAP Identifies an Endosomal Compartment Required for MHC Class I Cross-Presentation.* Science, 2009.

39. Lizee, G., et al., *Control of dendritic cell cross-presentation by the major histocompatibility complex class I cytoplasmic domain.* Nat Immunol, 2003. **4**(11): p. 1065-73.
40. Amigorena, S., *Fc gamma receptors and cross-presentation in dendritic cells.* J Exp Med, 2002. **195**(1): p. F1-3.
41. Zelenay, S., et al., *The dendritic cell receptor DNGR-1 controls endocytic handling of necrotic cell antigens to favor cross-priming of CTLs in virus-infected mice.* J Clin Invest, 2012. **122**(5): p. 1615-27.
42. Weck, M.M., et al., *hDectin-1 is involved in uptake and cross-presentation of cellular antigens.* Blood, 2008. **111**(8): p. 4264-72.
43. Bonifaz, L., et al., *In vivo targeting of antigens to maturing dendritic cells via the DEC-205 receptor improves T cell vaccination.* Journal of Experimental Medicine, 2004. **199**(6): p. 815-24.
44. Wagner, C.S., J.E. Grotzke, and P. Cresswell, *Intracellular events regulating cross-presentation.* Front Immunol, 2012. **3**: p. 138.
45. Kerrigan, A.M. and G.D. Brown, *C-type lectins and phagocytosis.* Immunobiology, 2009. **214**(7): p. 562-75.
46. Kovacsovics-Bankowski, M., et al., *Efficient major histocompatibility complex class I presentation of exogenous antigen upon phagocytosis by macrophages.* Proc Natl Acad Sci U S A, 1993. **90**(11): p. 4942-6.
47. Pfeifer, J.D., et al., *Phagocytic processing of bacterial antigens for class I MHC presentation to T cells.* Nature, 1993. **361**(6410): p. 359-62.
48. Reis e Sousa, C. and R.N. Germain, *Major histocompatibility complex class I presentation of peptides derived from soluble exogenous antigen by a subset of cells engaged in phagocytosis.* J Exp Med, 1995. **182**(3): p. 841-51.
49. Tran, K.K. and H. Shen, *The role of phagosomal pH on the size-dependent efficiency of cross-presentation by dendritic cells.* Biomaterials, 2009. **30**(7): p. 1356-62.
50. Norbury, C.C., et al., *Class I MHC presentation of exogenous soluble antigen via macropinocytosis in bone marrow macrophages.* Immunity, 1995. **3**(6): p. 783-91.
51. Matzinger, P., *Tolerance, danger, and the extended family.* Annu Rev Immunol, 1994. **12**: p. 991-1045.
52. Shi, Y., J.E. Evans, and K.L. Rock, *Molecular identification of a danger signal that alerts the immune system to dying cells.* Nature, 2003. **425**(6957): p. 516-21.
53. Ng, G., et al., *Receptor-independent, direct membrane binding leads to cell-surface lipid sorting and Syk kinase activation in dendritic cells.* Immunity, 2008. **29**(5): p. 807-18.
54. Flach, T.L., et al., *Alum interaction with dendritic cell membrane lipids is essential for its adjuvanticity.* Nat Med, 2011. **17**(4): p. 479-87.
55. Cunningham, C.C., et al., *Osteoarthritis-associated basic calcium phosphate crystals induce pro-inflammatory cytokines and damage-associated molecules via activation of Syk and PI3 kinase.* Clin Immunol, 2012. **144**(3): p. 228-36.
56. Doshi, N. and S. Mitragotri, *Macrophages recognize size and shape of their targets.* PLoS One, 2010. **5**(4): p. e10051.
57. Flannagan, R.S., V. Jaumouille, and S. Grinstein, *The cell biology of phagocytosis.* Annu Rev Pathol, 2012. **7**: p. 61-98.

58. Underhill, D.M. and H.S. Goodridge, *Information processing during phagocytosis.* Nat Rev Immunol, 2012. **12**(7): p. 492-502.
59. Steinman, R.M., *Decisions about dendritic cells: past, present, and future.* Annu Rev Immunol, 2012. **30**: p. 1-22.
60. Mellman, I. and R.M. Steinman, *Dendritic cells: specialized and regulated antigen processing machines.* Cell, 2001. **106**(3): p. 255-8.
61. Niess, J.H., et al., *CX3CR1-mediated dendritic cell access to the intestinal lumen and bacterial clearance.* Science, 2005. **307**(5707): p. 254-8.
62. Banchereau, J. and R.M. Steinman, *Dendritic cells and the control of immunity.* Nature, 1998. **392**(6673): p. 245-52.
63. Delamarre, L., et al., *Differential lysosomal proteolysis in antigen-presenting cells determines antigen fate.* Science, 2005. **307**(5715): p. 1630-4.
64. Suto, D., et al., *Inactivation of cysteine and serine proteases by singlet oxygen.* Arch Biochem Biophys, 2007. **461**(2): p. 151-8.
65. Rybicka, J.M., et al., *Phagosomal proteolysis in dendritic cells is modulated by NADPH oxidase in a pH-independent manner.* EMBO J, 2012. **31**(4): p. 932-44.
66. Savina, A., et al., *NOX2 controls phagosomal pH to regulate antigen processing during crosspresentation by dendritic cells.* Cell, 2006. **126**(1): p. 205-18.
67. Randolph, G.J., *Dendritic cell migration to lymph nodes: cytokines, chemokines, and lipid mediators.* Springer Semin Immunol, 2001. **13**(5): p. 267-74.
68. Lin, M.L., et al., *The cell biology of cross-presentation and the role of dendritic cell subsets.* Immunol Cell Biol, 2008. **86**(4): p. 353-62.
69. Geissmann, F., et al., *Development of monocytes, macrophages, and dendritic cells.* Science, 2010. **327**(5966): p. 656-61.
70. Nierkens, S., et al., *Antigen cross-presentation by dendritic cell subsets: one general or all sergeants?* Trends Immunol, 2013.
71. Kamphorst, A.O., et al., *Route of antigen uptake differentially impacts presentation by dendritic cells and activated monocytes.* J Immunol, 2010. **185**(6): p. 3426-35.
72. Heath, W.R. and F.R. Carbone, *The skin-resident and migratory immune system in steady state and memory: innate lymphocytes, dendritic cells and T cells.* Nat Immunol, 2013. **14**(10): p. 978-85.
73. Watowich, S.S. and Y.J. Liu, *Mechanisms regulating dendritic cell specification and development.* Immunol Rev, 2010. **238**(1): p. 76-92.
74. Waldmann, H. and H. Pope, *The influence of antigen presentation on the generation of T-helper cells with different functions.* Immunology, 1977. **33**(5): p. 721-5.
75. Haskins, K., et al., *The major histocompatibility complex-restricted antigen receptor on T cells. I. Isolation with a monoclonal antibody.* J Exp Med, 1983. **157**(4): p. 1149-69.
76. Hedrick, S.M., et al., *Isolation of cDNA clones encoding T cell-specific membrane-associated proteins.* Nature, 1984. **308**(5955): p. 149-53.
77. Yanagi, Y., et al., *A human T cell-specific cDNA clone encodes a protein having extensive homology to immunoglobulin chains.* Nature, 1984. **308**(5955): p. 145-9.
78. Smith-Garvin, J.E., G.A. Koretzky, and M.S. Jordan, *T cell activation.* Annu Rev Immunol, 2009. **27**: p. 591-619.
79. Huse, M., *The T-cell-receptor signaling network.* J Cell Sci, 2009. **122**(Pt 9): p. 1269-73.

80. Reis e Sousa, C., *Dendritic cells in a mature age.* Nat Rev Immunol, 2006. **6**(6): p. 476-83.
81. Steinman, R.M., D. Hawiger, and M.C. Nussenzweig, *Tolerogenic dendritic cells.* Annu Rev Immunol, 2003. **21**: p. 685-711.
82. Drutman, S.B. and E.S. Trombetta, *Dendritic cells continue to capture and present antigens after maturation in vivo.* J Immunol, 2010. **185**(4): p. 2140-6.
83. Platt, C.D., et al., *Mature dendritic cells use endocytic receptors to capture and present antigens.* Proc Natl Acad Sci U S A, 2010. **107**(9): p. 4287-92.
84. Carbone, F.R., G.T. Belz, and W.R. Heath, *Transfer of antigen between migrating and lymph node-resident DCs in peripheral T-cell tolerance and immunity.* Trends Immunol, 2004. **25**(12): p. 655-8.
85. Kawai, T. and S. Akira, *Toll-like receptors and their crosstalk with other innate receptors in infection and immunity.* Immunity, 2011. **34**(5): p. 637-50.
86. Geijtenbeek, T.B. and S.I. Gringhuis, *Signalling through C-type lectin receptors: shaping immune responses.* Nat Rev Immunol, 2009. **9**(7): p. 465-79.
87. Schenten, D. and R. Medzhitov, *The control of adaptive immune responses by the innate immune system.* Adv Immunol, 2011. **109**: p. 87-124.
88. Schroder, K. and J. Tschopp, *The inflammasomes.* Cell, 2010. **140**(6): p. 821-32.
89. Zygmunt, B. and M. Veldhoen, *T helper cell differentiation more than just cytokines.* Adv Immunol, 2011. **109**: p. 159-96.
90. Blander, J.M. and R. Medzhitov, *Regulation of phagosome maturation by signals from toll-like receptors.* Science, 2004. **304**(5673): p. 1014-8.
91. Zenaro, E., M. Donini, and S. Dusi, *Induction of Th1/Th17 immune response by Mycobacterium tuberculosis: role of dectin-1, Mannose Receptor, and DC-SIGN.* J Leukoc Biol, 2009. **86**(6): p. 1393-401.
92. Fritz, J.H., et al., *Nod1-mediated innate immune recognition of peptidoglycan contributes to the onset of adaptive immunity.* Immunity, 2007. **26**(4): p. 445-59.
93. Kumar, H., et al., *Cutting edge: cooperation of IPS-1- and TRIF-dependent pathways in poly IC-enhanced antibody production and cytotoxic T cell responses.* J Immunol, 2008. **180**(2): p. 683-7.
94. Wan, Y.Y., *Multi-tasking of helper T cells.* Immunology, 2010. **130**(2): p. 166-71.
95. Steinman, R.M., et al., *Endocytosis and the recycling of plasma membrane.* J Cell Biol, 1983. **96**(1): p. 1-27.
96. Jovic, M., et al., *The early endosome: a busy sorting station for proteins at the crossroads.* Histol Histopathol, 2010. **25**(1): p. 99-112.
97. Grant, B.D. and J.G. Donaldson, *Pathways and mechanisms of endocytic recycling.* Nat Rev Mol Cell Biol, 2009. **10**(9): p. 597-608.
98. Saftig, P. and J. Klumperman, *Lysosome biogenesis and lysosomal membrane proteins: trafficking meets function.* Nat Rev Mol Cell Biol, 2009. **10**(9): p. 623-35.
99. Compeer, E.B., et al., *Antigen processing and remodeling of the endosomal pathway: requirements for antigen cross-presentation.* Front Immunol, 2012. **3**: p. 37.
100. Soldati, T. and M. Schliwa, *Powering membrane traffic in endocytosis and recycling.* Nat Rev Mol Cell Biol, 2006. **7**(12): p. 897-908.
101. Swanson, J.A., *Shaping cups into phagosomes and macropinosomes.* Nat Rev Mol Cell Biol, 2008. **9**(8): p. 639-49.

102. Harrison, R.E. and S. Grinstein, *Phagocytosis and the microtubule cytoskeleton.* Biochem Cell Biol, 2002. **80**(5): p. 509-15.
103. Charles A. Janeway, J., *The immune system evolved to discriminate infectious nonself from noninfectious self.* Immunology Today, 1992. **12**(1): p. 11-16.
104. Pulecio, J., et al., *Cdc42-mediated MTOC polarization in dendritic cells controls targeted delivery of cytokines at the immune synapse.* J Exp Med, 2010. **207**(12): p. 2719-32.
105. Galvez, T., et al., *SnapShot: Mammalian Rab proteins in endocytic trafficking.* Cell, 2012. **151**(1): p. 234-234 e2.
106. Pulecio, J., et al., *Expression of Wiskott-Aldrich syndrome protein in dendritic cells regulates synapse formation and activation of naive CD8+ T cells.* J Immunol, 2008. **181**(2): p. 1135-42.
107. Radhakrishna, H. and J.G. Donaldson, *ADP-ribosylation factor 6 regulates a novel plasma membrane recycling pathway.* J Cell Biol, 1997. **139**(1): p. 49-61.
108. Mosmann, T.R., et al., *Two types of murine helper T cell clone. I. Definition according to profiles of lymphokine activities and secreted proteins.* J Immunol, 1986. **136**(7): p. 2348-57.
109. Hsieh, C.S., et al., *Development of TH1 CD4+ T cells through IL-12 produced by Listeria-induced macrophages.* Science, 1993. **260**(5107): p. 547-9.
110. O'Garra, A. and D. Robinson, *Development and function of T helper 1 cells.* Adv Immunol, 2004. **83**: p. 133-62.
111. Martinez, C.D.G.J., *T cells: the usual subsets.* Nature Reviews Immunology, 2010.
112. Henkart, P.A. and M. Catalfamo, *CD8+ effector cells.* Adv Immunol, 2004. **83**: p. 233-52.
113. Stetson, D.B., et al., *Th2 cells: orchestrating barrier immunity.* Adv Immunol, 2004. **83**: p. 163-89.
114. Mangan, P.R., et al., *Transforming growth factor-beta induces development of the T(H)17 lineage.* Nature, 2006. **441**(7090): p. 231-4.
115. Wong, M.T., et al., *Regulation of human Th9 differentiation by type I interferons and IL-21.* Immunol Cell Biol, 2010. **88**(6): p. 624-31.
116. Mantegazza, A.R., et al., *Presentation of Phagocytosed Antigens by MHC Class I and II.* Traffic, 2013. **14**(2): p. 135-52.
117. Greenberg, S. and S. Grinstein, *Phagocytosis and innate immunity.* Curr Opin Immunol, 2002. **14**(1): p. 136-45.
118. Huynh, K.K., et al., *Fusion, fission, and secretion during phagocytosis.* Physiology (Bethesda), 2007. **22**: p. 366-72.
119. Kovacsovics-Bankowski, M. and K.L. Rock, *A phagosome-to-cytosol pathway for exogenous antigens presented on MHC class I molecules.* Science, 1995. **267**(5195): p. 243-6.
120. Mant, A., et al., *The pathway of cross-presentation is influenced by the particle size of phagocytosed antigen.* Immunology, 2012. **136**(2): p. 163-75.
121. Thacker, R.I. and E.M. Janssen, *Cross-presentation of cell-associated antigens by mouse splenic dendritic cell populations.* Front Immunol, 2012. **3**: p. 41.
122. Desrosiers, M.D., et al., *Adenosine deamination sustains dendritic cell activation in inflammation.* J Immunol, 2007. **179**(3): p. 1884-92.

123. Mastronarde, D.N., *Automated electron microscope tomography using robust prediction of specimen movements.* J Struct Biol, 2005. **152**(1): p. 36-51.
124. Kremer, J.R., D.N. Mastronarde, and J.R. McIntosh, *Computer visualization of three-dimensional image data using IMOD.* J Struct Biol, 1996. **116**(1): p. 71-6.
125. Rybicka, J.M., et al., *NADPH oxidase activity controls phagosomal proteolysis in macrophages through modulation of the lumenal redox environment of phagosomes.* Proc Natl Acad Sci U S A, 2010. **107**(23): p. 10496-501.
126. Yates, R.M. and D.G. Russell, *Real-time spectrofluorometric assays for the lumenal environment of the maturing phagosome.* Methods Mol Biol, 2008. **445**: p. 311-25.
127. Liu, W., et al., *Intrinsic properties of immunoglobulin IgG1 isotype-switched B cell receptors promote microclustering and the initiation of signaling.* Immunity, 2010. **32**(6): p. 778-89.
128. Falo, L.D., Jr., et al., *Analysis of antigen presentation by metabolically inactive accessory cells and their isolated membranes.* Proc Natl Acad Sci U S A, 1985. **82**(19): p. 6647-51.
129. Shimonkevitz, R., et al., *Antigen recognition by H-2-restricted T cells. I. Cell-free antigen processing.* J Exp Med, 1983. **158**(2): p. 303-16.
130. Binnig, G., C.F. Quate, and C. Gerber, *Atomic force microscope.* Phys Rev Lett, 1986. **56**(9): p. 930-933.
131. Eibl, R.H. and M. Benoit, *Molecular resolution of cell adhesion forces.* IEE Proc Nanobiotechnol, 2004. **151**(3): p. 128-32.
132. Evans, E.A. and D.A. Calderwood, *Forces and bond dynamics in cell adhesion.* Science, 2007. **316**(5828): p. 1148-53.
133. Hosseini, B.H., et al., *Immune synapse formation determines interaction forces between T cells and antigen-presenting cells measured by atomic force microscopy.* Proc Natl Acad Sci U S A, 2009. **106**(42): p. 17852-7.
134. Helenius, J., et al., *Single-cell force spectroscopy.* J Cell Sci, 2008. **121**(Pt 11): p. 1785-91.
135. Bevan, M.J., *Cross-priming for a secondary cytotoxic response to minor H antigens with H-2 congenic cells which do not cross-react in the cytotoxic assay.* J Exp Med, 1976. **143**(5): p. 1283-8.
136. Kirschke, H., et al., *Cathepsin S from bovine spleen. Purification, distribution, intracellular localization and action on proteins.* Biochem J, 1989. **264**(2): p. 467-73.
137. Lennon-Dumenil, A.M., et al., *Analysis of protease activity in live antigen-presenting cells shows regulation of the phagosomal proteolytic contents during dendritic cell activation.* J Exp Med, 2002. **196**(4): p. 529-40.
138. Ackerman, A.L., A. Giodini, and P. Cresswell, *A role for the endoplasmic reticulum protein retrotranslocation machinery during crosspresentation by dendritic cells.* Immunity, 2006. **25**(4): p. 607-17.
139. Guermonprez, P. and S. Amigorena, *Pathways for antigen cross presentation.* Springer Semin Immunopathol, 2005. **26**(3): p. 257-71.
140. Di Pucchio, T., et al., *Direct proteasome-independent cross-presentation of viral antigen by plasmacytoid dendritic cells on major histocompatibility complex class I.* Nat Immunol, 2008. **9**(5): p. 551-7.
141. Gromme, M., et al., *Recycling MHC class I molecules and endosomal peptide loading.* Proc Natl Acad Sci U S A, 1999. **96**(18): p. 10326-31.

142. Savina, A. and S. Amigorena, *Phagocytosis and antigen presentation in dendritic cells.* Immunol Rev, 2007. **219**: p. 143-56.
143. Cross, A.R. and A.W. Segal, *The NADPH oxidase of professional phagocytes--prototype of the NOX electron transport chain systems.* Biochim Biophys Acta, 2004. **1657**(1): p. 1-22.
144. Leto, T.L. and M. Geiszt, *Role of Nox family NADPH oxidases in host defense.* Antioxid Redox Signal, 2006. **8**(9-10): p. 1549-61.
145. Yates, R.M., *Redox considerations in the phagosome: current concepts, controversies, and future challenges.* Antioxid Redox Signal, 2013. **18**(6): p. 628-9.
146. Yates, R.M., et al., *Macrophage activation downregulates the degradative capacity of the phagosome.* Traffic, 2007. **8**(3): p. 241-50.
147. Elliott, M.R. and K.S. Ravichandran, *Clearance of apoptotic cells: implications in health and disease.* J Cell Biol, 2010. **189**(7): p. 1059-70.
148. Ivashkiv, L.B., *Cross-regulation of signaling by ITAM-associated receptors.* Nat Immunol, 2009. **10**(4): p. 340-7.
149. Shi, Y., *To forge a solid immune recognition.* Protein Cell, 2012. **3**(8): p. 564-70.
150. Singh-Jasuja, H., et al., *Cross-presentation of glycoprotein 96-associated antigens on major histocompatibility complex class I molecules requires receptor-mediated endocytosis.* J Exp Med, 2000. **191**(11): p. 1965-74.
151. Giodini, A., C. Rahner, and P. Cresswell, *Receptor-mediated phagocytosis elicits cross-presentation in nonprofessional antigen-presenting cells.* Proc Natl Acad Sci U S A, 2009. **106**(9): p. 3324-9.
152. Datta, S.K., et al., *A subset of Toll-like receptor ligands induces cross-presentation by bone marrow-derived dendritic cells.* J Immunol, 2003. **170**(8): p. 4102-10.
153. Kreer, C., et al., *Cross-presentation: how to get there - or how to get the ER.* Front Immunol, 2011. **2**: p. 87.
154. Perrin-Cocon, L.A., P.N. Marche, and C.L. Villiers, *Purification of intracellular compartments involved in antigen processing: a new method based on magnetic sorting.* Biochem J, 1999. **338 (Pt 1)**: p. 123-30.
155. Tjelle, T.E., et al., *Isolation and characterization of early endosomes, late endosomes and terminal lysosomes: their role in protein degradation.* J Cell Sci, 1996. **109 (Pt 12)**: p. 2905-14.
156. Hammond, J.C., et al., *Evidence for abnormal forward trafficking of AMPA receptors in frontal cortex of elderly patients with schizophrenia.* Neuropsychopharmacology, 2010. **35**(10): p. 2110-9.